Development of a methodology for the operational evaluation of SBAS systems

Pedro Miguel Ferreira do Rosário Silva

Thesis to Obtain the Master of Science Degree in

Aerospace Engineering

Examination Committee

Chairperson: Prof. Doutor João Manuel Lage de Miranda Lemos (DEEC)
Supervisor: Prof. Doutor Agostinho Rui Alves da Fonseca (DEM)
Members of the Committee: Prof. Doutor João Manuel Gonçalves de Sousa Oliveira (DEM)

November 2013

Acknowledgements

I would like to thank Prof. Doutor Agostinho Fonseca for his guidance and the opportunity to write this thesis.

To my parents and my brother for their unending support throughout my academic career.

Abstract

As air travel keeps expanding, Air Traffic Management (ATM) is increasingly replacing older ground communications based navigation systems with Global Navigation Satellite Systems (GNSS). However, these systems alone cannot provide the necessary accuracy, integrity, continuity and availability that aviation requires; therefore augmentation systems are necessary to aid GNSS. One such type of augmentation is SBAS (Space Based Augmentation Systems).

This thesis aims to provide a systematic SBAS operational evaluation methodology using the EUROCONTROL PEGASUS software. To do so, several examples of evaluation will be shown by evaluating the performance of the European Geostationary Navigation Overlay Service (EGNOS), an SBAS, in several Portuguese airports as examples, using both a real GPS receiver and virtual reference stations.

Keywords: Global Navigation Satellite Systems (GNSS); Satellite Based Augmentation System (SBAS); EUROCONTROL PEGASUS; Civil Aviation; Operational Evaluation.

Resumo

À medida que o tráfego aéreo expande, a Gestão do Tráfego Aéreo está progressivamente a substituir as tecnologias de sistemas de navegação antigas baseadas em comunicações terrestres por sistemas de navegação por satélite (GNSS - Global Navigation Satellite Systems). Contudo, estes sistemas não são capazes de só por si fornecer a precisão, integridade, continuidade e disponibilidade do sinal que a aviação requer, logo são necessários sistemas para melhorar o desempenho dos GNSS. Um destes é o SBAS (Satellite Based Augmentation Systems).

O objetivo desta tese é oferecer uma metodologia de avaliação operational sistemática de sistemas SBAS usando o *software* EUROCONTROL PEGASUS. Para isso, serão apresentados vários exemplos de avaliação através da avaliação do desempenho do European Geostationary Navigation Overlay Service (EGNOS), um SBAS em vários aeroportos portugueses, usando tanto um recetor GPS real como várias estações de referência virtuais.

Palavras-chave: GNSS; SBAS; EUROCONTROL PEGASUS; Aviação Civil; Avaliação Operacional.

Contents

Acknowledgements i
Abstract ii
Resumo iii
Contents iv
List of Figures vi
List of Tables x
List of Acronyms xii
List of Symbols xv
1 Introduction 1
1.1 Objectives 1
1.2 Outline 2
2 Literature Review 3
2.1 GNSS Overview 3
2.2 GNSS Systems 6
2.2.1 Global Positioning System (GPS) 6
2.2.2 GLONASS 7
2.2.3 Galileo 8
2.3 GNSS errors 8
2.3.1 Clock error 8
2.3.2 Orbital Error 8
2.3.3 Ionospheric delay 8
2.3.4 Tropospheric Delay 9
2.3.5 Secondary Error Sources 9
2.3.6 Receiver Clock Errors 9
2.3.7 Receiver Measurement Noise 9
2.3.8 Multipath errors 9
2.3.9 Satellite Geometry 9
2.4 GNSS Augmentation 11
2.4.1 ABAS 11
2.4.2 GBAS 11
2.4.3 SBAS 11
2.5 GNSS Performance 12
2.6 EGNOS Overview 14
2.6.1 EGNOS Architecture 14

2.7 The EGNOS Signal ... 17
2.7.1 Ionospheric corrections ... 19
2.7.2 Long-term corrections ... 21
2.7.3 Fast corrections ... 22
2.7.4 Integrity Information ... 23
2.8 EGNOS Operational Evaluation ... 23
2.8.1 Software ... 23
2.8.2 Hardware ... 24
2.9 EGNOS Certification ... 24
2.9.1 Overview ... 24
3 Analysis of EGNOS Real Data ... 28
3.1 Procedure ... 28
3.2 DoIt Outputs ... 29
3.3 Real Receiver Evaluation ... 30
3.3.1 IST4 16 of October 2009 ... 30
3.3.2 IST4 15 of January 2012 ... 39
4 Analysis of Data Anomalies ... 48
4.1 January 23rd 2012 Occurrence ... 48
5 Analysis of Virtual Data ... 55
5.1 Virtual Receiver Stations (VRS) ... 55
5.2 Acceptability of VRS Data ... 56
5.3 Procedure ... 58
5.4 Virtual Receiver Station Evaluation ... 60
5.4.1 VirtPorto ... 60
5.4.2 VirtFaro ... 69
6 Conclusions and Future Work ... 75
6.1 Conclusions ... 75
6.2 Future Work ... 76
Annex A: DoIt Sample Report ... 77
Annex B: Location of Real and Virtual Receivers ... 89
Annex C: Evaluation Parameters Calculation ... 92
Protection Level Calculation ... 95
Bibliography ... 97

List of Figures

Figure 1 – Earth Centered Earth Fixed coordinate System 3

Figure 2 – Elliptical coordinate system 4

Figure 3 – Radius of curvature in the prime vertical 5

Figure 4 – Clock drift 6

Figure 5 – Dilution of precision 10

Figure 6 – EGNOS architecture 14

Figure 7 – Geographical distribution of the RIMS already in operation and the RIMS current under deployment 16

Figure 8 – EGNOS message structure 17

Figure 9 – Ionospheric Pierce Points 19

Figure 10 – IPP interpolation principle 20

Figure 11 – IGP grid 20

Figure 12 – Format of MT25 (long-term corrections) 22

Figure 13 – Format of MT2 to 5 (fast corrections) 22

Figure 14 – Real Data Analysis Procedure 28

Figure 15 – DoIt folder structure example 29

Figure 16 – DoIt receiver folder 29

Figure 17 – HPE, HPL and NSV Timeplot for IST4 16 of October 2009 PRN120 30

Figure 18 – VPE, VPL and NSV Timeplot for IST4 16 of October 2009 PRN120 30

Figure 19 – Horizontal Deviation From Reference for IST4 16 of October 2009 PRN120 31

Figure 20 – Horizontal Stanford Graph Generation 31

Figure 21 – Vertical Stanford Graph Generation 32

Figure 22 – Horizontal Stanford Plot for IST4 16 of October 2009 PRN120 32

Figure 23 – Vertical Stanford Plot for IST4 16 of October 2009 PRN120 32

Figure 24 – HPE Histogram for IST4 16 of October 2009 PRN120 33

Figure 25 – VPE Histogram for IST4 16 of October 2009 PRN120 33

Figure 26 – HPL Histogram for IST4 16 of October 2009 PRN120 33

Figure 27 – VPL Histogram for IST4 16 of October 2009 PRN120 33

Figure 28 – HPE, HPL and NSV Timeplot for IST4 16 of October 2009 PRN124 34

Figure 29 – VPE, VPL and NSV Timeplot for IST4 16 of October 2009 PRN124 34

Figure 30 – Horizontal Deviation From Reference for IST4 16 of October 2009 PRN124 35

Figure 31 – Horizontal Stanford Plot for IST4 16 of October 2009 PRN124 35

Figure 32 – Vertical Stanford Plot for IST4 16 of October 2009 PRN124 35

Figure 33 – HPE Histogram for IST4 16 of October 2009 PRN124 36

Figure 34 – VPE Histogram for IST4 16 of October 2009 PRN124 36
Figure 35 – HPL Histogram for IST4 16 of October 2009 PRN124 36
Figure 36 – VPL Histogram for IST4 16 of October 2009 PRN124 36
Figure 37 – HPE, HPL and NSV Timeplot for IST4 16 of October 2009 PRN126 37
Figure 38 – VPE, VPL and NSV Timeplot for IST4 16 of October 2009 PRN126 37
Figure 39 – Horizontal Deviation From Reference for IST4 16 of October 2009 PRN126 37
Figure 40 – Horizontal Stanford Plot for IST4 16 of October 2009 PRN126.. 37
Figure 41 – Vertical Stanford Plot for IST4 16 of October 2009 PRN126.. 37
Figure 42 – HPE Histogram for IST4 16 of October 2009 PRN126... 38
Figure 43 – HPE Histogram for IST4 16 of October 2009 PRN126... 38
Figure 44 – HPL Histogram for IST4 16 of October 2009 PRN126 39
Figure 45 – VPL Histogram for IST4 16 of October 2009 PRN126 39
Figure 46 – HPE, HPL and NSV Timeplot for IST4 15 of January 2012 PRN120 39
Figure 47 – VPE, VPL and NSV Timeplot for IST4 15 of January 2012 PRN120 39
Figure 48 – Horizontal Deviation from reference for IST4 15 of January 2012 PRN120 40
Figure 49 – Horizontal Stanford Plot for IST4 15 of January 2012 PRN120.. 40
Figure 50 – Vertical Stanford Plot for IST4 15 of January 2012 PRN120... 40
Figure 51 – HPE Histogram for IST4 15 of January 2012 PRN120.. 41
Figure 52 – VPE Histogram for IST4 15 of January 2012 PRN120 41
Figure 53 – HPL Histogram for IST4 15 of January 2012 PRN120 42
Figure 54 – VPL Histogram for IST4 15 of January 2012 PRN120 42
Figure 55 – HPE, HPL and NSV Timeplot for IST4 15 of January 2012 PRN124............................... 42
Figure 56 – VPE, VPL and NSV Timeplot for IST4 15 of January 2012 PRN124 42
Figure 57 – Horizontal Deviation from reference for IST4 15 of January 2012 PRN124...................... 43
Figure 58 – Horizontal Stanford Plot for IST4 15 of January 2012 PRN124.. 43
Figure 59 – Vertical Stanford Plot for IST4 15 of January 2012 PRN124.. 43
Figure 60 – HPE Histogram for IST4 15 of January 2012 PRN124... 44
Figure 61 – VPE Histogram for IST4 15 of January 2012 PRN124 44
Figure 62 – HPL Histogram for IST4 15 of January 2012 PRN124 44
Figure 63 – VPL Histogram for IST4 15 of January 2012 PRN124 44
Figure 64 – HPE, HPL and NSV Timeplot for IST4 15 of January 2012 PRN126............................... 45
Figure 65 – VPE, VPL and NSV Timeplot for IST4 15 of January 2012 PRN126 45
Figure 66 – Horizontal Deviation from reference for IST4 15 of January 2012 PRN126...................... 45
Figure 67 – Horizontal Stanford Plot for IST4 15 of January 2012 PRN126.. 46
Figure 68 – Vertical Stanford Plot for IST4 15 of January 2012 PRN126.. 46
Figure 69 – HPE Histogram for IST4 15 of January 2012 PRN126... 47

Figure 70 – VPE Histogram for IST4 15 of January 2012 PRN126 47
Figure 71 – HPL Histogram for IST4 15 of January 2012 PRN126 47
Figure 72 – VPL Histogram for IST4 15 of January 2012 PRN126 47
Figure 73 – Horizontal Evaluation Data for IST4 in January 23rd 2012 PRN 120 48
Figure 74 – Vertical Evaluation Data for IST4 in January 23rd 2012 PRN 120 48
Figure 75 – Horizontal Evaluation Data for IST4 in January 23rd 2012 PRN 124 48
Figure 76 – Vertical Evaluation Data for IST4 in January 23rd 2012 PRN 124 48
Figure 77 – Horizontal Evaluation Data for IST4 in January 23rd 2012 PRN 126 49
Figure 78 – Vertical Evaluation Data for IST4 in January 23rd 2012 PRN 126 49
Figure 79 – Vertical Position Error for IST4 from 01:41 to 02:13 of January 23rd 2012 PRN 120 49
Figure 80 – Horizontal Protection Level for IST4 from 01:41 to 02:13 of January 23rd 2012 PRN 120 49
Figure 81 –Vertical Protection Level for IST4 from 01:41 to 02:13 of January 23rd 2012 PRN 120 50
Figure 82 – Vertical Position Error for IST4 from 01:41 to 02:13 of January 23rd 2012 PRN 124 50
Figure 83 – Vertical Protection Level for IST4 from 01:41 to 02:13 of January 23rd 2012 PRN 124 50
Figure 84 – Horizontal Protection Level for IST4 from 01:41 to 02:13 of January 23rd 2012 PRN 124 51
Figure 85 – Vertical Position Error for IST4 from 01:41 to 02:13 of January 23rd 2012 PRN 126 51
Figure 86 – Horizontal Protection Level for IST4 from 01:41 to 02:13 of January 23rd 2012 PRN 126 51
Figure 87 – Vertical Protection Level for IST4 from 01:41 to 02:13 of January 23rd 2012 PRN 126 52
Figure 88 – PRC 01 values for PRN=120 AND TYPE=4 filter on January 23rd 2012 52
Figure 89 – PRC 01 values for PRN=124 AND TYPE=4 filter on January 23rd 2012 53
Figure 90 – PRC 01 values for PRN=126 AND TYPE=4 filter on January 23rd 2012 53
Figure 91 – GNSS Solution Parameters Advanced Configuration 53
Figure 92 – Time Series Graphic of HPL for 0:00 to 6:00 January 23rd 2012 PRN 120 using all GPS Satellites 54
Figure 93 – Time Series Graphic of HPL for January 23rd 2012 PRN 120 using all GPS Satellites except PRN29 54
Figure 94 – Geographical Institute of the Army GPS Receiver Network 56
Figure 95 – CNO_L1 of GPS satellite PRN 20 for EGNOS PRN 120 IST4 data during October 10th 2011 57
Figure 96 – CNO_L1 of GPS satellite PRN 20 for EGNOS PRN 120 VRS4 data during October 10th 2011 57
Figure 97 – NSV_LOCK of GPS satellite PRN 20 for EGNOS PRN 120 IST4 data during October 10th 2011 57
Figure 98 – NSV_LOCK of GPS satellite PRN 20 for EGNOS PRN 120 VRS4 data during October 10th 2011 57
Figure 99 – Virtual Data Evaluation Procedure 59
Figure 100 – PEGASUS Main Window 59
Figure 101 – Convertor Parameters Screen 60

Figure 102 – GNSS Solution Parameter Screen 60
Figure 103 – HPE and HPL for VirtPorto in February 9th 2012 PRN 120 61
Figure 104 – VPE and VPL for VirtPorto in February 9th 2012 PRN 120 61
Figure 105 – Horizontal Stanford Plot for VirtPorto in February 9th 2012 PRN 120 61
Figure 106 – Vertical Stanford Plot for VirtPorto in February 9th 2012 PRN 120 61
Figure 107 – Horizontal deviation from reference for VirtPorto in February 9th 2012 PRN 120 62
Figure 108 – HPE histogram for VirtPorto in February 9th 2012 PRN 120 62
Figure 109 – HPL histogram for VirtPorto in February 9th 2012 PRN 120 62
Figure 110 – VPE histogram for VirtPorto in February 9th 2012 PRN 120 63
Figure 111 – VPL histogram for VirtPorto in February 9th 2012 PRN 120 63
Figure 112 – Horizontal Stanford Plot for VirtPorto in February 9th 2012 PRN 124 64
Figure 113 – Vertical Stanford Plot for VirtPorto in February 9th 2012 PRN 124 64
Figure 114 – Horizontal deviation from reference for VirtPorto in February 9th 2012 PRN 124 64
Figure 115 – HPE and HPL for VirtPorto in February 9th 2012 PRN 124 65
Figure 116 – VPE and VPL for VirtPorto in February 9th 2012 PRN 124 65
Figure 117 – HPE histogram for VirtPorto in February 9th 2012 PRN 124 65
Figure 118 – HPL histogram for VirtPorto in February 9th 2012 PRN 124 65
Figure 119 – VPE histogram for VirtPorto in February 9th 2012 PRN 124 65
Figure 120 – VPL histogram for VirtPorto in February 9th 2012 PRN 124 65
Figure 121 – Horizontal Stanford Plot for VirtPorto in February 9th 2012 PRN 126 66
Figure 122 – Vertical Stanford Plot for VirtPorto in February 9th 2012 PRN 126 66
Figure 123 – HPE and HPL for VirtPorto in February 9th 2012 PRN 126 67
Figure 124 – VPE and VPL for VirtPorto in February 9th 2012 PRN 126 67
Figure 125 – Horizontal deviation from reference for VirtPorto in February 9th 2012 PRN 126 67
Figure 126 – HPE histogram for VirtPorto in February 9th 2012 PRN 126 68
Figure 127 – HPL histogram for VirtPorto in February 9th 2012 PRN 126 68
Figure 128 – VPE histogram for VirtPorto in February 9th 2012 PRN 126 68
Figure 129 – VPL histogram for VirtPorto in February 9th 2012 PRN 126 68
Figure 130 – Horizontal Stanford Plot for VirtFaro in February 9th 2012 PRN 120 69
Figure 131 – Vertical Stanford Plot for VirtFaro in February 9th 2012 PRN 120 69
Figure 132 – Horizontal deviation from reference for VirtFaro in February 9th 2012 PRN 120 70
Figure 133 – HPE and HPL for VirtFaro in February 9th 2012 PRN 120 70
Figure 134 – VPE and VPL for VirtFaro in February 9th 2012 PRN 120 70
Figure 135 – HPE histogram for VirtFaro in February 9th 2012 PRN 120 71
Figure 136 – HPL histogram for VirtFaro in February 9th 2012 PRN 120 71
Figure 137 – VPE histogram for VirtFaro in February 9th 2012 PRN 120 71

Figure 138 – VPL histogram for VirtFaro in February 9th 2012 PRN 120 71
Figure 139 – Horizontal Stanford Plot for VirtFaro in February 9th 2012 PRN 124 72
Figure 140 – Vertical Stanford Plot for VirtFaro in February 9th 2012 PRN 124 72
Figure 141 – Horizontal Stanford Plot for VirtFaro in February 9th 2012 PRN 126 73
Figure 142 – Vertical Stanford Plot for VirtFaro in February 9th 2012 PRN 126 73
Figure 143 – IST4 location 89
Figure 144 – VirtPorto location 90
Figure 145 – VirtFaro location 91
Figure 146 – Horizontal Standard Deviation 94

List of Tables

Table 1 – ICAO Accuracy, Integrity, Continuity and Availability requirements 13
Table 2 – ICAO Alert Limit requirements 13
Table 3 – EGNOS Space Segment 15
Table 4 – EGNOS SIS transmitted Message Types 18
Table 5 – Bit mask 18
Table 6 – PRN mask 19
Table 7 – IGP numbering principle 20
Table 8 – GIVE Indicators 21
Table 9 – UDRE Indicators 22
Table 10 – EGNOS Certification 25
Table 11 – Protection Level Statistics for IST4 16 of October 2009 PRN120 34
Table 12 – Position Error Statistics for IST4 16 of October 2009 PRN120 34
Table 13 – Availability Statistics for IST4 16 of October 2009 PRN120 34
Table 15 – Protection Level Statistics for IST4 16 of October 2009 PRN124 35
Table 16 – Position Error Statistics for IST4 16 of October 2009 PRN124 35
Table 17 – Availability Statistics for IST4 16 of October 2009 PRN124 36
Table 19 – Protection Level Statistics for IST4 16 of October 2009 PRN126 38
Table 20 – Position Error Statistics for IST4 16 of October 2009 PRN126 38
Table 21 – Availability Statistics for IST4 16 of October 2009 PRN126 38
Table 23 – Protection Level Statistics for IST4 15 of January 2012 PRN120 40
Table 24 – Position Error Statistics for IST4 15 of January 2012 PRN120 41
Table 25 – Availability Statistics for IST4 15 of January 2012 PRN120 41
Table 27 – Protection Level Statistics for IST4 15 of January 2012 PRN124 43
Table 28 – Position Error Statistics for IST4 15 of January 2012 PRN124 43

Table 29 – Availability Statistics for IST4 15 of January 2012 PRN124 44
Table 31 – Protection Level Statistics for IST4 15 of January 2012 PRN126...................................... 46
Table 32 – Position Error Statistics for IST4 15 of January 2012 PRN126.. 46
Table 33 – Availability Statistics for IST4 15 of January 2012 PRN126 46
Table 35 – Protection level statistics for PRN 120 IST4 data during October 10^{th} 2011 57
Table 36 – Position error statistics for PRN 120 IST4 data during October 10^{th} 2011.......................... 58
Table 37 – Availability statistics for PRN 120 IST4 data during October 10^{th} 2011 58
Table 38 – Protection level statistics for VRS4 data during October 10^{th} 2011 58
Table 39 – Position error statistics for PRN 120 VRS4 data during October 10^{th} 2011........................ 58
Table 40 – Availability statistics for PRN 120 VRS4 data during October 10^{th} 2011 58
Table 41 – Protection Level Statistics for VirtPorto and IST4 in February 9^{th} 2012 PRN 120 63
Table 42 – Position Error Statistics for VirtPorto and IST4 in February 9^{th} 2012 PRN 120 63
Table 43 – Availability statistics for VirtPorto and IST4 in February 9^{th} 2012 PRN 120........................ 63
Table 44 – Protection level statistics for VirtPorto and IST4 in February 9^{th} 2012 PRN 124 66
Table 45 – Position error statistics for VirtPorto and IST4 in February 9^{th} 2012 PRN 124 66
Table 46 – Availability statistics for VirtPorto and IST4 in February 9^{th} 2012 PRN 124........................ 66
Table 47 – Protection level statistics for VirtPorto and IST4 in February 9th 2012 PRN 126............... 68
Table 48 – Position error statistics for VirtPorto and IST4 in February 9th 2012 PRN 126 68
Table 49 – Availability statistics for VirtPorto and IST4 in February 9th 2012 PRN 126 69
Table 50 – Protection level statistics for VirtFaro and IST4 in February 9th 2012 PRN 120 71
Table 51 – Position Error statistics for VirtFaro and IST4 in February 9th 2012 PRN 120................... 72
Table 52 – Availability statistics for VirtFaro and IST4 in February 9th 2012 PRN 120........................ 72
Table 53 – Protection level statistics for VirtFaro and IST4 in February 9th 2012 PRN 124 72
Table 54 – Position error statistics for VirtFaro and IST4 in February 9th 2012 PRN 124 73
Table 55 – Availability statistics for VirtFaro and IST4 in February 9th 2012 PRN 124........................ 73
Table 56 – Protection level statistics for VirtFaro and IST4 in February 9th 2012 PRN 126 73
Table 57 – Position Error statistics for VirtFaro and IST4 in February 9th 2012 PRN 126................... 74
Table 58 – Availability statistics for VirtFaro and IST4 in February 9th 2012 PRN 126........................ 74

List of Acronyms

ABAS	Aircraft-Based Augmentation System
ANSP	Air Navigation Service Providers
APV	Approach with Vertical Guidance
ASQF	Application Specific Qualification Facility
ATM	Air Traffic Management
C/A	Coarse/Acquisition
CAT	Category
CDMA	Code Division Multiple Access
CDDS	Commercial Data Distribution Service
CN&S	Communication Navigation & Surveillance
CPF	Central Processing Facility
CS	Commercial Services
DOP	Dilution of Precision
DU	Do not Use
EASA	European Aviation Safety Agency
EC	European Commission
ECEF	Earth-Centered Earth-Fixed
EDCN	EGNOS Data Collection Network
EGNOS	European Geostationary Navigation Overlay Service
ESA	European Space Agency
ESSP	European Satellite Services Provider
EU	European Union
EWAN	EGNOS Wide Area Network
FDMA	Frequency Division Multiple Access
GBAS	Ground-based Augmentation System
GBRS	Ground-based Ranging Source
GDOP	Geometric Dilution Of Precision
GEO	Geosynchronous Earth Orbit
GIVE	Grid Ionospheric Vertical Error
GIVEi	GIVE Indicator
GIVD	Grid Ionospheric Vertical Delay
GLONASS	Globalnaya Navigazionnaya Sputnikovaya Sistema
GNSS	Global Navigation Satellite System
GPRS	General Packet Radio Service

GPS	Global Positioning System
GRAS	Ground-based Regional Augmentation Systems
GSA	GNSS Supervisory Authority
GSM	Global System for Mobile Communication
HP	High Precision
HAL	Horizontal Alert Limit
HDOP	Horizontal Dilution Of Precision
HPE	Horizontal Position Error
HPL	Horizontal Protection Level
ICAO	International Civil Aviation Organization
IgeoE	Instituto Geográfico do Exército
IGP	Ionospheric Grid Points
IGS	International Geodetic Service
IODE	Issue Of Data Ephemeris
IODF	Issue Of Data Fast corrections
IODI	Issue Of Data Ionosphere
IODP	Issue Of Data PRN
IPP	Ionospheric Pierce Points
MCC	Mission Control Centers
NED	North-East-Down
NEU	North-East-Up
MEO	Medium Earth Orbit
MOPS	Minimum Operational Performance Standards
NSV	Number of Satellites in View
MT	Message Types
NLES	Navigation Land Earth Stations
NM	Not Monitored
NSA	National Supervisory Authority
OS	Open Service
PACF	Performance Assessment and Checkout Facility
PDOP	Position Dilution of Precision
PEGASUS	Prototype EGNOS and GBAS Analysis System Using SAPPHIRE
PRN	Pseudo-random Noise
PPS	Precise Positioning Service
PRC	Pseudorange Corrections
RIMS	Ranging Integrity Monitoring Stations

RINEX	Receiver Independent Exchange Format
RTCA	Radio Technical Commission for Aeronautics
RTK	Real-Time Kinematic
SARPs	Standards and Recommended Practices
SAS	Société par Actions Simplifiée
SBAS	Satellite Based Augmentation System
SES	Single European Sky
SIS	Signal-in-Space
SoL	Safety of Life Service
SP	Standard Precision
SPS	Standard Positioning Service
TTA	Time To Alert
UDRE	User Differential Range Error
VAL	Vertical Alert Limit
VDOP	Vertical Dilution of Precision
VPE	Vertical Position Error
VPL	Vertical Protection Level
VRS	Virtual Reference Station
WGS-84	World Geodetic System

List of Symbols

a	Semi-major axis of WGS-84
C	Covariance matrix
e	First eccentricities
f	Flattening factor of WGS-84
$\underline{\underline{H}}$	Derivate matrix
k_i	Empirical parameter
N	Radius of curvature in the prime vertical
$\underline{\underline{T_{WGS}^{NED}}}$	Rotation matrix
W	Weight matrix for weight least square solution
(x,y,z)	Receiver position in ECEF coordinates
$(\hat{x}_u, \hat{y}_u, \hat{z}_u, d\hat{t}_r,)$	Reference variables for linearization
$\frac{\partial \hat{\rho}_i}{\partial d\hat{t}_r} = \mathrm{c}$	Pseudorange derivate by time
$\frac{\partial \hat{\rho}_i}{\partial \hat{x}_u} = a_{xi}$	Pseudorange derivate by x
$\frac{\partial \hat{\rho}_i}{\partial \hat{y}_u} = a_{yi}$	Pseudorange derivate by y
$\frac{\partial \hat{\rho}_i}{\partial \hat{z}_u} = a_{zi}$	Pseudorange derivate by z
Δdt_r	Receiver time variation
ΔE	Error vector
Δx_u	Receiver position variation along x
Δy_u	Receiver position variation along y
Δz_u	Receiver position variation along z
$\hat{\rho}_i$	Estimated Pseudorange
$(\sigma_N, \sigma_E, \sigma_D)$	Standard deviation of the North, East and Down position components
${\sigma_{NN}}^2$	North variance in NED coordinates
${\sigma_{EE}}^2$	East variance in NED coordinates
${\sigma_{DD}}^2$	Down variance in NED coordinates
${\sigma_{NE}}^2$	North-East variance in NED coordinates
${\sigma_{ND}}^2$	North-Down variance in NED coordinates
${\sigma_{DE}}^2$	Down-East variance in NED coordinates
(ϕ,λ,h)	Receiver position in elliptical coordinates

1 Introduction

Ever since its beginnings in the 1970s with the creation of the Global Positioning System (GPS), the field of satellite based navigation has undergone massive changes. The last decade in particular has seen a massive increase in development and use of Global Navigation Satellite Systems (GNSS) based consumer technologies. For example, a great percentage of automobiles and mobile phones sold today are equipped with a GPS receiver [1]. GNSS is also being used in increasingly varied fields possibly never imagined by the original systems designers, such as environmental remote sensing, precision agriculture [2], search and rescue and even location based social networking and gaming.

One field in particular in which the use of GNSS is greatly growing in importance is that of air navigation. For decades, the main method of air navigation was the use of radio ground stations to determine position and bearing. In the early 1980s, the International Civil Aviation Organization (ICAO) Council established a special committee on Future Air Navigation Systems (FANS) to develop recommendations for the future development of air navigation for civil aviation over the following 25 years. In September 1991, the ICAO 10th Air Navigation Conference endorsed the FANS Concept. After acceptance by the ICAO Council, it came to be known as “communications, navigation, and surveillance/air traffic management (CNS/ATM) systems”. In order to progress implementation of said systems, ICAO developed a document, now known as the Global Air Navigation Plan for CNS/ATM Systems (ICAO Global Plan) as a strategic document to guide their respective implementation. The ICAO Global Plan recognizes the GNSS as a key element of CNS/ATM systems, which can provide seamless navigation for all phases of flight, and a foundation upon which States can deliver improved aeronautical navigation services [3].

With GNSS, aircraft have the possibility of determining their position anywhere in the world at any time. However, in certain circumstances the GNSS signal must be accurate, reliable and near constantly available, since a lack of any of those attributes would cause potential disaster. Unfortunately, the GNSS signal alone can lack those qualities, hence the use of GNSS augmentation systems.

GNSS augmentation systems are systems capable of improving GNSS attributes; namely accuracy, reliability, continuity and availability. GNSS augmentation systems can be classified within several categories, one of which is Satellite Based Augmentation Systems (SBAS). SBAS provide augmentation via a series of ground stations which broadcast correction data to geostationary satellites. There are several SBAS systems currently in operation, one of them being the European Geostationary Navigation Overlay Service (EGNOS). EGNOS was developed by the European Space Agency (ESA), the European Commission and EUROCONTROL. It is capable of supplementing the GPS system. EGNOS was certified for aviation applications in the 2nd of March, 2011.

1.1 Objectives

The main goal of this thesis is the development of a systematic methodology for the operational evaluation of EGNOS. We will use the PEGASUS software to do so and provide examples by evaluating EGNOS’ performance in several Portuguese airports using real GNSS receivers as well as virtual ones.

1.2 Outline

The structure of this thesis is as follows:

Chapter 2 gives us an overview of GNSS, the existing GNSS systems and the main causes of error in those systems, followed by a brief overview of GNSS augmentation and finally a detailed description of EGNOS.

Chapter 3 details the resources used to perform the operational evaluation of EGNOS in this thesis.

Chapter 4 describes the procedure used for analyzing EGNOS performance with a real EGNOS receiver.

Chapter 5 describes how to proceed if the analysis ever gives out unusual or anomalous results.

Chapter 6 describes the procedure used in the analysis of EGNOS performance using Virtual Reference Stations.

Finally, Chapter 7 summarizes the conclusions reached and offers proposals for future work.

2 Literature Review

In this chapter, the literature consulted for this thesis will be used to provide an overview of GNSS and GNSS augmentation, followed by a focus on SBAS and finally, EGNOS.

2.1 GNSS Overview

The International Civil Aviation Organization (ICAO) defines GNSS as a "worldwide position and time determination system that includes one or more satellite constellations, aircraft receivers and system integrity monitoring, augmented if necessary to support the required Navigation Performances for the intended operation" [4], though GNSS can also be used for applications besides aviation. Also, according to ICAO, GNSS has the means to "provide a seamless, harmonized and cost-effective navigational service from departure to final approach that will provide benefits in safety, efficiency and capacity" [5]. Indeed, GNSS is currently used as a supplementary means of navigation for En-route, Terminal Area and Non-Precision Approaches. However, current satellite navigation systems (GPS and GLONASS) don't have the capacity to meet the requirements for this sort of operations, hence the need for supplementary support via Augmentation Systems, as we'll see later on.

Since GNSS deals in positioning, first and foremost a suitable coordinate system must be defined. In GNSS applications, the most convenient coordinate system is the Earth-Centered Earth-Fixed (ECEF) coordinate system. The ECEF coordinate system is a right-handed Cartesian system (x, y, z) with its origin coinciding with the Earth's center of mass while its z-axis coincides with the mean rotational axis of the Earth. The x-axis points to the mean Greenwich meridian, while the y-axis is directed to complete a right-handed system In other words, the z-axis is pointing to a mean pole of the Earth's rotation. Such a mean pole, defined by international convention, is called the Conventional International Origin (CIO). Then the xy-plane is called mean equatorial plane, and the xz-plane is called mean zero-meridian [6]. The ECEF system is illustrated in the figure below:

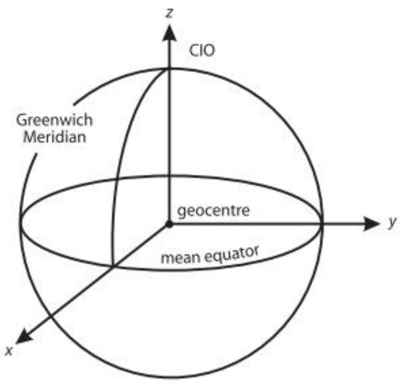

Figure 1 – Earth Centered Earth Fixed coordinate System [6]

In order to obtain latitude, longitude and altitude, we must convert the ECEF coordinate system to an ellipsoidal coordinate system (since the Earth is not shaped like a perfect sphere, but rather like an ellipsoid). An ellipsoid coordinate system is illustrated in Figure 2:

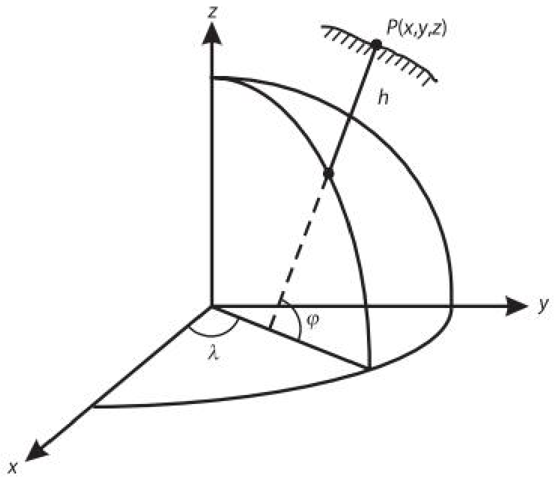

Figure 2 – Elliptical coordinate system [6]

The ellipsoidal system is also known as the geodetic coordinate system. Geocentric longitude and geodetic longitude are identical. The two geometric parameters could be the semi-major radius (denoted by a) and the semi-minor radius (denoted by b) of the rotating ellipse, or the semi-major radius and the flattening (denoted by f) of the ellipsoid. They are equivalent sets of parameters. As stated in [6], the relationship between (x, y, z) and (ϕ,λ,h) is:

$$\begin{pmatrix} x \\ y \\ z \end{pmatrix} = \begin{pmatrix} (N+h)cos\varphi\cos\lambda \\ (N+h)cos\varphi\sin\lambda \\ (N(1-e^2)+h)sin\varphi \end{pmatrix} \qquad (2.1)$$

Or

$$\begin{cases} tan\varphi = \frac{z}{\sqrt{x^2+y^2}}\left(1-e^2\frac{N}{N+h}\right)^{-1} \\ \tan\lambda = y/x \\ h = \frac{\sqrt{x^2+y^2}}{\cos\varphi} - N \end{cases} \qquad (2.2)$$

Where

$$N = \frac{a}{\sqrt{1-e^2 sin^2\varphi}} \qquad (2.3)$$

N is the radius of curvature in the prime vertical, and e is the first eccentricities. The geometric meaning of N is shown here:

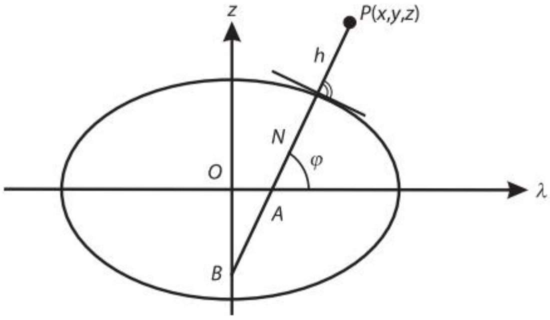

Figure 3 – Radius of curvature in the prime vertical [6]

The flattening and the first eccentricities are defined thusly, again according to [6]:

$$f = \frac{a-b}{a} \qquad (2.4)$$

$$e = \frac{\sqrt{a^2-b^2}}{a} \qquad (2.5)$$

In the World Geodetic System 1984 (WGS-84), the standard used by both EGNOS and GPS are (a = 6 378 137 m, f = 1 / 298.2572236) [6].

The fundamental measures in satellite navigation are the ranges. The ranges are defined as the measures of the distances between each satellite and the receiver's antenna. Said distances are obtained by multiplying the speed of light c by the time the signal has taken from the satellite to the receiver. The transmitting time is measured through maximum correlation analysis of the receiver code and the GPS signal. The receiver code is derived from the clock used in the GPS receiver. The GPS signal is, of course, generated by the clock used in the GPS satellite. However, since there are inevitably accuracy errors in the time measured by the receiver (the errors on the time measured by the satellite being negligible since they use atomic clocks), thus making them different from the true geometric distance between the satellites and receiver, the measures of the distances obtained by the GNSS are referred to as pseudoranges. It is also notable that the path of the signal transmission differs slightly from the geometric path. The transmitting medium not only delays the transmitting of the signal, but also bends the transmitting path of the signal [6] [7] [8].

In order to obtain a position in a three dimensional space, it is necessary to obtain the pseudoranges from at least four different satellites: three to determine the position in accordance to the principle of triangulation and one more to resolve the extra unknown of the time measurement error on ground [6] [7] [8], as seen in the following figure:

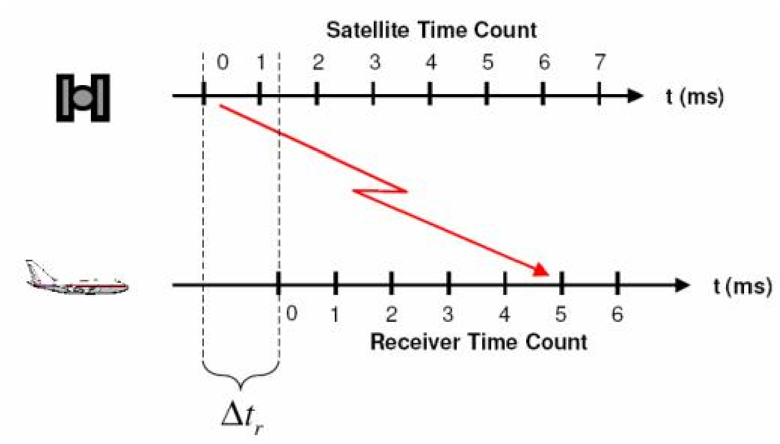

Figure 4 – Clock drift [9]

Thus the final pseudorange equation system becomes [10]:

$$\begin{cases} \sqrt{(x-x_1)^2+(y-y_1)^2+(z-z_1)^2} = (\rho_1 - c\Delta t) \\ \sqrt{(x-x_2)^2+(y-y_2)^2+(z-z_2)^2} = (\rho_2 - c\Delta t) \\ \sqrt{(x-x_3)^2+(y-y_3)^2+(z-z_3)^2} = (\rho_3 - c\Delta t) \\ \sqrt{(x-x_4)^2+(y-y_4)^2+(z-z_4)^2} = (\rho_4 - c\Delta t) \end{cases} \qquad (2.6)$$

Where (x, y, z) is the receiver's position, (x_i, y_i, z_i) is the ith satellite's position, ρ_i is the pseudorange between the receiver and the ith satellite and Δt is the time measurement error, or clock drift.

2.2 GNSS Systems

In this section, two GNSS in operation today and one which will be operating in the coming years are described:

2.2.1 Global Positioning System (GPS)

The Global Positioning System was designed, built, is operated and maintained by the U.S. Department of Defense. The first GPS satellite was launched in 1978, and the system was fully operational in the mid-1990s. The GPS constellation consists of 24 satellites in six orbital planes with four satellites in each plane. The ascending nodes of the orbital planes are equally spaced by 60 degrees and said orbital planes are inclined 55 degrees. Each GPS satellite is in a nearly circular orbit with a semi-major axis of 26 578 km and a period of about twelve hours. Each satellite carries four atomic clocks with long term frequency stability of the clocks reaches better than a few parts of 10^{-13} over a day. The atomic clocks aboard the satellite produce the fundamental L-band frequency, 10.23 MHz [6].

The GPS satellites are monitored by five base stations, with the main base station in Colorado Springs, Colorado and the other four located on Ascension Island (Atlantic Ocean), Diego Garcia (Indian Ocean), Kwajalein and Hawaii (both Pacific Ocean) [6].

All stations are equipped with precise cesium clocks and receivers to determine the broadcast ephemerides and to model the satellite clocks. Transmitted to the satellites are ephemerides and clock adjustments. The satellites in turn use these updates in the signals that they send to GPS receivers [6].

Each GPS satellite currently transmits data on the L1 (1575.42 MHz) and L2 (1227.60 MHz) frequency bands, with the L1 band being available for civilian use and the L2 for military use. There are plans in course to modernize GPS by adding new civilian use signals for both the L1 and L2 bands (called L1C and L2C respectively) as well as an entirely new band for Safety of Life (SoL) operations: L5 (1176.45 MHz) [11] [12] [13]. The L1, L2 and L5 carrier frequencies are generated by multiplying the fundamental frequency by 154, 120 and 115, respectively. GPS uses the Code Division Multiple Access (CDMA) channel access method [12]. Pseudo-random noise (PRN) codes, along with satellite ephemerides, ionospheric model, and satellite clock corrections are superimposed onto the carrier frequencies L1, L2 and L5. The measured transmitting times of the signals that travel from the satellites to the receivers are used to compute the pseudoranges [6]. The Coarse/Acquisition (C/A) code, sometimes called the Standard Positioning Service (SPS), is a pseudo-random noise code that is modulated onto the L1 carrier. The precision (P) code, sometimes called the Precise Positioning Service (PPS), is modulated onto the L1, L2 and L5 carriers allowing for the removal of the effects of the ionosphere. [6] The Global Positioning System (GPS) was conceived as a ranging system from known positions of satellites in space to unknown positions on land and sea, as well as in air and space. The orbits of the GPS satellites are available by broadcast or by the International Geodetic Service (IGS). IGS orbits are precise ephemerides after post-processing or quasi-real time processing. All GPS receivers have an almanac programmed into their computer, which tells them where each satellite is at any given moment, the almanac being a data file that contains information of orbits and clock corrections of all satellites. The almanac is transmitted by a GPS satellite to a GPS receiver, where it facilitates rapid satellite vehicle acquisition within GPS receivers [6].

2.2.2 GLONASS

GLONASS is a GNSS managed by the Russian Space Forces and it is operated by the Coordination Scientific Information Center (KNITs) of the Ministry of Defense of the Russian Federation. The first GLONASS satellite was launched in 1982. The system consists of 21 satellites in three orbital planes, with three on-orbit spares. The ascending nodes of three orbital planes are separated 120 degrees, and the satellites within the same orbit plane are equally spaced by 45 degrees. The arguments of the latitude of satellites in equivalent slots in two different orbital planes differ by 15 degrees. Each satellite operates in nearly circular orbits with a semi-major axis of 25 510 km. Each orbital plane has an inclination angle of 64.8 degrees, and each satellite completes an orbit in approximately 11 hours 16 minutes [6].

Cesium clocks are used on board the GLONASS satellites, with their stability reaching better than a few parts of 10^{-13} over a day. The satellites transmit coded signals in two frequencies located on two frequency bands, 1602–1615.5 MHz and1246–1256.5 MHz, with a frequency interval of 0.5625 MHz and 0.4375 MHz, respectively. GLONASS uses the frequency division multiple access (FDMA) channel access method though current modernization plans suggest it will eventually switch to CDMA [12]. The antipodal satellites, separated by 180 degrees in the same orbit plane in argument of latitude, transmit on the same frequency. The signals can be received by users anywhere on the Earth’s surface to identify their position and velocity in real time based on ranging measurements. The coordinate and time systems used in GLONASS are different from those of GPS. GLONASS satellites are also distinguished by slightly different carrier frequencies instead of by different PRN codes. The ground control stations of the GLONASS are maintained only in the territory of the former Soviet Union due to historical reasons. This lack of global coverage is not optimal for the monitoring of a global navigation satellite system. GLONASS and GPS are not entirely compatible with each other; however, they are generally interoperable [6].

2.2.3 Galileo

Galileo is a GNSS initiated by the European Union (EU) and the European Space Agency (ESA) for providing a highly accurate, guaranteed global positioning service under civilian control. As an independent navigation system, Galileo will meanwhile be interoperable with the two other global satellite navigation systems, GPS and GLONASS. A user will be able to position with the same receiver from any of the satellites in any combination. Galileo will guarantee availability of service with higher accuracy. The first Galileo satellite was launched in December 2005. The Galileo constellation consists of 30 Medium Earth Orbit (MEO) satellites in three orbital planes with nine equally spaced operational satellites in each plane plus one inactive spare satellite. The ascending nodes of the orbital planes are equally spaced by 120 degrees. The orbital planes are inclined 56 degrees. Each Galileo satellite is in a nearly circular orbit with semi-major axis of 29 600 km and a period of about 14 hours. The Galileo satellite rotates about its Earth-pointing axis so that the flat surface of the solar arrays always faces the Sun to collect maximum solar energy. The Galileo satellite has four clocks, two of each type (passive maser and rubidium whose stabilities are 0.45 ns and 1.8 ns over 12 hours, respectively). At any time, only one of each type is operating. The operating maser clock produces the reference frequency from which the navigation signal is generated. If the maser clock were to fail, the operating rubidium clock would take over instantaneously and the two reserve clocks would start up. The second maser clock would take the place of the rubidium clock after a few days when it is fully operational. The rubidium clock would then go on standby or reserve again. In this way, the Galileo satellite is guaranteed to generate a navigation signal at all times. Galileo will provide ten navigation signals in the Right Hand Circular Polarization (RHCP) in the frequency ranges 1 164–1215 MHz (E5a and E5b), 1215–1300 MHz (E6) and 1 559–1592 MHz (E2-L1-E1). The interoperability and compatibility of Galileo and GPS is realized by having two common center frequencies in E5a/L5 and L1 as well as adequate geodetic coordinate and time reference frames [6].

2.3 GNSS errors

In this section, the main causes of error in GNSS are examined:

2.3.1 Clock error

Any error in the synchronization of the different satellite clocks will have a direct effect on the range measurement accuracy. If navigation errors of more than a meter are to be avoided, an atomic clock must deviate by less than about 4 nanoseconds from perfect synchronization with the other satellite clocks. These errors are similar for all users able to view a given satellite [7].

2.3.2 Orbital Error

In order to determine pseudorange as accurately as possible, it is is vital to have a very precise knowledge of the location of the ranging source (i.e. the satellites). The ranging signals carry the required data to determine the satellites' orbits and to establish their position at any given time. Nevertheless, perturbations in the satellites' orbits do occur, introducing an error ranging from 2 to 5 meters [9].

2.3.3 Ionospheric delay

The ionosphere is the uppermost layer of the Earth's atmosphere, extending from an altitude of approximately 50 to 750 km [6]. As its name indicates, it's mostly comprised of atmospheric atoms and molecules ionized by solar radiation. The size of the error will depend on the level of solar activity (following approximately an 11-year cycle) and the satellite elevation above the horizon. For a low elevation satellite at 5° above the horizon, the error affecting the measurement is about 3 times larger than the error affecting a satellite seen at the zenith. The amount of the ionospheric delay or advance of the GPS signal can vary from a few meters to more than twenty meters within one day. Ionospheric effects are extremely difficult to model due to complicated physical interactions among the geomagnetic field and solar activities. However, since the ionosphere is a dispersive medium, the ionospheric effect is mostly dependent on signal frequency. Using this property, GNSS systems are designed with several working frequencies; so that ionospheric effects can be measured or corrected (GPS for example uses dual-frequency observations for this very purpose) [6].

2.3.4 Tropospheric Delay

Troposphere is the lowest layer of the atmosphere, extending from the surface of the Earth up to about 50 Km above. It is composed of gases and water vapor, which lengthen the propagation path due to refraction. The delay the signals suffer is a function of the local refractive index, which depends on the local temperature, pressure and relative humidity. Unlike the ionosphere delay, the troposphere delay does not vary with the signals' frequency and thus dual-frequency observations cannot correct it. The delay is also influenced by the elevation angle of the ranging sources, typically varying from 2 to 9 meters for satellites with over 15 degrees of elevation above the horizon.

2.3.5 Secondary Error Sources

Pseudorange measurement secondary error sources are those that are strictly linked with the user's equipment and location. The error sources that these introduce, along with errors arising from atmospheric delays variation, account for variations in measurements between nearby receivers [9].

2.3.6 Receiver Clock Errors

GNSS receivers are equipped with quartz clocks, which are much less accurate than the atomic clocks used by the satellites and thus they will exhibit much larger errors. These errors are usually corrected by introducing the receiver clock bias into the navigation equations, as seen earlier [9].

2.3.7 Receiver Measurement Noise

The receiver measurement noise results from the physical characteristics of the receiver's electronics. The contribution of this term to the range error will thus heavily depend on the design and quality of the receiver [9].

2.3.8 Multipath errors

Multipath is a propagation phenomenon which results in a radio signal reaching a receiving antenna via multiple paths. This is usually a result of environmental features, namely reflection and diffraction by the atmosphere, nearby buildings and objects, etc. Effects of multipath include constructive and destructive interference, and phase shifting of the signal [14], which can cause distortion of the receiver correlation function and ultimately the discrimination function and hence errors in range estimation.

2.3.9 Satellite Geometry

The disposition of the visible satellites in space can affect the position calculation accuracy. If the visible satellites are too close to each other, errors are generated.

For example, assuming the worst (and impractical) case in which all the satellites are in the same place, every satellite will correspond to an equal pseudorange, thus rendering the position impossible to calculate. On the other hand, the bigger the spread between satellites in the sky, the greater the accuracy of the resulting measurement becomes.

The following figure shows a two-dimensional representation of the issue:

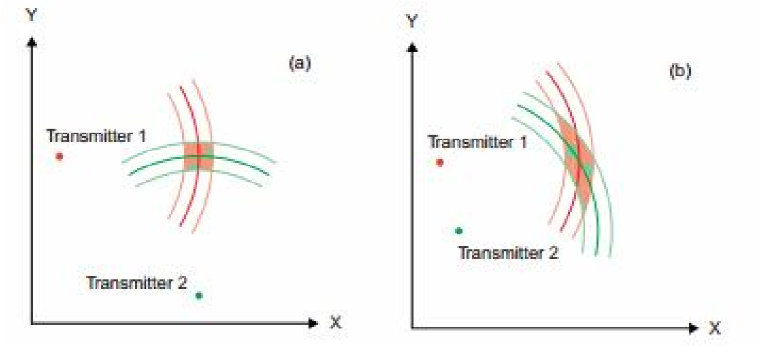

Figure 5 – Dilution of precision [15]

Here, Transmitter 1 generates a probable region delimited by the red circumferences and Transmitter 2 generates another delimitated by green circumferences. The probable region determined by both is the region marked in orange. As we can see, moving the transmitters closer together increases the probable area and thus increases the uncertainty of the result.

Dilution of Precision (DOP) thus serves as a measure of the strength of the satellite geometry. Mathematically, it is the ration of the standard deviation of one coordinate to the measurement accuracy and a scalar quantity, representing the geometrical contribution of a certain scalar factor to the uncertainty (for example, standard deviation) of a GPS measurement. A low DOP factor is considered good while a high DOP factor is considered bad.

The main form of DOP used in GNSS positioning is the Geometric DOP (GDOP), which measures accuracy in a 3-dimensional position and time:

$$GDOP = \frac{\left(\sigma_E^2+\sigma_N^2+\sigma_U^2+(c\cdot\delta_T)^2\right)^{1/2}}{\sigma_R} \qquad (2.7)$$

Where σ_E, σ_N and σ_U are the standard deviation in East, North and Up value, respectively; c is the speed of light and σ_R is the overall standard deviation in range.

Positional Dilution of Precision (PDOP) measures the accuracy in 3-dimensional position alone:

$$PDOP = \frac{\left(\sigma_E^2+\sigma_N^2+\sigma_U^2\right)^{1/2}}{\sigma_R} \qquad (2.8)$$

Other positional parameters are Horizontal DOP (HDOP):

$$HDOP = \frac{\left(\sigma_E^2+\sigma_N^2\right)^{1/2}}{\sigma_R} \qquad (2.9)$$

And Vertical DOP (VDOP) [8]:

$$VDOP = \frac{\sigma_U}{\sigma_R} \qquad (2.10)$$

2.4 GNSS Augmentation

One of the main ways of improving GNSS performance is via GNSS augmentation. GNSS augmentation is the process in which a GNSS signal's attributes are enhanced via an external system.

There are four classes of augmentation systems which have been recognized by the international aviation community: aircraft based augmentation systems (ABAS), satellite based augmentation systems (SBAS), ground based augmentation systems (GBAS), and a hybrid architecture known as ground-based regional augmentation systems (GRAS) [12].

2.4.1 ABAS

ABAS augments and/or integrates GNSS information with information available on-board the aircraft to enhance the performance of the core satellite constellations.

The most common ABAS technique is called receiver autonomous integrity monitoring (RAIM). RAIM requires redundant satellite range measurements to detect faulty signals and alert the pilot. The requirement for redundant signals means that navigation guidance with integrity provided by RAIM may not be available 100 per cent of the time. Another ABAS technique involves integration of GNSS with other sensors such as inertial navigation systems [16].

2.4.2 GBAS

As the name implies, Ground-Based Augmentation Systems enhance GNSS performance via a series of ground stations.

GBAS consists of a ground subsystem containing two to four GNSS reference receivers and an airborne subsystem. Using data from reference receivers, the ground-based subsystem provides corrections to the pseudoranges for all visible satellites. Said subsystem also monitors the quality of the information transmitted to the airborne subsystem by performing tests on the differential corrections and the pseudoranges. Those corrections are then transmitted to the aircraft via the VDB (VHF Data Broadcast) system. GBAS systems can provide coverage to aircraft in an area up to 23 nautical miles [17].

2.4.3 SBAS

An SBAS is typically comprised of three modules: a Ground Segment, which includes reference stations, processing centers, a communication network, and Navigation Land Earth Stations (NELS), a Space Segment which includes geostationary satellites, and a User Segment which consists of the user equipment. The SBAS reference stations transmit differential corrections and integrity messages for navigation satellites that are within their sight to the geostationary satellites, which in turn transmit to the user's receiver.

Currently, there are several SBAS covering several world regions: the Wide Area Augmentation System (WAAS) in the USA, the European Geostationary Navigation Overlay System (EGNOS) in the European Union, the nation-wide Canadian DGPS Service (CDGPS), the Japanese MTSAT Satellite Augmentation System (MSAS) and GPS/GLONASS and Geostationary Augmentation Navigation (GAGAN) system in India. As said earlier, EGNOS is our primary concern, since it covers all of continental Europe including Portugal [18].

2.5 GNSS Performance

The performance of a satellite navigation system is assessed by the following four criteria: Accuracy, Integrity, Continuity and Availability [19].

The accuracy of a navigation system is naturally defined as the closeness of a navigation system's positioning to its "true value". Accuracy is measured via positioning errors: the lower the errors, the more accurate the system is [19]. In RTCA requirements, accuracy is measured by the 95th percentile of the position errors during the period of study (i.e. the value which 95% of the measured errors are lower than)

The availability of a navigation system is the ability of the system to provide the required function and performance at the initiation of the intended operation. In other words, it is an indication of the ability of the system to provide usable service within the specified coverage area. Signal availability is defined as the percentage of time that navigational signals transmitted from external sources are available for use. Availability depends on the physical characteristics of the environment as well as the technical capabilities of the transmitter facilities [19].

The continuity of a system is the total system's (i.e. all elements necessary to maintain aircraft position within the defined airspace) ability to perform its function without interruption during the intended operation. Specifically, continuity is the likelihood that the specified system performance will be maintained for the duration of a phase of operation, presuming that the system was available at the beginning of that phase of operation and was predicted to operate throughout the operation [19].

Integrity is a measure of the trust which can be placed in the correctness of the information supplied by a given system. Integrity includes the ability of a system to provide timely and valid warnings to the user (alerts) when the system must not be used for the intended operation (or phase of flight). Integrity services should protect the user from GNSS satellite failure (drifting or biased pseudoranges) by detecting and excluding faulty satellites through the measurement of GNSS signals with the network of reference ground stations as well as transmission of faulty differential corrections. These faulty corrections may in turn be induced from either undetected failures in the ground segment or processing of reference data corrupted by the noise induced by the measurement and algorithmic process [19].

The concept of integrity relies on the following concepts:

● Integrity risk: the probability that the position error is higher than the alert limit defined for the intended operation and the user is not warned within the time to alert (TTA).

● Alert Limit: the error tolerance not to be exceeded without issuing an alert (ICAO SARPS definition). There is a Horizontal Alert Limit (HAL) and a Vertical Alert Limit (VAL) for each operation (i.e.: alert limits for APV-I are more demanding than for NPA).

● Protection levels:

◦ The Horizontal Protection Level (HPL) is the radius of a circle in the horizontal plane, with its center being at the true position, which describes the region which is assured to contain the indicated horizontal position;

◦ The Vertical Protection Level (VPL) is the half length of a segment on the vertical axis with its center being at the true position, which describes the region which is assured to contain the indicated vertical.

In other words, the HPL bounds the horizontal position error with a confidence level derived from the integrity risk requirement. Similarly, the VPL bounds the Vertical Position Error [19].

"Out of tolerance": The out of tolerance condition is defined as a horizontal error larger than the HPL or a vertical error larger than the VPL. Horizontal error is referred to as HPE (Horizontal Position

Error), while vertical error is referred to as VPE (Vertical Position Error). Thus, an out of tolerance event occurs when either: HPE > HPL or VPE > VPL (in absolute value). Out of tolerance events are also known as integrity events.

● Time To Alert (TTA): The maximum allowable time elapsed from the onset of the navigation system being out of tolerance until the user equipment enunciates the alert.

The ICAO Standards and Recommended Practices (SARPs) requirements of each element for each operation are detailed in the tables below [19]:

Typical operation	Accuracy horizontal 95% (Notes 1 and 3)	Accuracy vertical 95% (Notes 1 and 3)	Integrity (Note 2)	Time-to-alert (Note 3)	Continuity (Note 4)	Availability (Note 5)
En-route	3.7 km (2.0 NM) (Note 6)	N/A	$1-1\times10^{-7}$/h	5 min	$1-1\times10^{-4}$/h to $1-1\times10^{-8}$/h	0.99 to 0.99999
En-route, Terminal	0.74 km (0.4 NM)	N/A	$1-1\times10^{-7}$/h	15 s	$1-1\times10^{-4}$/h to $1-1\times10^{-8}$/h	0.99 to 0.99999
Initial approach, Intermediate approach, Non-precision approach (NPA), Departure	220 m (720 ft)	N/A	$1-1\times10^{-7}$/h	10 s	$1-1\times10^{-4}$/h to $1-1\times10^{-8}$/h	0.99 to 0.99999
Approach operations with vertical guidance (APV-I)	16.0 m (52 ft)	20 m (66 ft)	$1-2\times10^{-7}$ per approach	10 s	$1-8\times10^{-6}$ in any 15 s	0.99 to 0.99999
Approach operations with vertical guidance (APV-II)	16.0 m (52 ft)	8.0 m (26 ft)	$1-2\times10^{-7}$ per approach	6 s	$1-8\times10^{-6}$ in any 15 s	0.99 to 0.99999
Category I precision approach (Note 8)	16.0 m (52 ft)	6.0 m to 4.0 m (20 ft to 13 ft) (Note 7)	$1-2\times10^{-7}$ per approach	6 s	$1-8\times10^{-6}$ in any 15 s	0.99 to 0.99999

Table 1 – ICAO Accuracy, Integrity, Continuity and Availability requirements

The definition of the integrity requirement includes an alert limit against which the requirement can be assessed. These alert limits are:

Typical operation	Horizontal alert limit	Vertical alert limit
En-route (oceanic/continental low density)	7.4 km (4 NM)	N/A
En-route (continental)	3.7 km (2 NM)	N/A
En-route, Terminal	1.85 km (1 NM)	N/A
NPA	556 m (0.3 NM)	N/A
APV-I	40 m (130 ft)	50 m (164 ft)
APV- II	40.0 m (130 ft)	20.0 m (66 ft)
Category I precision approach	40.0 m (130 ft)	15.0 m to 10.0 m (50 ft to 33 ft)

Table 2 – ICAO Alert Limit requirements

2.6 EGNOS Overview

EGNOS was developed by European Space Agency, the European Commission and EUROCONTROL. It was designed to support the GPS, GLONASS and the Galileo system and its official start of operations was announced on 1 October 2009.

EGNOS is designed to provide three services: Open Service, Safety-of-Life Service and the EDAS (EGNOS Data Access Server).

The Open Service (OS) was launched on October 2009 and is accessible in Europe to any user equipped with an appropriate GPS/SBAS compatible receiver for which no specific certification is required. The minimum OS accuracy is around 3 m in the horizontal plane and 4 m in the vertical plane, with 99 % availability [20].

The Safety of Life (SoL) service was officially launched on 2 March 2011 and it is intended for most transport applications in different domains (aviation, maritime, terrestrial, etc.) where lives could be endangered if the performance of the navigation system were degraded below specific accuracy limits without giving notice in the specified time to alert EGNOS. As of the publication date, only the aviation domain has specific service requirements, as well as certification and individual authorization procedures developed and implemented [18].

The EGNOS Commercial Data Distribution Service (CDDS) is planned to be provided on the basis of commercial agreements between the EGNOS Service Provider and its customers. The CDSS encompasses corrections, integrity messages and raw data from all Ranging and Integrity Monitoring Stations (RIMS) all provided in real time.

2.6.1 EGNOS Architecture

Like other SBAS systems, EGNOS is comprised of two segments: the Space Segment and the Ground Segment. The two segments are shown in the following figure:

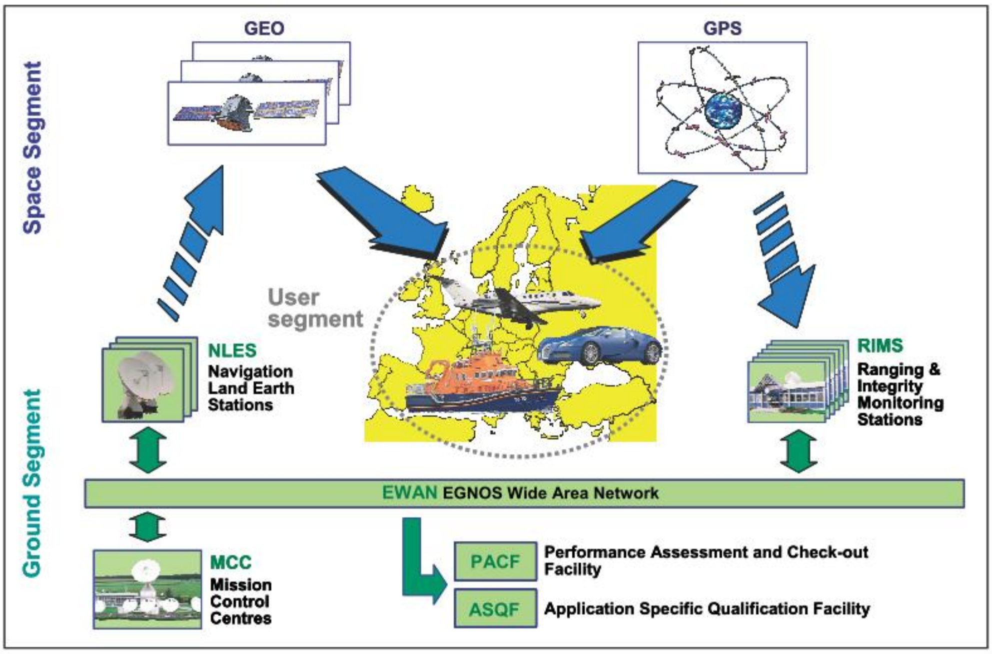

Figure 6 – EGNOS architecture [18]

The EGNOS Space Segment is comprised of 3 geosynchronous earth orbit (GEO) satellites that broadcast corrections and integrity information for GPS satellites in the L1 frequency band (1575,42 MHz). As of 2011 the 3 GEO satellites used by EGNOS are:

GEO Name	Pseudo-random Noise (PRN) Number	Orbital Slot
INMARSAT AOR-E	PRN 120	15.5 W
INMARSAT IOR-W	PRN 126	25.0 E
ARTEMIS	PRN 124	21.5 E

Table 3 – EGNOS Space Segment[17]

The space segment's configuration is designed to provide a high level of redundancy over the entire service area.

This space segment configuration provides a high level of redundancy over the whole service area in case of a geostationary satellite link failure. The EGNOS operations are handled in such a way that, at any point in time, typically two of the three GEOs broadcast an operational signal. Since it is only necessary to track a single GEO satellite link to benefit from the EGNOS SoL, this secures a switching capability in case of interruption and ensures a high level of continuity of service. It is intended that the EGNOS space segment will be replenished over time in order to maintain a similar level of redundancy. The exact orbital location of future satellites may vary, though this will not impact the service offered to users. Similarly, different PRN code numbers may be assigned to future GEOs. However, all SBAS user receivers are designed to automatically detect and use any code in a pre-allocated set reserved for SBAS. Such evolutions will therefore be transparent for end users and will not necessitate any human intervention or change of receiving equipment.

The EGNOS Ground Segment comprises a network of Ranging Integrity Monitoring Stations (RIMS), four Mission Control Centers (MCC), six Navigation Land Earth Stations (NLES), and the EGNOS Wide Area Network (EWAN) which provides the communication network for all the components of the ground segment. Two additional facilities are also deployed as part of the ground segment to support system operations and service provision, namely the Performance Assessment and Checkout Facility (PACF) and the Application Specific Qualification Facility (ASQF), which are operated by the EGNOS Service Provider, the European Satellite Services Provider SAS (ESSP SAS).

The main function of the RIMS (the locations of which are shown in Figure 8) is to collect measurements from GPS satellites and to transmit these raw data every second to the Central Processing Facilities (CPF) of each MCC. The initial configuration includes 34 RIMS sites located over a wide geographical area. In order to improve the performance of the EGNOS system and enlarge the area where the EGNOS services can be used, an extension of the monitoring network is expected soon which will see the deployment of additional RIMS in La Palma, (Spain), Athens (Greece) and Alexandria (Egypt). A further extension is also planned in a slightly longer timeframe that should improve the EGNOS performance in the southern parts of the service area.

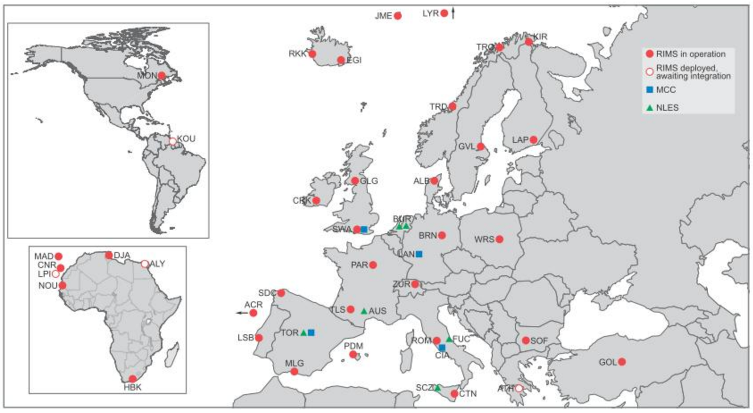

Figure 7 – Geographical distribution of the RIMS already in operation and the RIMS current under deployment [18]

The Central Processing Facility (CPF) is a module of the Mission Control Centers that uses the data received from the network of RIMS stations to:

● Elaborate clock corrections for each GPS satellite in view of the network of RIMS stations. These corrections are valid throughout the geostationary broadcast area (i.e. wherever the EGNOS signal is received);

● Elaborate ephemeris corrections to improve the accuracy of spacecraft orbital positions. In principle, these corrections are also valid throughout the geostationary broadcast area. However, due to the geographical distribution of the EGNOS ground monitoring network, the accuracy of these corrections will degrade when moving away from the core service area;

● Elaborate a model for ionospheric errors over the EGNOS service area in order to compensate for ionospheric perturbations to the navigation signals. This function requires a dense network of monitoring stations. For this reason, the ionospheric model broadcast by EGNOS is not available for the whole geostationary broadcast area but is only provided for a region centered over Europe. These three sets of corrections are then broadcast to users to improve positioning accuracy.

In addition, the CPF estimates the residual errors that can be expected by the users once they have applied the set of corrections broadcast by EGNOS. These residual errors are characterized by two parameters:

● User Differential Range Error: this is an estimate of the residual range error after the application of clock and ephemeris error correction for a given GPS satellite;

● Grid Ionospheric Vertical Error: this is an estimate of the vertical residual error after application of the ionospheric corrections for a given geographical grid point.

These two parameters can be used to determine an aggregate error bounded by the horizontal and vertical position errors. Such information is of special interest for Safety of Life users but may also be beneficial to other communities needing to know the uncertainty in the position determined by the user receiver [18] [20].

Finally, the CPF includes a large number of monitoring functions designed to detect any anomaly in GPS and in the EGNOS system itself and is able to warn users within a very short timeframe (less than 6 seconds) in case of an error exceeding a certain threshold. These monitoring functions are tailored to the Safety of Life functions and will not be further detailed in this document.

The messages elaborated by the CPF at the Master MCC are transmitted to the NLESs. The NLESs (two for each GEO for redundancy purposes) transmit the EGNOS message received by the CPF to the GEO satellites for broadcast to users and to ensure the synchronization with the GPS signal.

The EGNOS system is controlled through a Central Control Facility (CCF) located in each of the Mission Control Centers. These facilities are manned on a 24/7 basis in order to ensure permanent service monitoring and control [18] [20].

2.7 The EGNOS Signal

This section describes the structure and contents of the EGNOS signal in order to later demonstrate how this knowledge can be used to discover the cause of anomalies in collected data.

The EGNOS system transmits its messages over band L1 (1575.42 MHz) at a rate of 250 bits per second with the same modulation as GPS, but with a five times higher transmission rate. The size of the transmitted message is 250 bits, which enables one message to be transmitted per second [17].

The EGNOS Message data blocks are 250 bits long (1 second), and consist of a 8 bit preamble, a 6 bit field indicating the message type, the 212 bits message and a 24 bits Cyclic Redundancy Check (CRC). The data block format of the EGNOS message is as follows:

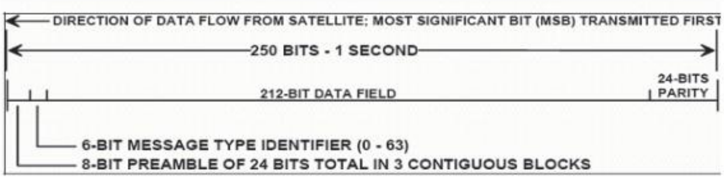

Figure 8 – EGNOS message structure [17]

The preamble is part of a 24 bit unique word distributed over three successive blocks. There are three possible preambles: 01010011, 10011010, and 11000110, which enable the initial part of the data to be synchronized during the acquisition phase. The next 6 bits identify the message type (0 to 63) followed by 212 bits that contain the useful data in the message, specific to its respective type. The last 24 bits are the parity bits, which ensure that the data was not corrupted during transmission (i.e. no bit error). The contents and purpose of each Message Type are explained in the following table (from [17]):

Message Type	Contents	Purpose
0	Don't Use (SBAS test mode)	Discard any ranging, corrections and integrity data from that PRN signal. Used also during system testing.
1	PRN Mask	Indicates the slots for GPS and GEO satellites provided data
2-5	Fast corrections	Range corrections and accuracy
6	Integrity information	Accuracy for all satellites in one message
7	Fast correction degradation factor	Information about the degradation of the fast term corrections
9	GEO ranging function parameters	EGNOS satellites orbit information (ephemeris)
10	Degradation parameters	Information about the degradation of the long term corrections
12	SBAS network Time/UTC offset parameters	Parameters for synchronisation of SBAS Network time with UTC
17	GEO satellite almanacs	GEO Almanacs
18	Ionospheric grid point masks	Indicates for which geographical point ionopheric correction data is provided
24	Mixed fast/long-term satellite error corrections	Fast-term error corrections for up to six satellites and long-term satellite error correction for one satellite in one message
25	Long-term satellite error corrections	Corrections for satellite ephemeris and clock errors for up to two satellites
26	Ionospheric delay corrections	Vertical delays/accuracy at given geographical points
27	EGNOS service message	Defines the geographic region of the service
63	Null message	Filler message if no other message is available

Table 4 – EGNOS SIS transmitted Message Types

Each GPS and EGNOS satellite has a unique pseudo-random noise (PRN) code, which makes it identifiable by the user.

Message type 1 (MT1) contains what is known as “PRN mask” data. This mask enables the size of EGNOS messages to be optimized by showing to which satellites (PRN) the data contained in the other subsequent messages are related. The mask contains 51 bits. An nth bit at 1 shows that the nth satellite is being monitored by EGNOS [17].

Bit mask	Satellite PRN
1-37	GPS PRN constellation
62-119	Glonass slot number plus 37
38-61	Future constellations
120-138	GEO/SBAS PRN
139-210	Future constellations

Table 5 – Bit mask

The table below provides an example: the PRN mask shows that EGNOS will supply in its subsequent messages corrections and integrity information for the GPS satellites whose PRN codes are 3, 5 and 7. The first correction supplied by EGNOS will correspond to PRN3, the second to PRN5, etc

Bit No.	1	2	3	4	5	6	7	…
PRN Mask	0	0	1	0	1	0	1	…
PRN Code No.			GPS PRN 3		GPS PRN 5		GPS PRN 7	

Table 6 – PRN mask

IODs are attributes of masks and of current long-term and fast corrections that allow the transmitted data and the successive updates to be handled coherently:

•IODP (Issue of Data PRN) identifies the current PRN mask;

•IODFj = IOD Fast Corrections identifies current fast corrections (j refers to the type of message (2 to 5));

•IODE = IOD Ephemeris identifies current long-term corrections;

•IODI = IOD Ionosphere identifies current ionospheric corrections.

2.7.1 Ionospheric corrections

To estimate the ionospheric error in each line of sight between the receiver and the satellite, the receiver must identify the Ionospheric Pierce Points (IPPs).

Each IPP is defined as the intersection between the atmospheric layer located at an altitude of 350 km and the line originating at the receiver's position and directed at the GPS satellite in question, as shown in Figure 10:

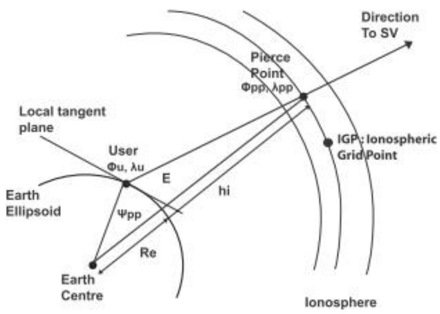

Figure 9 – Ionospheric Pierce Points [17]

The ionospheric corrections transmitted by EGNOS allow the ionospheric error to be estimated for each IPP. These ionospheric corrections are broadcast for all the points on an imaginary grid situated at an altitude of 350 km. These points are called Ionospheric Grid Points (IGPs) [17].

By knowing the position of these points and their respective estimated delay, the receiver is thus able to estimate both the ionospheric delay for each IPP and therefore each pseudorange. For that to be possible, the receiver performs an interpolation between the values provided for the IGPs close to each PP. The receiver also takes into account the angle at which the ionosphere is traversed (obliquity factor) [17].

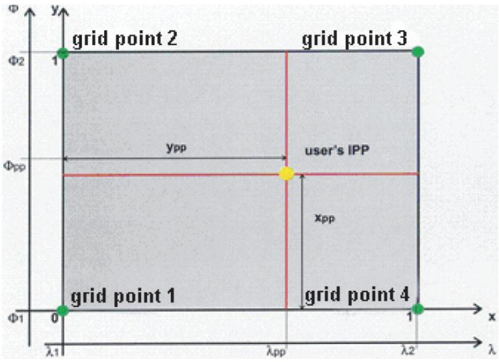

Figure 10 – IPP interpolation principle [17]

The IGP grid consists of 11 bands numbered 0 to 10 (Mercator projection). Bands 0 to 8 are vertical, and bands 9 and 10 are defined horizontally around the poles, there being a total of 1808 IGPs. The following figure shows bands 0 to 8:

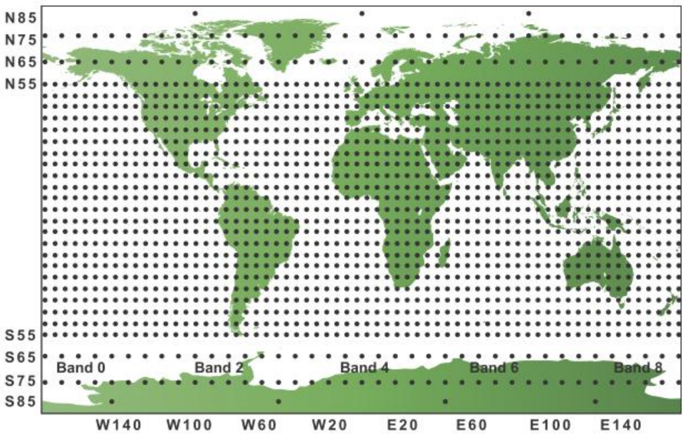

Figure 11 – IGP grid [17]

In each of the bands 0 to 8, the IGPs are numbered 1 to 201, as shown in this table:

	North								
West	28	51	78	101	128	151	178	201	East
	27	50	77	100	127	150	177	151	
	..	..	..	..	..	..	..	..	
	..	..	..	..	..	..	..	..	
	..	..	..	..	..	..	..	..	
	2	30	53	80	103	130	153	180	
	1	29	52	79	102	129	152	179	
	South								

Table 7 – IGP numbering principle

In bands 9 (North Pole) and 10 (South Pole), the IGPs are numbered 1 to 192 from West to East and by increasing latitude.

Message type 18 provides the IGP mask: Again with the aim of optimizing message size, the mask principle is applied to associate ionospheric corrections with the IGPs to which they relate. Each message contains the mask for one band. A bit positioned at 1 means that the information is provided for the corresponding IGP [17].

Type 26 messages provide, for the IGPs present in the mask, data for computing the ionospheric corrections or Grid Ionospheric Vertical Delay (GIVD) and a parameter for estimating the accuracy of corrections (σ 2GIVE), called a GIVE indicator (GIVEi).

This information can be provided for a maximum of 15 IGPs per message. As the ionospheric bands can contain up to 201 IGPs, the IGPs present in the mask are grouped into blocks of 15 IGPs. Thus, block 0 contains data for the first 15 IGPs activated in the mask and so on [17].

The σ^2_{GIVE} values are obtained through correspondence with the GIVE indicators transmitted in the message:

GIVEi	σ^2_{GIVE} (m^2)	IGP Status
0	0.0084	Use
1	0.0333	Use
2	0.0749	Use
3	0.1331	Use
4	0.2079	Use
5	0.2994	Use
6	0.4075	Use
7	0.5322	Use
8	0.6735	Use
9	0.8315	Use
10	1.1974	Use
11	1.8709	Use
12	3.3260	Use
13	20.7870	Use
14	187.0826	Use
15	Not Monitored	Not Monitored

Table 8 – GIVE Indicators

2.7.2 Long-term corrections

Long-term corrections are broadcast by EGNOS to correct long-term variations in the ephemeris errors (orbit parameters: δx,δy ,and δz) and clock errors (δa_{f0}) of the GPS satellites [17].

These corrections are provided in type 25 messages (long-term satellite error corrections).

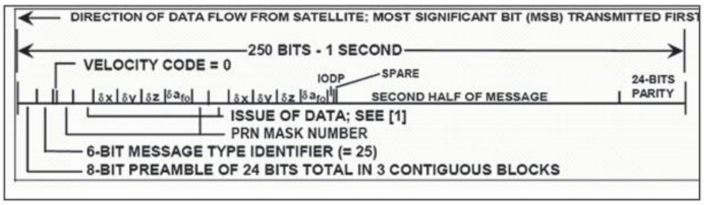

Figure 12 – Format of MT25 (long-term corrections) [17]

2.7.3 Fast corrections

Fast corrections are broadcast by EGNOS to correct rapid variations in the ephemeris errors and clock errors of the GPS satellites.

Fast corrections are provided in messages type 2 to 5. Message type 2 contains the data for the first 13 satellites of the mask that have the same IODP (Issue Of Data PRN) value, message type 3 contains data on satellites 14 to 26 of the mask that have the same IODP value and so on. If the number of satellites in the mask (or in the remaining part of the mask) is less than 6, type 2 to 5 messages can be replaced by a message type 24 [17].

The structure of type 2 to 5 messages is as follows:

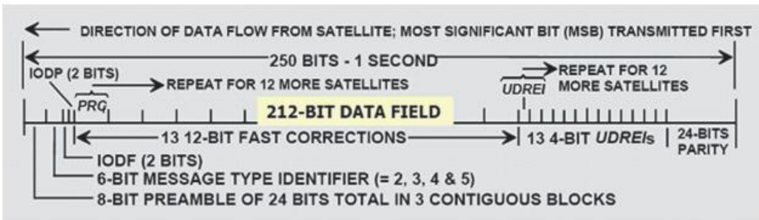

Figure 13 – Format of MT2 to 5 (fast corrections) [17]

Type 2, 3, 4 and 5 messages also contain a parameter enabling the accuracy of corrections to be estimated, known as UDRE indicators (UDREi) [17]:

UDREi	σ^2_{UDRE} (m^2)	Status of Satellite
0	0.0520	OK
1	0.0924	OK
2	0.1444	OK
3	0.2830	OK
4	0.4678	OK
5	0.8315	OK
6	1.2992	OK
7	1.8709	OK
8	2.5465	OK
9	3.3260	OK
10	5.1968	OK
11	20.7870	OK
12	230.9661	OK
13	2078.695	OK
14	N/A	Not Monitored (NM)
15	N/A	Do Not Use (DU)

Table 9 – UDRE Indicators

2.7.4 Integrity Information

EGNOS transmits, for each GPS satellite being monitored, an integrity signal with three values showing whether the status of the satellite is in keeping with use for a safety of life application (OK), an anomaly has been detected with the satellite (Do not Use – DU) or the data on the satellite are insufficient to monitor it (Not Monitored – NM) [17].

The system has 6 seconds in which to inform the user of any integrity fault, that is, no more than 6 seconds may elapse between the moment when the problem impacts the user and the moment when the alert is available to the user. The alert is repeated in the signal for 4 consecutive seconds in order to counteract any message loss [17].

Anomaly information (“Do not Use” and “Not Monitored”) is transmitted within UDRE parameters (values 14 and 15).

EGNOS also transmits for each IGP being monitored an integrity signal with three values and showing its status if an anomaly is detected or if it is not being monitored. However, the «Do not Use» alert is generated through the maximum value of the GIVD ionospheric delay, not by a particular GIVE value.

As with the satellite alerts, the system has 6 seconds in which to inform the user of any integrity fault. Again, the alert is repeated 4 times.

The parameters transmitted to estimate the accuracy of the corrections (GIVE and GIVD) enable the receiver to compute horizontal and vertical protection levels.

Generally, only receivers used for aviation purposes calculate and automatically generate protection levels. However, the entire set of parameters needed to calculate them is broadcast, in particular through type 2 to 5, 6, 24, 18 and 26 messages [17].

Message type 6 is a special case: Type 6 messages are used in two instances: to refresh UDRE indicators (UDREi) and to be able to broadcast satellite alerts very quickly if necessary (DU).

It should be pointed out that although UDREi are contained in messages 2 to 5 with the fast differential corrections, their validity period may require more frequent updating.

Similarly, if broadcasting of an alert cannot wait until the next type 2, 3, 4 or 5 message is broadcast, a message type 6 will be broadcast immediately.

A message type 6 contains integrity information on all the mask’s satellites (the maximum number of satellites in the PRN mask is 51) [17].

2.8 EGNOS Operational Evaluation

This section provides an overview of the software tools and the methodology used for the operational evaluation of EGNOS in this thesis:

2.8.1 Software

To analyze our data, two pieces of software are used: EUROCONTROL PEGASUS and DoIt.

PEGASUS Software Package

PEGASUS (Prototype EGNOS and GBAS Analysis System Using SAPPHIRE) is a prototype software program which allows analysis of GNSS data collected from different SBAS and GBAS systems using only algorithms contained in the published standards. PEGASUS has been developed in the frame of the GNSS-1 operational validation activity defined in the EUROCONTROL SBAS project with the aim of becoming a first step towards the development of a standard processing and analysis tool for future EGNOS operational validation.

PEGASUS was designed to automate the GNSS Data processing process in a customizable way, log the different data processing activity in order to keep traceability of the process and to find a data & results storage solution allowing the combination and the easy access to all the data. PEGASUS has been validated against the RTCA DO-229 Minimum Operational Performance Standards (MOPS) [21].

With PEGASUS it is possible to create data processing jobs, with three different slots to be configured: scenario (list of data processing tasks to be run in sequence), processing parameters (list of parameters customizing the data processing), and the location of the input file (data to be processed).

It is also important to note that the data analysis is open and fully documented. Access to all processing steps allows extrapolation to future CAT III systems by adapting monitoring algorithms and performing error simulations, thereby contributing to the development of detailed performance and interface descriptions at ICAO and European level.

DoIt Program Package

DoIt is a program comprised of a series of Windows batch files designed to automate the use of PEGASUS to analyze data and create reports in a convenient .pdf format. However, it can only be used to analyse real data since virtual data requires heavy manipulation that is not automated at this time.

2.8.2 Hardware

EGNOS static real data is collected via three hardware elements: an antenna, a compatible receiver and a computer that treats the received data with PEGASUS (listed in software) at the rate of 1Hz. As part of the activities undertaken for EGNOS Signal-In-Space Validation, EUROCONTROL established the EGNOS Data Collection Network (EDCN) in 2001 [22]. The EDCN consists of a series of monitor stations each comprised of the aforementioned 3 elements set up across Europe by European Navigation Service Providers as well as European universities, including IST.

2.9 EGNOS Certification

2.9.1 Overview

In order for EGNOS to provide Safety of Life services to aviation it must first be *certified*. The EGNOS certification process can be described as “the demonstration and authorization that the EGNOS system, service provision and equipment, are acceptable in order that EGNOS can be made available for safety critical operations by airspace users”. Certification involves many of EGNOS’s areas, including user equipment on-board, service provision, system design, operations and procedures [23].

The Europe-wide process requires the involvement of several actors and certification bodies:

• GSA - coordinates the certification process;

• European Space Agency (ESA) - EGNOS design authority and in charge of procuring the system development and operations;

• European Organization for the Safety of Air Navigation (EUROCONTROL) - provides support to the operational introduction of EGNOS into civil aviation;

• ICAO - Issues international standards for aviation;

• National supervisory authority (NSA) - responsible to deliver certificates for service providers under the Single European Sky regulation;

• Air Navigation Service Providers (ANSPs) - national organizations responsible for air traffic service provision;

• European Aviation Safety Agency (EASA) - certification body for receiver equipment;

• EGNOS Service provider - responsible to operate the system and provide Safety of Life services [23].

The certification process itself is done on a number of different levels:

• Demonstrating that the system is fit for purpose (i.e, meeting ICAO SARPS);

• Certifying an EGNOS service provider;

• Certifying EGNOS equipment;

• Authorizing the operational use of EGNOS applications for civil aviation.

The approach for the first two items is to follow the framework established by the EC Single European Sky (SES) – namely regulation for service provision and interoperability. The Single European Sky is an initiative to reform the architecture of air traffic control in the European Union in order to meet future capacity and safety need. As the name suggests, SES seeks to organize air space and air navigation at a European level, as opposed to a local level [24]. Technologies like GALILEO and EGNOS are thus key in providing improvements in efficiency and safety of air travel.

EGNOS receiver equipment must meet applicable international receiver standards. As the following table shows, each level of certification involves the presentation of solid evidence to the appropriate authority:

	Regulation	**Evidence**	**Certifying Body**
System Certification	Compliance with SES interoperability regulation 552/2004 essential requirements	Technical file and declaration to be issued. Main part of technical file is an EGNOS Safety Case demonstrating compliance to ICAO SARPS	Submitted to NSA in charge
Service Provider Certification	Compliance with SES service regulation 550/2004 & 2096/ 2005 requirements for Communication Navigation & Surveillance providers (CN&S)	Demonstration of compliance with regulatory requirements Work based on qualification exercise managed by ESA	Application to NSA in charge
Operational Approval for EGNOS Applications	National regulations	Application safety cases for specific operation and airspace prepared by national Air Navigation Service Providers (ANSPs)	Submitted by each ANSP to national regulators (NSA)
Receiver Certification	Technical Standard Orders and Minimum Operational Performance Standards (MOPS) for Satellite Based Augmentation System (SBAS) Receivers	Demonstration of compliance to standards through aviation to certification body	EASA provides type approval after submission of design documents by manufactures

Table 10 – EGNOS Certification

In the Civil Aviation domain, the European Commission's regulations for the Single European Sky provide the rules for the EGNOS Certification for civil aviation. In this frame, the following Regulations are considered of interest for the EGNOS services provision. Such regulations are in place; their applicability for the European GNSS components is foreseen to be supervised and supported by the European GNSS Supervisory Authority (GSA).

According to the EC Regulation (EC/549/2004), laying down the framework for the creation of Single European Sky (the "Framework Regulation"), in addition to the designated Air Traffic Service providers, a navigation services provider can be individually certified. The following articles are of interest:

- Regulation (EC) No 549/2004, Article 2.4. 'air navigation services' means air traffic services; communication, navigation and surveillance services; meteorological services for air navigation; and aeronautical information services [25];
- Reg.549/2004, Article 2.5. 'air navigation service providers' means any public or private entity providing air navigation services for general air traffic [25].

Such definitions are applicable to the GNSS services, then such regulation, and the following derived for the same frame, are applicable to the GNSS case.

The EC Regulation 550/2004 on the provision of the Air Navigation Services in the Single European Sky (the "Service Provision Regulation") is applicable for the certification of the EGNOS operating entity as Service Provider [26]. According to such regulation, the EGNOS operating entity apply to the National Supervisory Authority of the Country where his principal place of business is located. Then the NSA, supported by a Notified Body if the case, release the "certification of conformity" to the Common requirements [27] for the Navigation service provision of the EGNOS operating entity. Such certificate shows the capability to operate and control the configuration of the system according to the ICAO standards [28].

Finally, the EC Regulation 552/2004 about the interoperability of the European Air Traffic Management network (the "Interoperability regulation") require the achieved performance and safety requirements to be documented [29]. On this purpose, the European GNSS certified service provider issues to his NSA a "declaration of verification", together with a technical file, which confirm the compliance to the implementing rules for interoperability in order to make the system be integrated in the European Air Traffic Management Network (EATMN); such implementing rules could need to be specifically issued for the GNSS. Such "declaration of verification" contains also the "declaration of conformity" or "suitability use" of the system constituents to the implementing rules.

Important inputs for the preparation of the technical file for the "declaration of verification" are the EGNOS Safety Cases. The EGNOS System Safety Case has been developed by ESA and will be updated with each new ESR. During the Initial Operations Phase, ESSP is working on the development of the EGNOS Operation Safety Case, which will be maintained throughout the system's life time.

The challenges and issues to be tackled with regards to EGNOS certification are the following:

- Clarification of the service provision organizational scenario;
- Designation of the authority and responsibility;
- Provider's certification by the competent National Supervisory Agency supported by notified body/ies;
- Clarification of liability issues;
- Issues linked to the complexity and number of different actors involved;
- Necessary time scales for the certification process.

To be certified as a Navigation Service Provider, EGNOS requires the demonstration of compliance with the many requirements placed on providers through the SES regulation. The EGNOS service provider will need to demonstrate to the NSA in charge that it meets a set of common requirements covering:

- Technical and operational competence and suitability;
- Adequate safety and quality management systems;
- Security;
- Reporting systems;
- Quality of services;
- Appropriate liability and insurance cover;
- Organization structure;
- Prevention of conflicts of interest;
- Human resources plans.

3 Analysis of EGNOS Real Data

This chapter explains the necessary steps to evaluate real receiver data as well as provide an example of said evaluation.

The receiver used for the collection of real data used in this thesis is called IST4. Said station is comprised of a Septentrio PolaRx2 Prototype L1/L2 receiver with version 2.70 firmware, a Septentrio PolaNt L1/L2 antenna located at Lisbon Airport, specifically at coordinates 38º 47’ 20.46672’,’ -9º 07’ 48.94063’’, 160.070m.

3.1 Procedure

To process real data with DoIt, the following steps must be taken:

1. Create a folder in your main drive marked “Data”. If the drive doesn’t named “C:/” then alter the line “set DoIt_rootdisk=c:” in DoIt.bat.
2. Inside the “Data” folder create a folder with the 4 character receiver acronym (e.g. IST4).
3. Inside the receiver folder create another folder named “XXYYY” with XX and YYY being the last two digits of the year and the number of the day the data was collected respectively.
4. Create a new .bat file and write the line “call DoIt [arg1] [arg2] [arg3] [arg4] [arg 5]”, the arguments being as follows:
    a. Arg1 is the Receiver name 4 character acronym e.g. IST4.
    b. Arg2 is the SBAS PRN number e.g. 120 | 124 | 126 | all |
    c. Arg3 is the FTP flag (FTP|NOFTP). If the flag is FTP, then the results will be uploaded to an FTP server.
    d. Arg4 is the day offset (-2= two days ago, -1=yesterday, 0=today, +1=tomorrow, etc).
    e. Arg5 is the reference date: format yyyymmdd. If the argument is not given, it assumes that the reference date is the current date.
5. Run the .bat file.
6. Analyze the generated graphics.

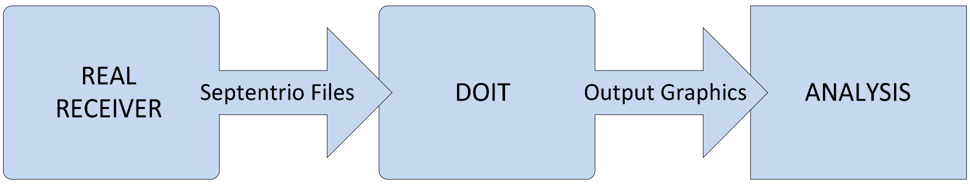

Figure 14 – Real Data Analysis Procedure

The average processing time for the static evaluation of real station data can be quite extensive, typically taking one hour for a single satellite and 3 hours for all of them in a mid-range computer (2.6 Ghz Dual core processor). Raw data for a complete day typically occupies about 400 MB of disk space while processed data takes up around 700 MB.

Combining a real GPS receiver that automatically uploads its data to a server combined with DoIt allows for EGNOS performance data to be analyzed and stored in an entirely automated fashion. By having the receiver upload the data in intervals of 24 hours followed by running DoIt and storing the respective reports a continuous monitoring of EGNOS performance can be achieved. However it is still possible that over the course of reviewing this data that unexpected results may happen. We will see how to deal with that situation in a later section.

3.2 DoIt Outputs

Once a Septentrio file is processed by DoIt, it automatically organizes the output with a certain folder structure: outputs are placed in DoIt/Data/Processed and organized by date, via nested folders separating the data by calendar year (YXXX), month (MXX), day (DXX_YYY where XX is the calendar day and YYY is the day number) and receiver. An example is shown in the following figure:

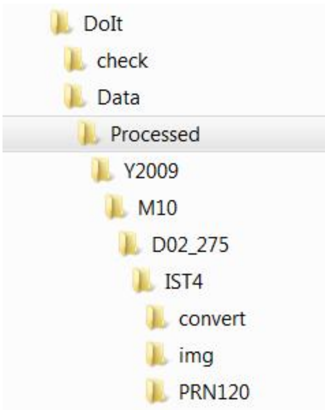

Figure 15 – DoIt folder structure example

The receiver folder contains the following:

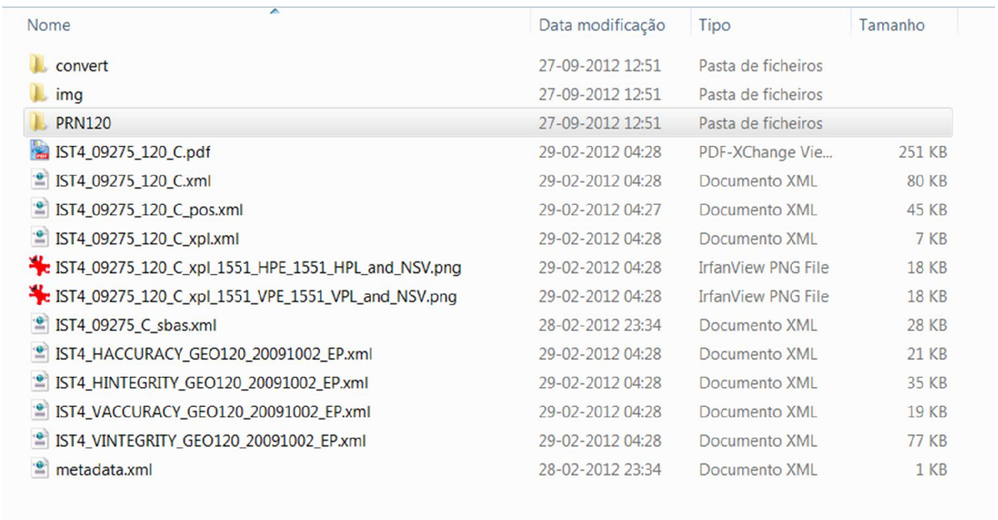

Figure 16 – DoIt receiver folder

DoIt generates a report with the statistics and graphics shown earlier in PDF format under the name “XXXX_YYYYY_ZZZ_C.pdf”, where XXXX is the name of the receiver, YYYYY is the same date format used to name the folder and ZZZ is the PRN number. The data used for the report is stored in the XML file of the same name. This file can be examined to obtain the data if the PDF report is not generated. The “convert” folder shows the output of the PEGASUS Convertor model, the “img” folder contains the report graphics in image format and the “PRN 120/124/126” folder contains the output of the PEGASUS GNSS Solution module after processing the .rng file of the “convert” folder for the satellite in question.

3.3 Real Receiver Evaluation

EGNOS’ performance will now be evaluated for two sets of IST4 data: the data received during 16 of October 2009 at 00:00 until 23:59 and the data received during 15 of January 2012 00:00 until 23:59 by the IST4 real station. While the exact day and month were arbitrarily chosen to provide this example, the years are significant since the data collected during 2009 was used to evaluate EGNOS for certification. 2012 data was also chosen to demonstrate the EGNOS evaluation procedure.

3.3.1 IST4 16 of October 2009

After following the steps detailed in section 4.1 with the 2009 data, the graphs shown in this section are generated. The graphs displaying the Horizontal and Vertical Position Errors (HPE and VPE), the Horizontal and Vertical Protection Levels (HPL and VPL) and the Number of Satellites in View (NSV) are shown in the following figures:

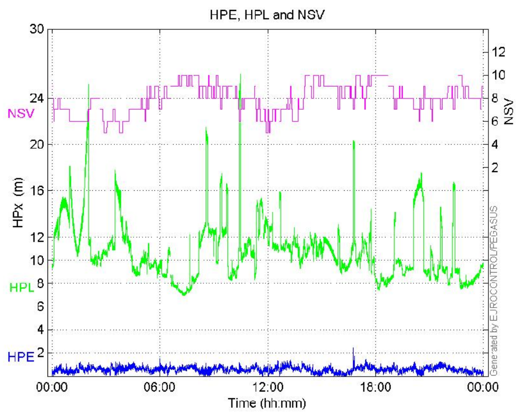

Figure 17 – HPE, HPL and NSV Timeplot for IST4 16 of October 2009 PRN120

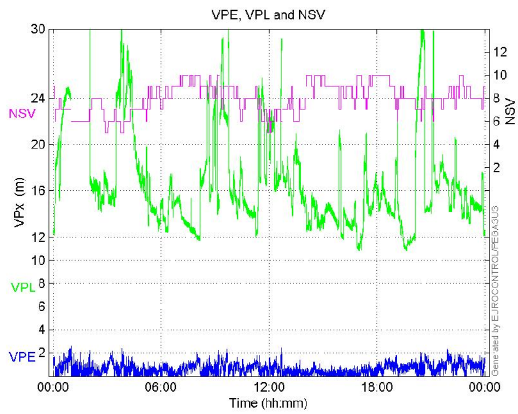

Figure 18 – VPE, VPL and NSV Timeplot for IST4 16 of October 2009 PRN120

As the figures show, the position errors both remained low and below their protection levels at all times, meaning no integrity events occurred. It can also be verified that Protection Level is correlated with the number of visible satellites: as NSV increases, the protection level decreases.

The following figure shows a scatter plot displaying the horizontal deviation from reference in the North and East coordinates (the closer the samples are of the origin, the better):

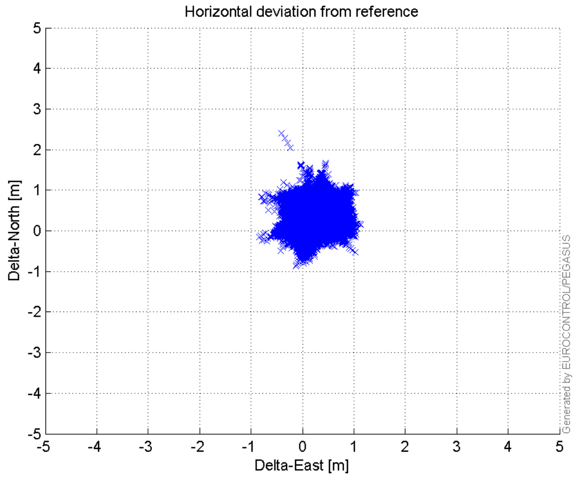

Figure 19 – Horizontal Deviation From Reference for IST4 16 of October 2009 PRN120

This graph shows that the horizontal error mostly remained below 2 meters apart from a few outliers. You can also see that the errors are mostly clustered around a point North and East of the actual origin. This is also seen in many other readings on IST4, as demonstrated further ahead, meaning there's some sort of systematic bias. This error is not due to bad placement of the antenna, since exhaustive measures were put in place to ensure the minimization of error in its location. Therefore, it can be concluded that this bias is due to IST4's position relative to the EGNOS satellites: since Portugal is located near the West and South most edge of the EGNOS coverage area and the EGNOS satellites are located near the center of Europe, then the latter's corrections will naturally be skewed towards the location of the satellites.

PEGASUS (and by extension DoIt, via the former) are capable of generating Stanford Plots, in which the Position Errors and Protection Levels are sorted according to whether they fulfill the requirements of APV-I, APV-II or CAT-I, according to the criteria shown in the following two figures:

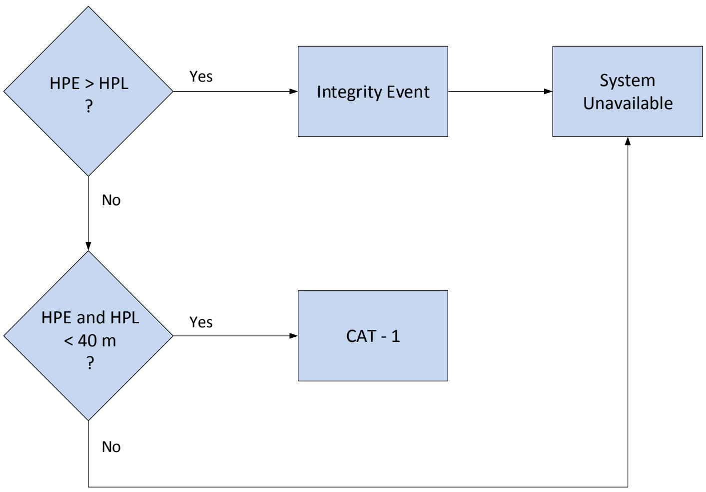

Figure 20 – Horizontal Stanford Graph Generation

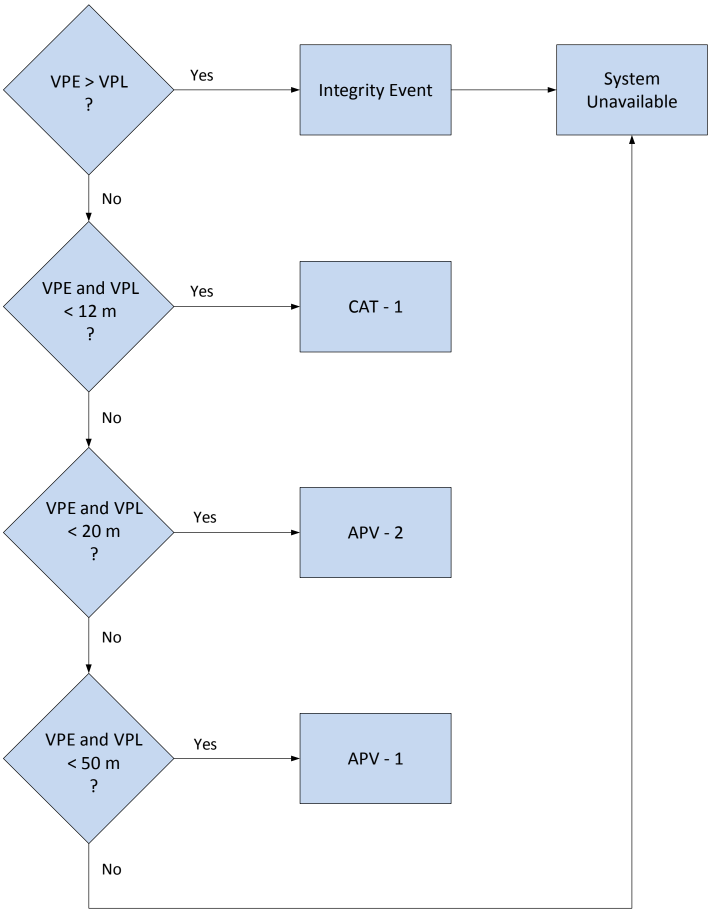

Figure 21 – Vertical Stanford Graph Generation

The Stanford Plots for this particular set of data are shown here:

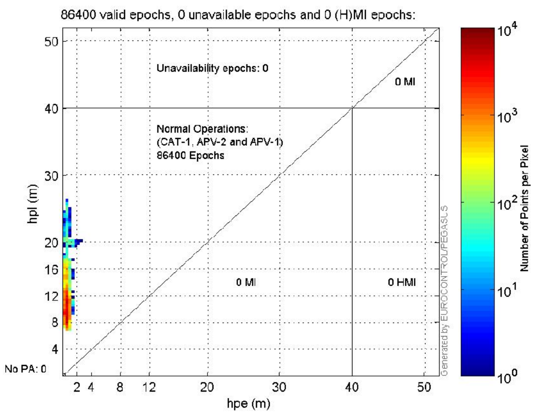

Figure 22 – Horizontal Stanford Plot for IST4 16 of October 2009 PRN120

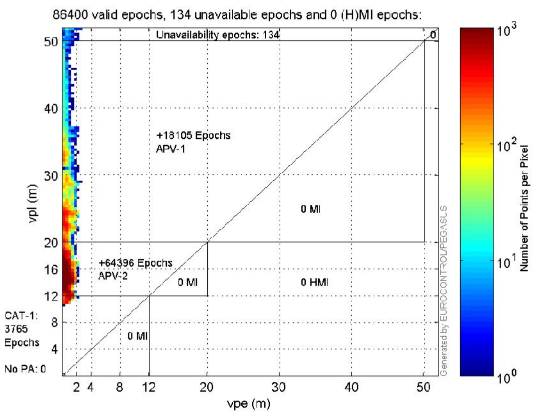

Figure 23 – Vertical Stanford Plot for IST4 16 of October 2009 PRN120

The Stanford plots show that the vast majority of samples fulfilled APV-I requirements or better, with only 134 epochs (corresponding to 134 seconds) having EGNOS completely unavailable.

The following figures show the generated histograms displaying the distribution of the Horizontal and Vertical position errors and protection levels:

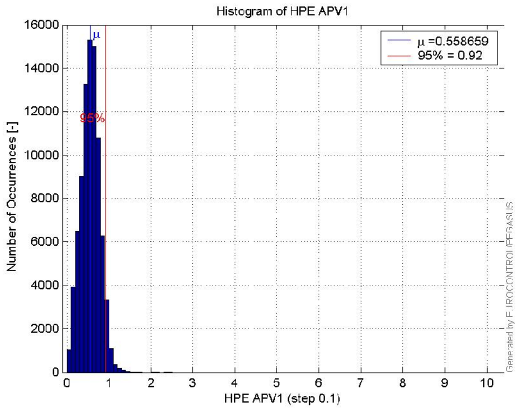

Figure 24 – HPE Histogram for IST4 16 of October 2009 PRN120

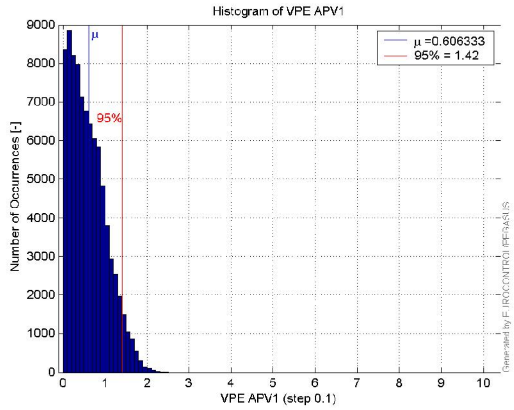

Figure 25 – VPE Histogram for IST4 16 of October 2009 PRN120

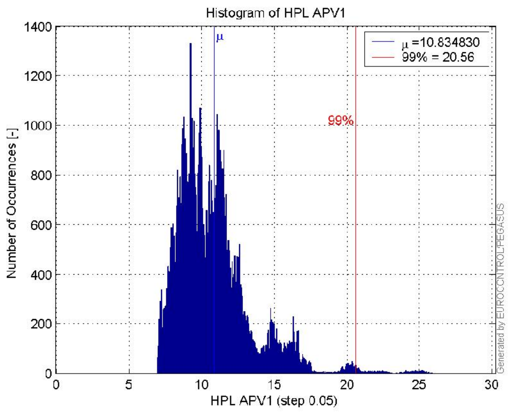

Figure 26 – HPL Histogram for IST4 16 of October 2009 PRN120

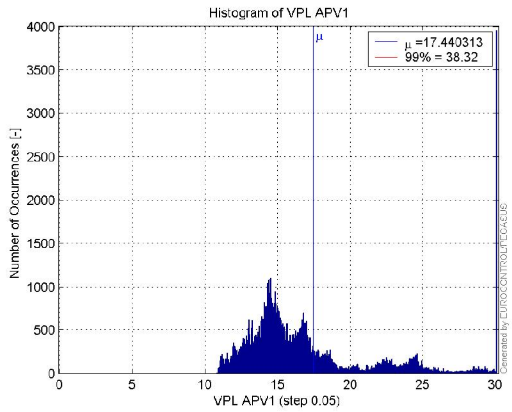

Figure 27 – VPL Histogram for IST4 16 of October 2009 PRN120

The position error histograms show that on average, the error was below 0.6m. The red line shows the 95th percentile of the obtained data: this value is significant since, as mentioned in section 2.4, the ICAO SARPs use the 95th percentile to determine the accuracy requirements of each operation. The 95th percentile horizontal error requirement for APV-I, APV-II and CAT-I is 16.0 m while the vertical error requirement is 20 m, 8.0 m and 6.0 to 4.0 m for APV-I, APV-II and CAT-I respectively.

These protection level graphics show that the latter overall remained about 10 m in the horizontal plane and 15 in the vertical plane. However, the 99th percentiles for VPL remained above the maximum for APV-II (20.0 m).

DoIt also generates a PDF report in which we obtain the following statistics:

Protection level statistics	
	99%
HPL	20.56
VPL	38.32

Table 11 – Protection Level Statistics for IST4 16 of October 2009 PRN120

Position error statistics	
	95%
HPE	0.92
VPE	1.42

Table 12 – Position Error Statistics for IST4 16 of October 2009 PRN120

Availability			
	APV-I	APV-II	CAT-I
Minimum Required	99%	99%	NA
Availability	99.845%	78.89%	4.358%
Estimated Availability	99.89%	84.76%	-

Table 13 – Availability Statistics for IST4 16 of October 2009 PRN120

These tables support the graphs shown earlier: In both the horizontal and vertical case, the position error remains below two meters. We further find that CAT-I was only achieved for a short time and that the APV-II availability requirements weren't met by over 15% but that APV-I conditions were maintained throughout the day.

The graphics for the PRN 124 satellite will now be shown:

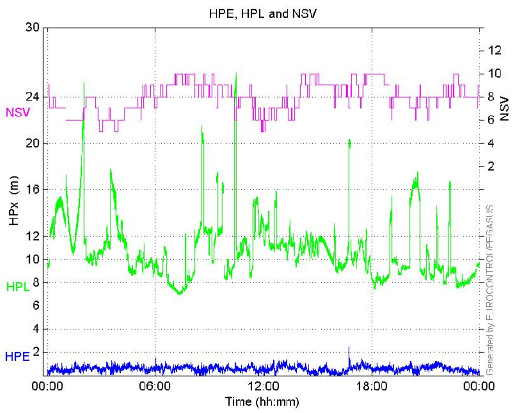

Figure 28 – HPE, HPL and NSV Timeplot for IST4 16 of October 2009 PRN124

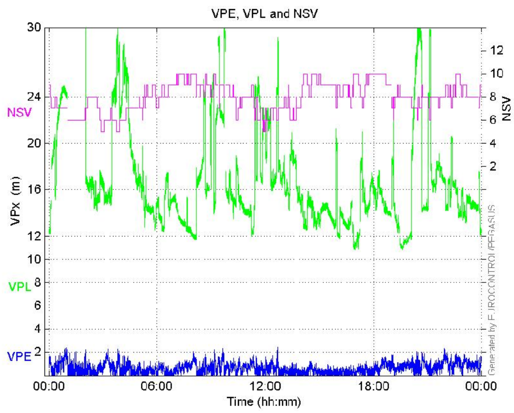

Figure 29 – VPE, VPL and NSV Timeplot for IST4 16 of October 2009 PRN124

The Position Error and Protection Level graphics are similar to those found for PRN 120. No integrity events occurred and the error remained mostly below 2 meters in both the vertical and horizontal plane.

As the following graphic shows, the horizontal deviation remained below 2 meters apart from 4 outliers:

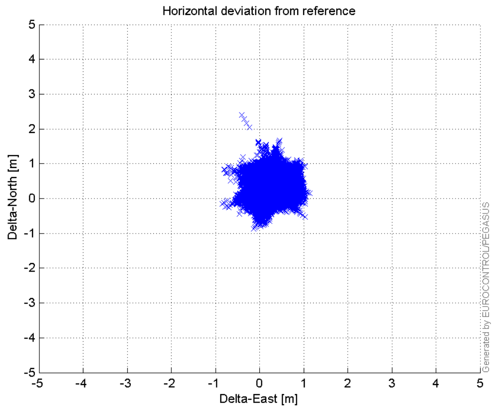

Figure 30 – Horizontal Deviation From Reference for IST4 16 of October 2009 PRN124

The Stanford Plots show that apart from a total of 125 seconds, APV-I or matter was maintained throughout the day:

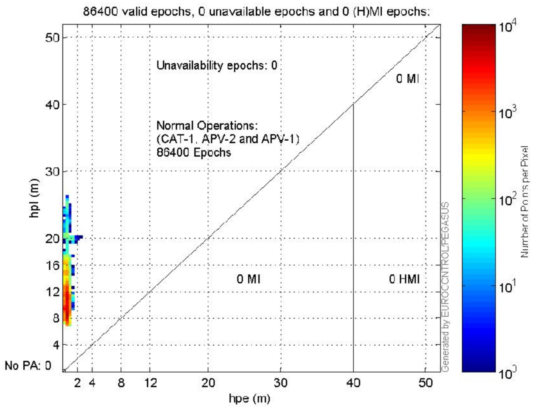

Figure 31 – Horizontal Stanford Plot for IST4 16 of October 2009 PRN124

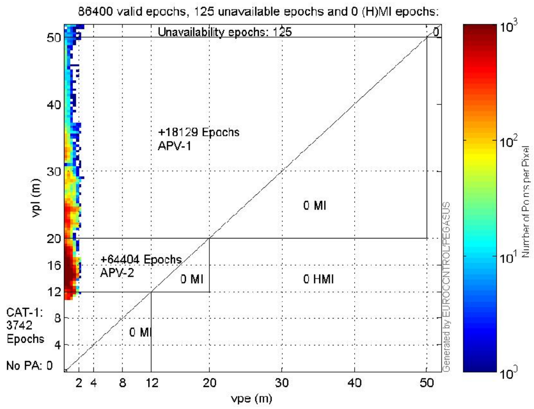

Figure 32 – Vertical Stanford Plot for IST4 16 of October 2009 PRN124

Examining the generated XML file provides the following data:

Protection level statistics	
	99%
HPL	20.55
VPL	38.45

Table 14 – Protection Level Statistics for IST4 16 of October 2009 PRN124

Position error statistics	
	95%
HPE	0.92
VPE	1.43

Table 15 – Position Error Statistics for IST4 16 of October 2009 PRN124

Availability			
	APV-I	APV-II	CAT-I
Minimum Required	99%	99%	NA
Availability	99.86%	78.87%	4.331%
Estimated Availability	99.9%	84.75%	-

Table 16 – Availability Statistics for IST4 16 of October 2009 PRN124

Once again, APV-I requirements were met and performance was nearly identical to the one verified with the PRN 120 satellite.

Position Error and Protection Level distribution also remained similar as the following graphics show:

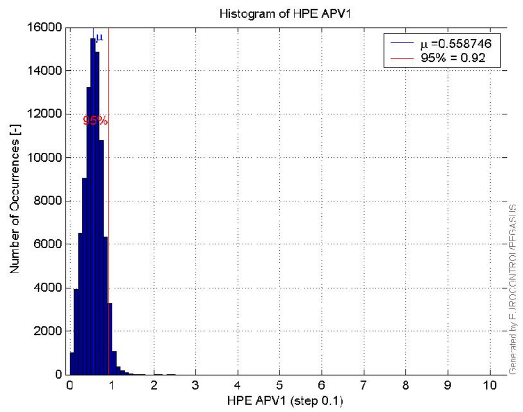

Figure 33 – HPE Histogram for IST4 16 of October 2009 PRN124

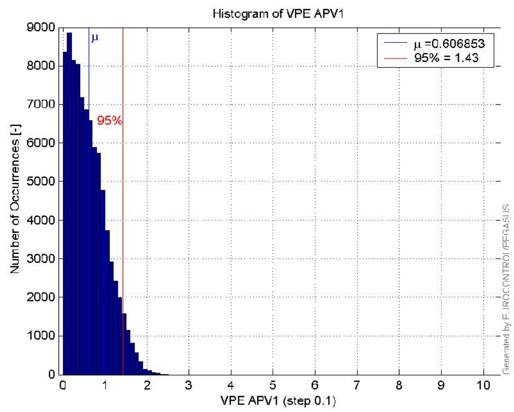

Figure 34 – VPE Histogram for IST4 16 of October 2009 PRN124

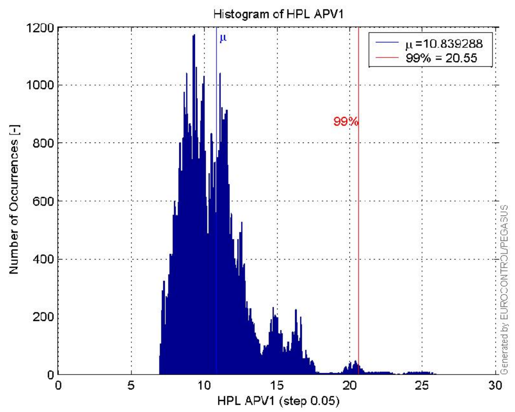

Figure 35 – HPL Histogram for IST4 16 of October 2009 PRN124

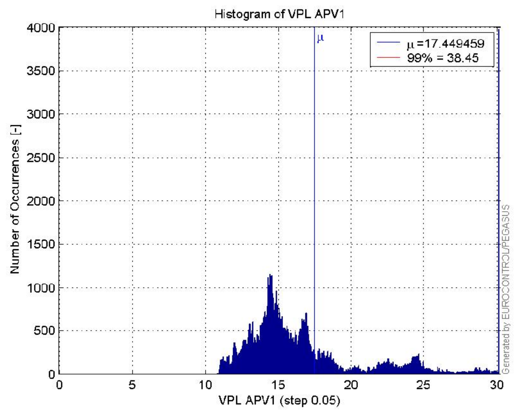

Figure 36 – VPL Histogram for IST4 16 of October 2009 PRN124

Finally, the PRN 126 data is examined:

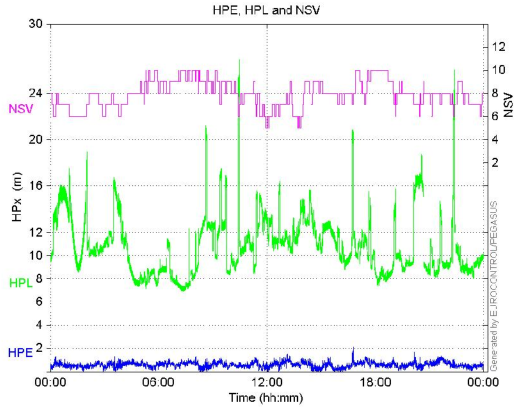

Figure 37 – HPE, HPL and NSV Timeplot for IST4 16 of October 2009 PRN126

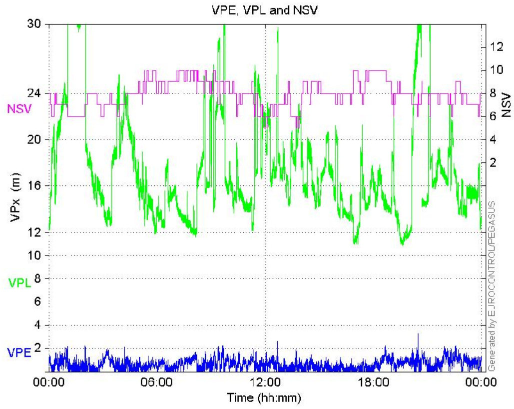

Figure 38 – VPE, VPL and NSV Timeplot for IST4 16 of October 2009 PRN126

Horizontal deviation has also remained below the previous seen amounts (2 meters):

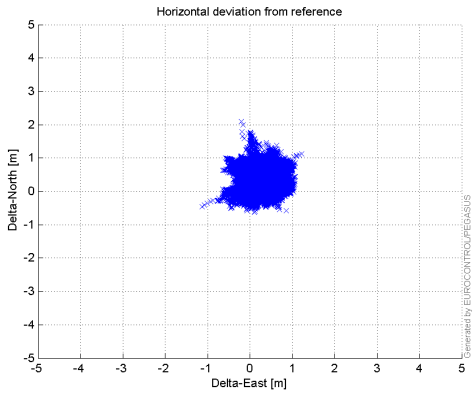

Figure 39 – Horizontal Deviation From Reference for IST4 16 of October 2009 PRN126

The Stanford Plots show that APV-I was actually maintained for 100% of samples:

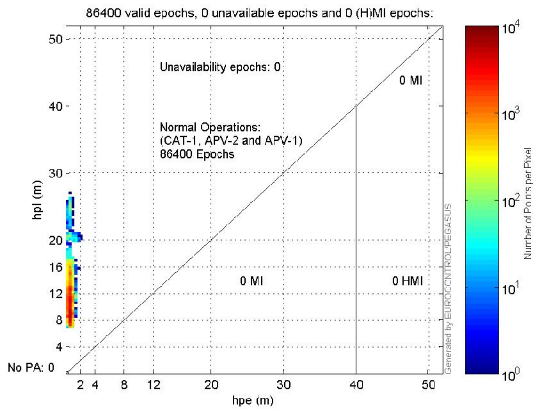

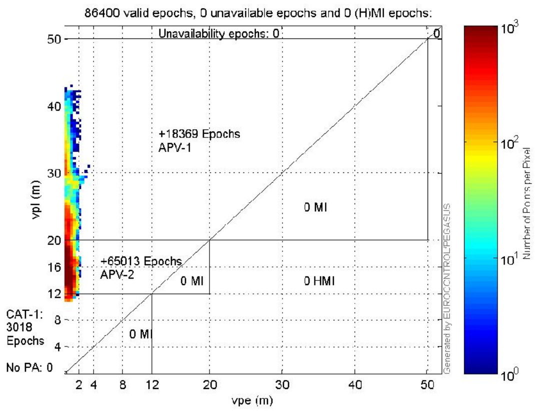

Figure 40 – Horizontal Stanford Plot for IST4 16 of October 2009 PRN126

Figure 41 – Vertical Stanford Plot for IST4 16 of October 2009 PRN126

This is supported by the data seen in the XML file:

Protection level statistics	
	99%
HPL	20.52
VPL	35.75

Table 17 – Protection Level Statistics for IST4 16 of October 2009 PRN126

Position error statistics	
	95%
HPE	0.94
VPE	1.39

Table 18 – Position Error Statistics for IST4 16 of October 2009 PRN126

Availability			
	APV-I	APV-II	CAT-I
Minimum Required	99%	99%	NA
Availability	100%	78.74%	3.493%
Estimated Availability	100%	85.51%	-

Table 19 – Availability Statistics for IST4 16 of October 2009 PRN126

Once again, Position Error and Protection Level distribution is very similar to the previous two satellites as both the preceding and following graphics show:

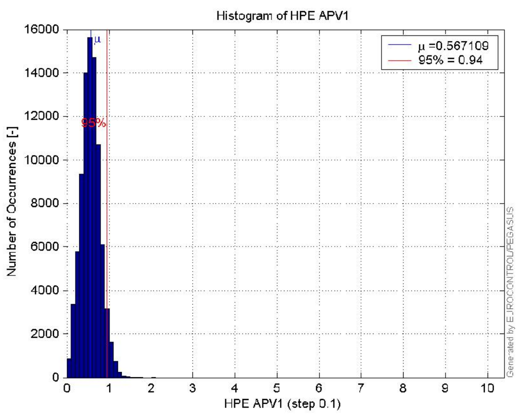

Figure 42 – HPE Histogram for IST4 16 of October 2009 PRN126

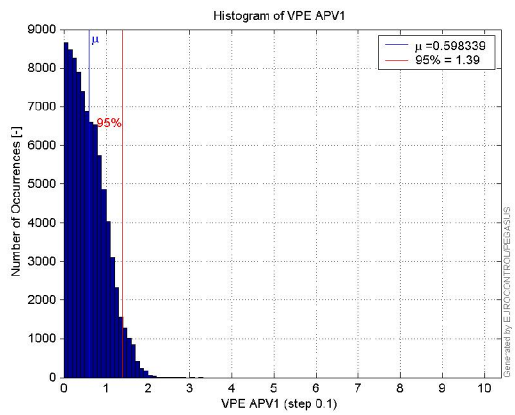

Figure 43 – HPE Histogram for IST4 16 of October 2009 PRN126

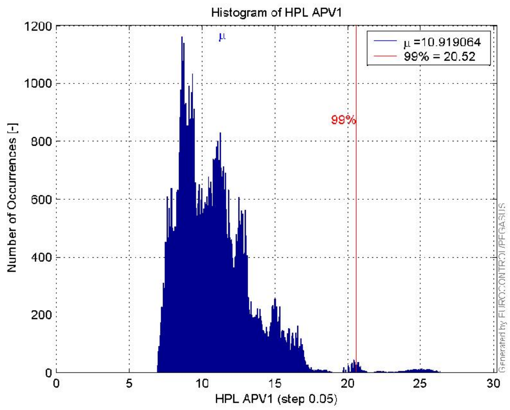

Figure 44 – HPL Histogram for IST4 16 of October 2009 PRN126

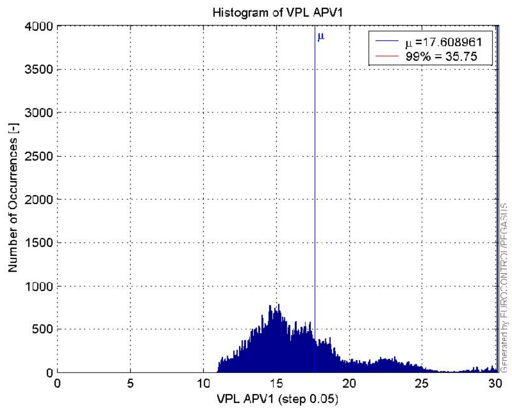

Figure 45 – VPL Histogram for IST4 16 of October 2009 PRN126

Once again the Protection Level and Position Error values are similar to the ones provided by the previous 2 satellites. However, in PRN 126, APV-I was maintained throughout the entire 24 hour period, though APV-II was maintained though less time.

It can be concluded by this date's data that performance stayed consistent between PRN 120, PRN 124 and PRN 126. This is an important result since if any of the satellites suffers some sort of outage, the others can provide redundancy.

3.3.2 IST4 15 of January 2012

The same analysis is now performed for the 2012 data (after the certification year). Once again, graphs showing the Position Error, Protection Level and Number of Satellites Viewed are generated:

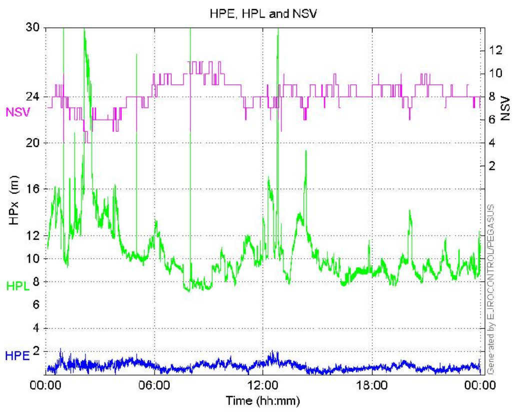

Figure 46 – HPE, HPL and NSV Timeplot for IST4 15 of January 2012 PRN120

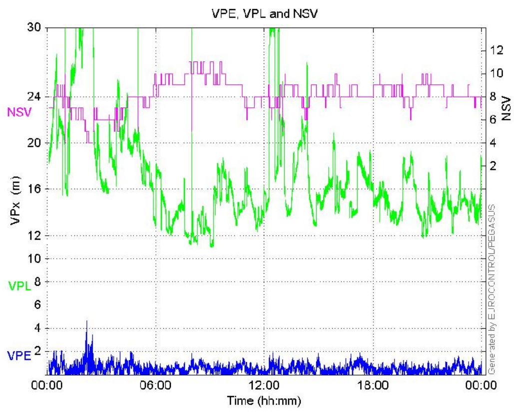

Figure 47 – VPE, VPL and NSV Timeplot for IST4 15 of January 2012 PRN120

As in the 2009 data, no integrity events occurred.

The figure below shows the Horizontal deviation from the reference position for the 2012 data samples:

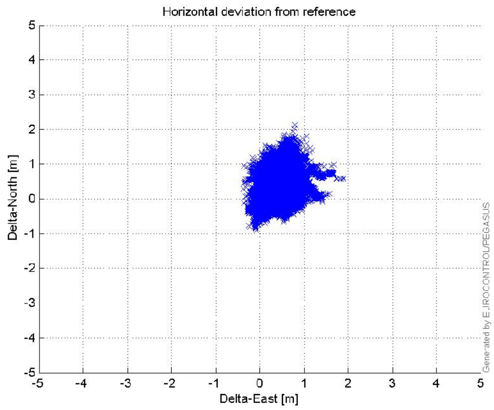

Figure 48 – Horizontal Deviation from reference for IST4 15 of January 2012 PRN120

This graphic shows that the horizontal error has mostly remained below 1 meter.

The generated Horizontal and Vertical Stanford Plots are shown here:

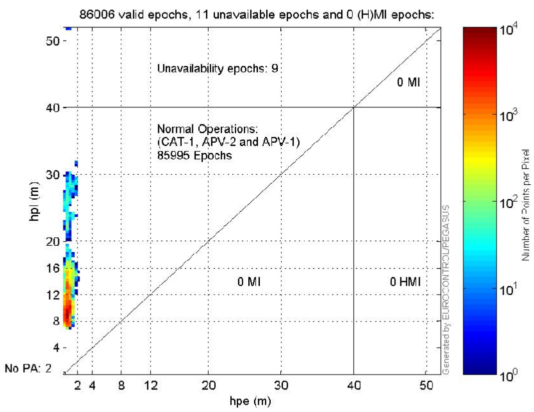

Figure 49 – Horizontal Stanford Plot for IST4 15 of January 2012 PRN120

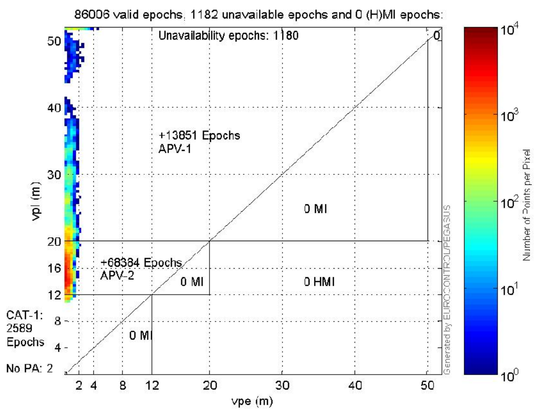

Figure 50 – Vertical Stanford Plot for IST4 15 of January 2012 PRN120

These plots show that there were more unavailable epochs that in the 2009 data, meaning that overall APV-I may not have been achieved. To verify this, we turn to the generated XML data:

Protection level statistics	
	99%
HPL	18.10
VPL	34.08

Table 20 – Protection Level Statistics for IST4 15 of January 2012 PRN120

Position error statistics	
	95%
HPE	1.17
VPE	1.12

Table 21 – Position Error Statistics for IST4 15 of January 2012 PRN120

Availability			
	APV-I	APV-II	CAT-I
Minimum Required	99%	99%	NA
Availability	98.62%	82.52%	3.010%
Estimated Availability	98.48%	86.4%	-

Table 22 – Availability Statistics for IST4 15 of January 2012 PRN120

These tables show that the position error is somewhat larger in the vertical plane than in the corresponding 2009 data. We also discover that there is slightly lower availability for APV-II and that APV-I requirements aren't met, albeit by a very small margin. However, the Protection Levels are overall lower.

The following figures show the Protection Level distribution histograms for the 2012 data:

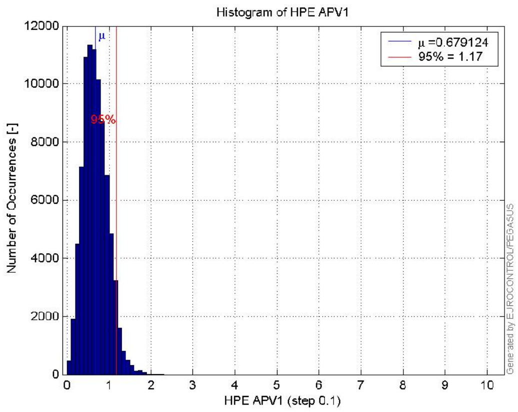

Figure 51 – HPE Histogram for IST4 15 of January 2012 PRN120

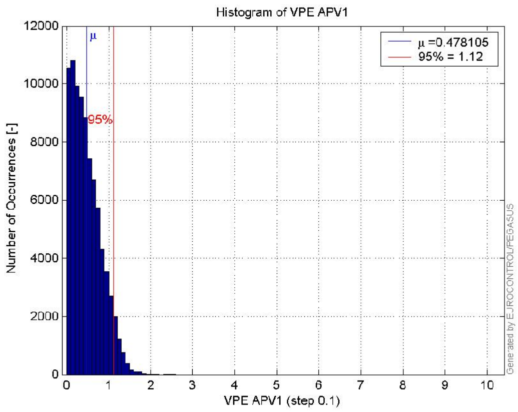

Figure 52 – VPE Histogram for IST4 15 of January 2012 PRN120

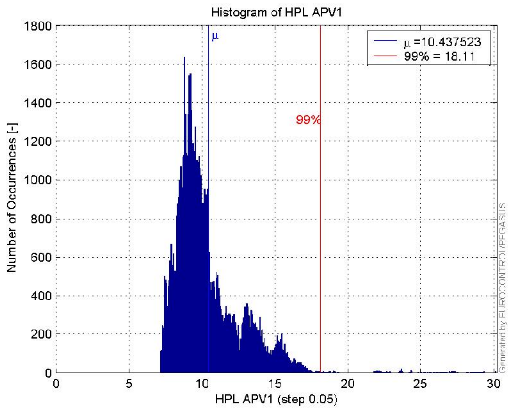

Figure 53 – HPL Histogram for IST4 15 of January 2012 PRN120

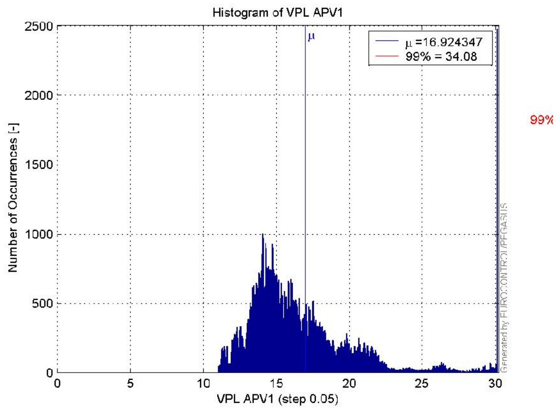

Figure 54 – VPL Histogram for IST4 15 of January 2012 PRN120

Similar to the previous data, the horizontal protection level is mostly around the 10 meter range. The vertical protection level however, is more spread, especially in the 15-20 meter range.

The PRN 124 data is now examined, starting with the Position Error and Protection Level graphs:

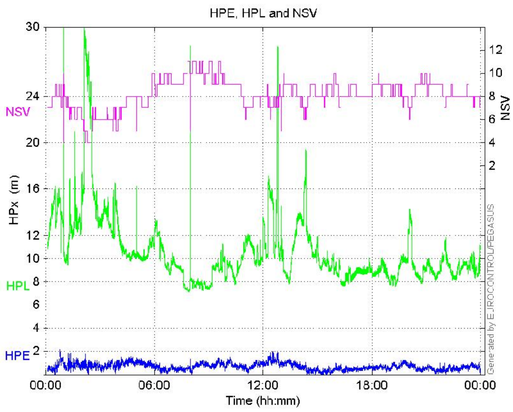

Figure 55 – HPE, HPL and NSV Timeplot for IST4 15 of January 2012 PRN124

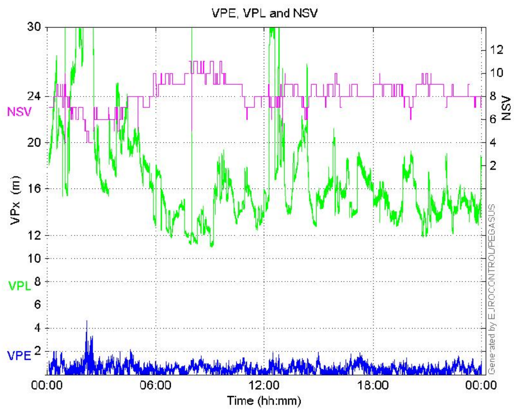

Figure 56 – VPE, VPL and NSV Timeplot for IST4 15 of January 2012 PRN124

As it can be seen above, the graphics are nearly identical to the ones for PRN 120.

Horizontal deviation also remained below 2 meters, as seen in the following figure:

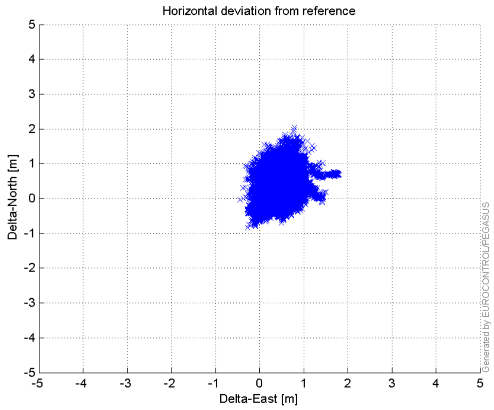

Figure 57 – Horizontal Deviation from reference for IST4 15 of January 2012 PRN124

The Stanford Plots also show similar results though PRN 124 has slightly less (23 to be exact) unavailable epochs in the horizontal plane:

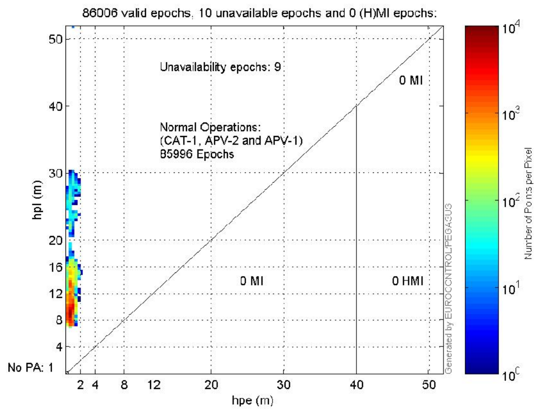

Figure 58 – Horizontal Stanford Plot for IST4 15 of January 2012 PRN124

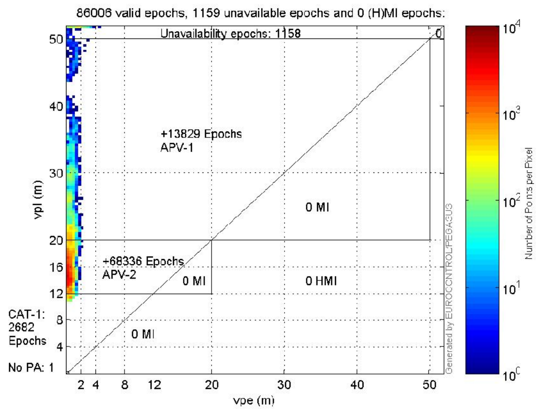

Figure 59 – Vertical Stanford Plot for IST4 15 of January 2012 PRN124

Examining the XML files provides the following data:

Protection level statistics	
	99%
HPL	17.29
VPL	34.01

Table 23 – Protection Level Statistics for IST4 15 of January 2012 PRN124

Position error statistics	
	95%
HPE	1.17
VPE	1.12

Table 24 – Position Error Statistics for IST4 15 of January 2012 PRN124

Availability			
	APV-I	APV-II	CAT-I
Minimum Required	99%	99%	NA
Availability	98.65%	82.57%	3.118%
Estimated Availability	98.5%	86.54%	-

Table 25 – Availability Statistics for IST4 15 of January 2012 PRN124

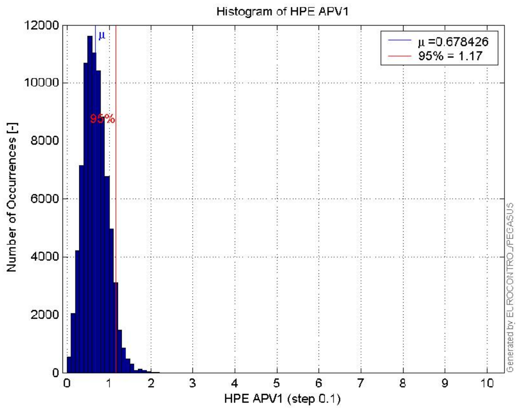

Figure 60 – HPE Histogram for IST4 15 of January 2012 PRN124

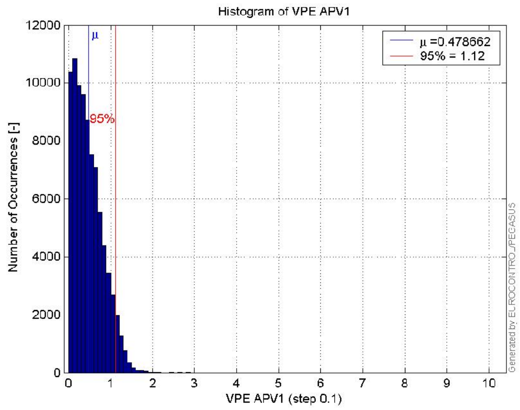

Figure 61 – VPE Histogram for IST4 15 of January 2012 PRN124

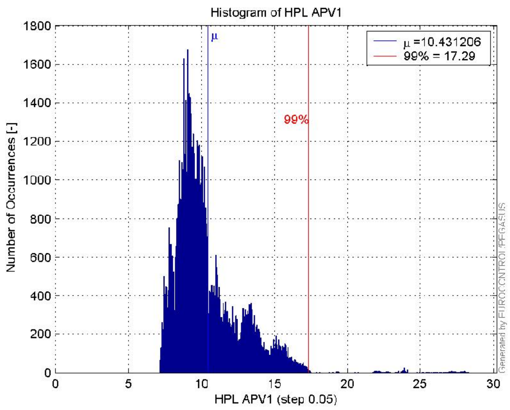

Figure 62 – HPL Histogram for IST4 15 of January 2012 PRN124

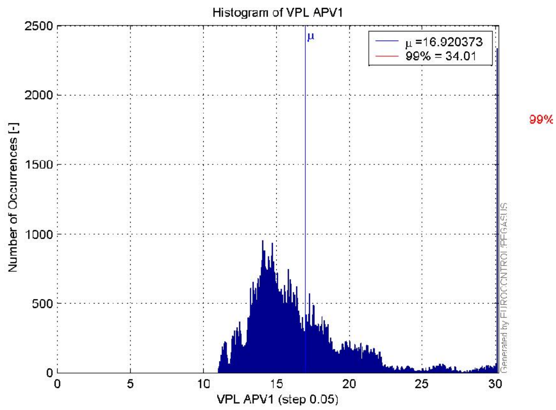

Figure 63 – VPL Histogram for IST4 15 of January 2012 PRN124

Finally, the PRN 126 data is examined:

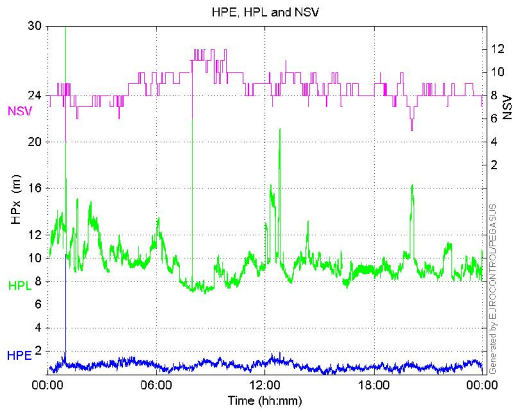

Figure 64 – HPE, HPL and NSV Timeplot for IST4 15 of January 2012 PRN126

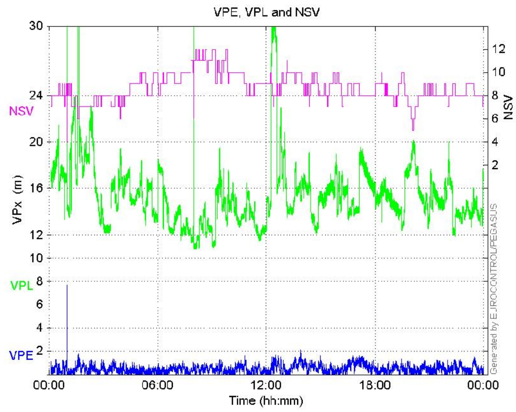

Figure 65 – VPE, VPL and NSV Timeplot for IST4 15 of January 2012 PRN126

As the graphics show, the Protection Levels showed multiple outliers and the Position Error showed one (over 10 meters in the horizontal plane and nearly 8 in the vertical plane).

Horizontal deviation also remained similar apart from the aforementioned outliers:

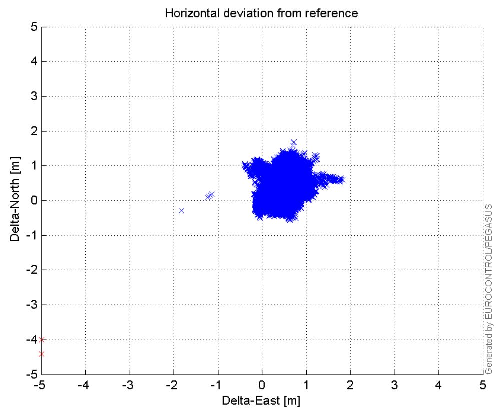

Figure 66 – Horizontal Deviation from reference for IST4 15 of January 2012 PRN126

The Stanford Plots show substantial improvement compared to the PRN 120 and 124: as seen below, samples became more concentrated around the APV-2 area and only 7 epochs were unavailable:

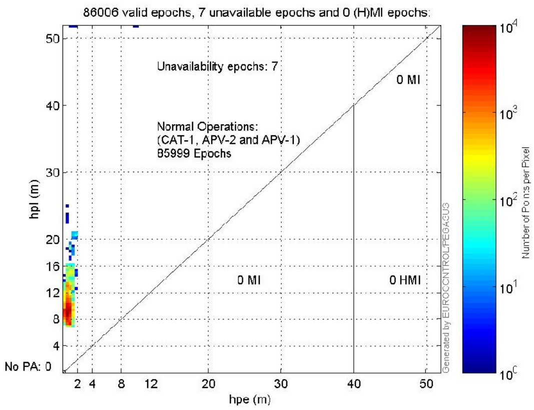

Figure 67 – Horizontal Stanford Plot for IST4 15 of January 2012 PRN126

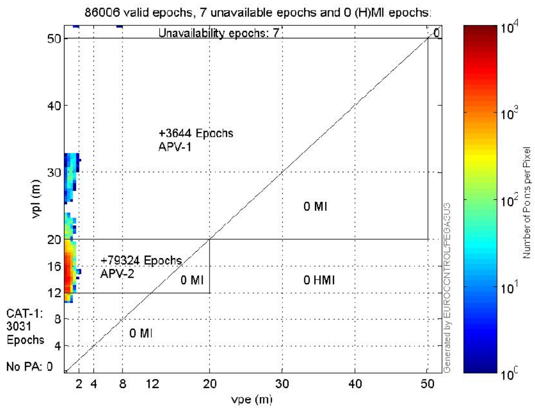

Figure 68 – Vertical Stanford Plot for IST4 15 of January 2012 PRN126

Examining the XML file confirms that availability is much higher than seen in PRN 120 and 124:

Protection level statistics	
	99%
HPL	15.48
VPL	29.46

Table 26 – Protection Level Statistics for IST4 15 of January 2012 PRN126

Position error statistics	
	95%
HPE	1.19
VPE	1.08

Table 27 – Position Error Statistics for IST4 15 of January 2012 PRN126

Availability			
	APV-I	APV-II	CAT-I
Minimum Required	99%	99%	NA
Availability	99.99%	95.75%	3.524%
Estimated Availability	99.82%	96.64%	-

Table 28 – Availability Statistics for IST4 15 of January 2012 PRN126

Unlike earlier results, here PRN 126 managed to provide considerably better performance than PRN 120 and 124, allowing for APV-I to be met throughout the day. Both Protection Levels and Position Errors were lower as well. Overall, while PRN 120 and 124 showed worse performance than in the 2009 data, PRN 126 showed higher performance, thus allowing APV-I to be met during this date.

PE and PL distribution is similar to the other two satellites, which is supported by the following histograms:

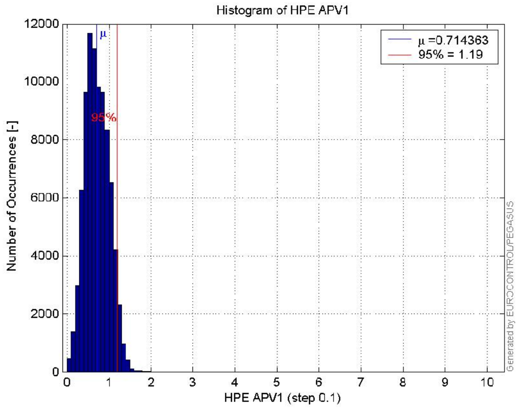

Figure 69 – HPE Histogram for IST4 15 of January 2012 PRN126

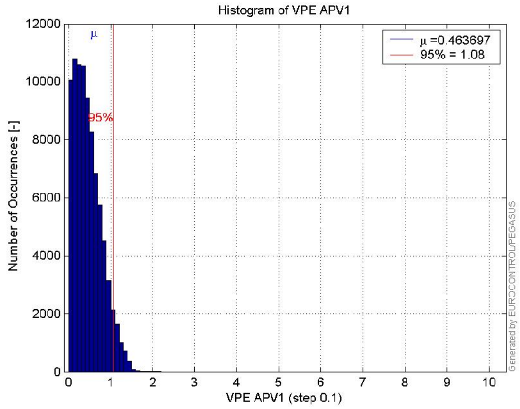

Figure 70 – VPE Histogram for IST4 15 of January 2012 PRN126

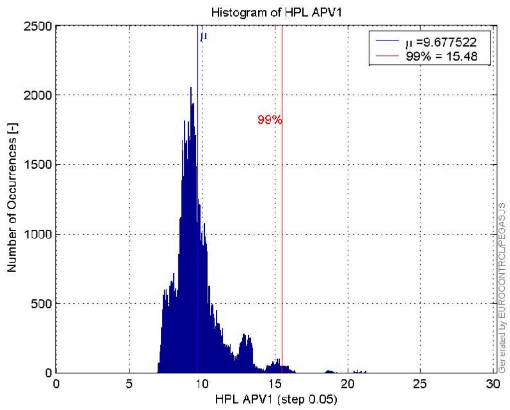

Figure 71 – HPL Histogram for IST4 15 of January 2012 PRN126

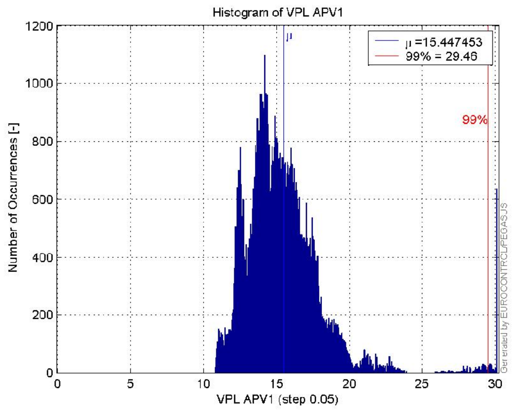

Figure 72 – VPL Histogram for IST4 15 of January 2012 PRN126

Overall, EGNOS performance was worse during the 2012 data than the 2009 date. This is likely due to work being performed on the RIMS in preparation for the extension of the EGNOS operation area due in February 2012 [30].

4 Analysis of Data Anomalies

This section will demonstrate how knowledge of the inner workings of EGNOS (namely its message structure) coupled with PEGASUS can be used to determine the cause of anomalies in collected data.

4.1 January 23rd 2012 Occurrence

On January 23rd 2012, the data collected from the PRN 120 and PRN 124 satellites on IST4 exhibited some unusually high position errors with rapid temporal variation during the first 6 hours of the day, with said errors being especially pronounced in the vertical plane. However, PRN 126 wasn't affected, as the following graphs show:

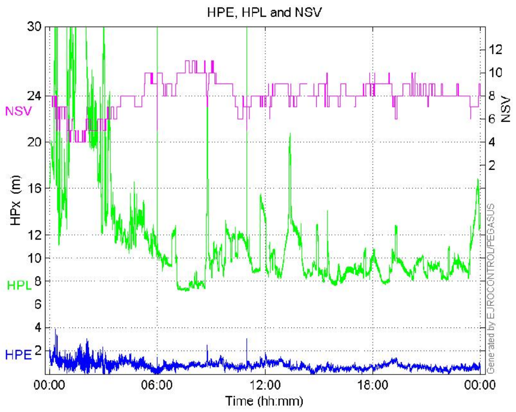

Figure 73 – Horizontal Evaluation Data for IST4 in January 23rd 2012 PRN 120

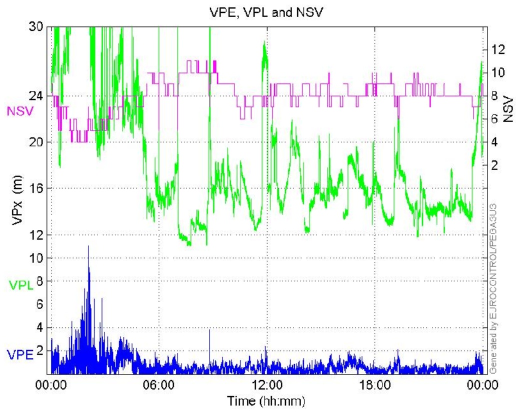

Figure 74 – Vertical Evaluation Data for IST4 in January 23rd 2012 PRN 120

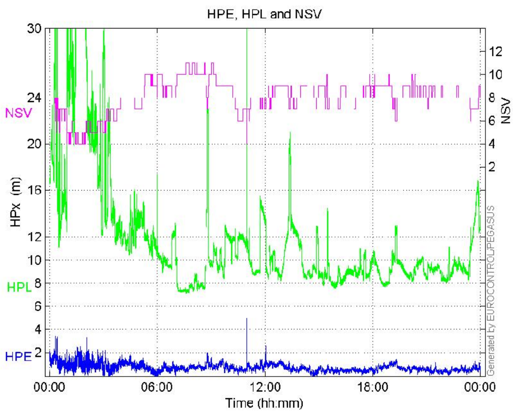

Figure 75 – Horizontal Evaluation Data for IST4 in January 23rd 2012 PRN 124

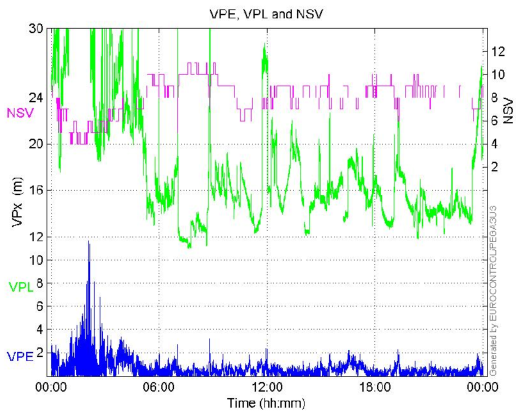

Figure 76 – Vertical Evaluation Data for IST4 in January 23rd 2012 PRN 124

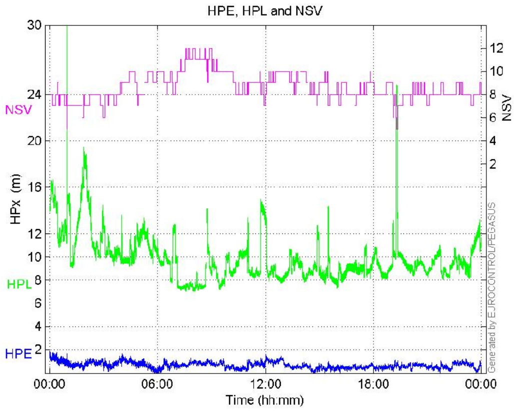

Figure 77 – Horizontal Evaluation Data for IST4 in January 23rd 2012 PRN 126

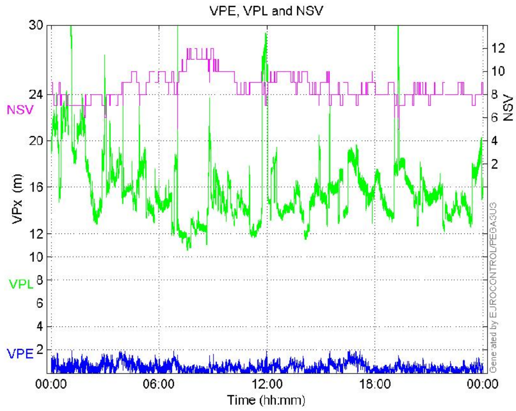

Figure 78 – Vertical Evaluation Data for IST4 in January 23rd 2012 PRN 126

Using the File Watch module, we can take a closer look at the measured position for the first few hours of the day, when the anomaly occurred. Performance usually stays consistent between all three (PRN 120, PRN 124 and PRN 126). Thus if there is any substantial difference, that means there is some problem with the satellite. If the anomaly is consistent across all three then the problem must be related to reception or some other factor:

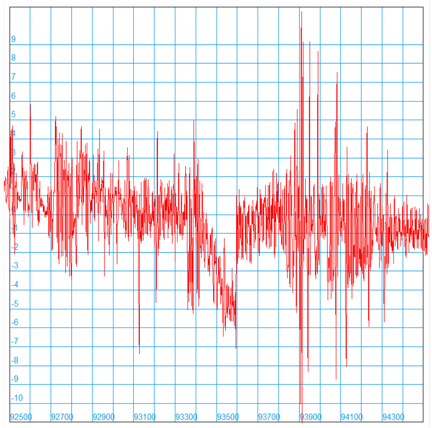

Figure 79 – Vertical Position Error for IST4 from 01:41 to 02:13 of January 23rd 2012 PRN 120

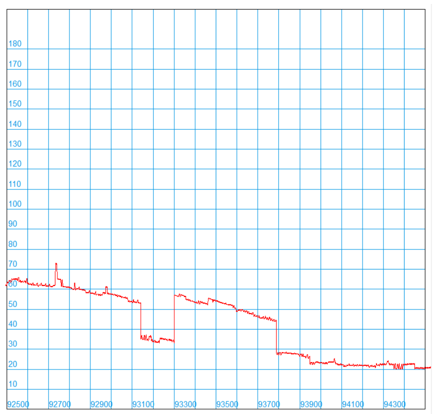

Figure 80 – Horizontal Protection Level for IST4 from 01:41 to 02:13 of January 23rd 2012 PRN 120

Figure 81 –Vertical Protection Level for IST4 from 01:41 to 02:13 of January 23rd 2012 PRN 120

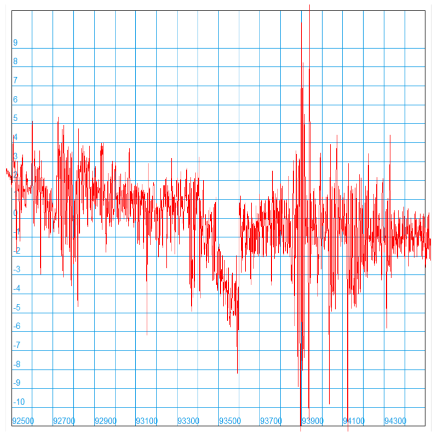

Figure 82 – Vertical Position Error for IST4 from 01:41 to 02:13 of January 23rd 2012 PRN 124

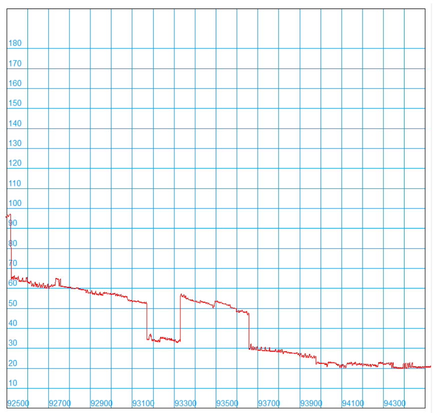

Figure 83 – Vertical Protection Level for IST4 from 01:41 to 02:13 of January 23rd 2012 PRN 124

Figure 84 – Horizontal Protection Level for IST4 from 01:41 to 02:13 of January 23rd 2012 PRN 124

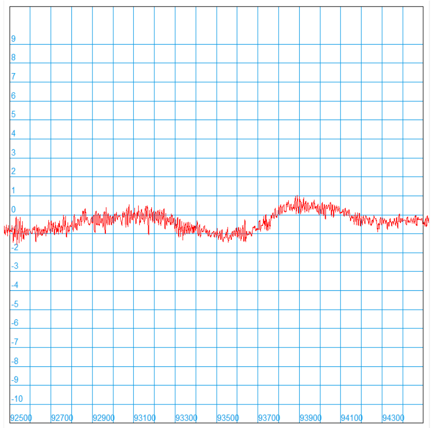

Figure 85 – Vertical Position Error for IST4 from 01:41 to 02:13 of January 23rd 2012 PRN 126

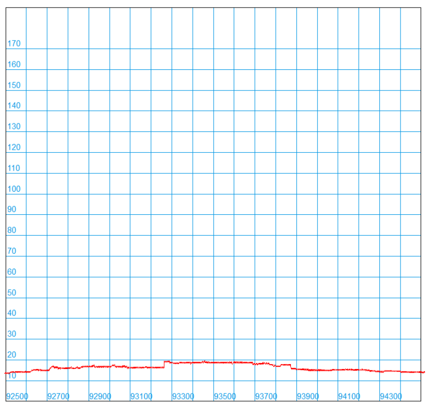

Figure 86 – Horizontal Protection Level for IST4 from 01:41 to 02:13 of January 23rd 2012 PRN 126

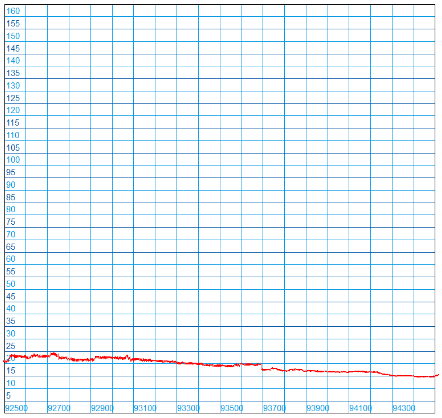

Figure 87 – Vertical Protection Level for IST4 from 01:41 to 02:13 of January 23rd 2012 PRN 126

As we can see, the PRN 120 and PRN 124 position data had much greater variations than that of PRN 126. Therefore, the problem must be related to the satellites and its cause will now be determined.

In order to investigate the causes behind this occurrence, PEGASUS' File Watch module will be used to analyze the EGNOS data for that day. After examining each of the generated files with the program, a data anomaly was found in the generated .sfc file, which contains the data corresponding to EGNOS' fast corrections. This anomaly was found by using the Filter function of File Watch module to examine the message types and the PRN one by one. After inspection, a discrepancy was noted in PRC values for Type 4: the values of the corrections were very high in PRN 120 and 124 but non existent in 126:

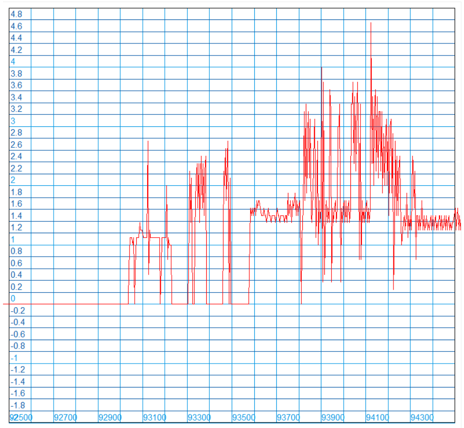

Figure 88 – PRC 01 values for PRN=120 AND TYPE=4 filter on January 23rd 2012

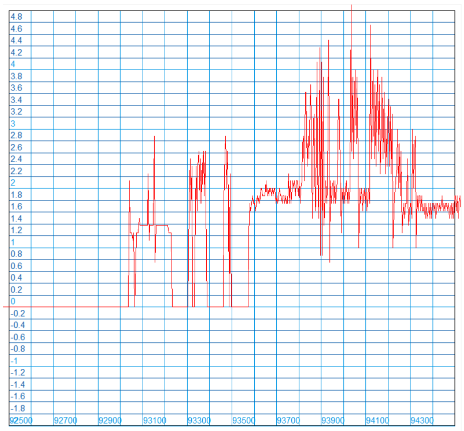

Figure 89 – PRC 01 values for PRN=124 AND TYPE=4 filter on January 23rd 2012

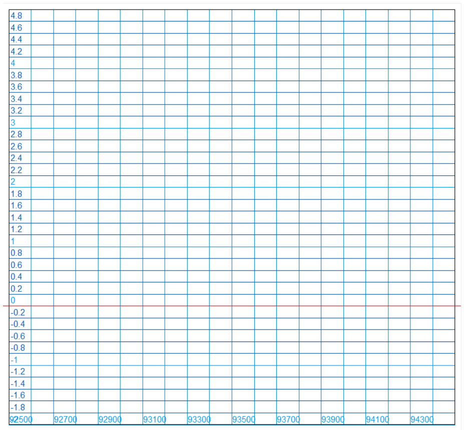

Figure 90 – PRC 01 values for PRN=126 AND TYPE=4 filter on January 23rd 2012

Examining these graphs leads us to the conclusion that the problem is in Message Type 4. Message concerns GPS satellites PRN27 through PRN37. Using the GNSS Solution module of PEGASUS, we can remove data from individual GPS satellites using the "Advanced" options in the "Parameters" screen:

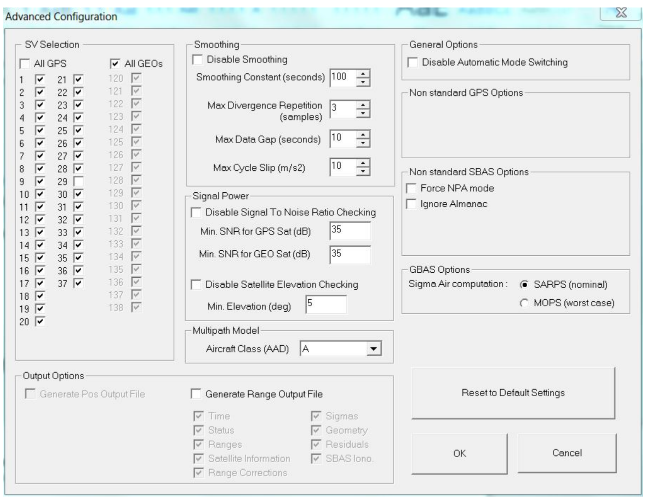

Figure 91 – GNSS Solution Parameters Advanced Configuration

By running the module several times while turning off the 27-37 satellites one by one, and comparing the generated graphics with a job where all the satellites are used, the problem is isolated in satellite PRN29.

:

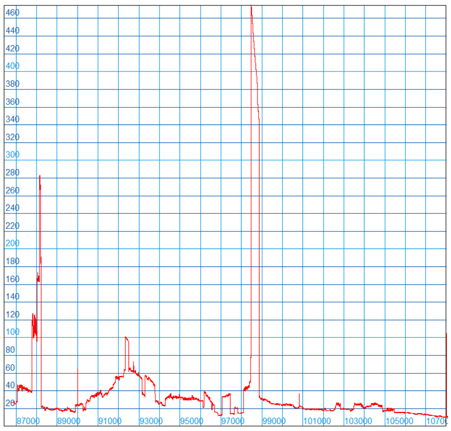

Figure 92 – Time Series Graphic of HPL for 0:00 to 6:00 January 23rd 2012 PRN 120 using all GPS Satellites

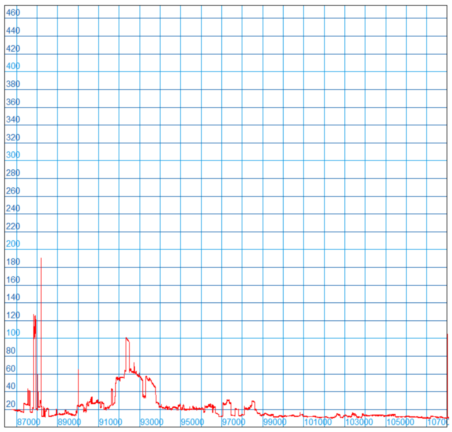

Figure 93 – Time Series Graphic of HPL for January 23rd 2012 PRN 120 using all GPS Satellites except PRN29

As the above graphics show, HPL is much lower when the PRN29 data is not considered than when it is. Therefore, the problem lies in satellite PRN29. This is confirmed by the EUROCONTROL EGNOS Data Collection Network which reported a problem with PRN29 during that date.[1]

As it was just demonstrated, if a hypothetical automated data collection system ends up producing anomalous data, PEGASUS can be used to examine that data separately to discover the cause of said anomaly.

[1] http://edcn2.pildo.com/newsletter/newsletter_2012_1.html.

5 Analysis of Virtual Data

Here we will demonstrate how a VRS can be used as an adequate replacement for a real receiver and explain how to evaluate performance using VRS and PEGASUS.

5.1 Virtual Receiver Stations (VRS)

Having a physical GPS reference station on which ever site in which performance evaluation is necessary may not be possible due to a variety of issues (cost, difficulty in access, etc). An alternative to this is the use of virtual receivers.

In order to generate Virtual Receiver Stations, a network of real reference stations must be connected to a computation server.

Each receiver will allow the creation of a distance-dependent error database. In order to do so, it is needed to measure all the carrier phase information and solve carrier phase ambiguities (reference stations' position must be known).

If it is a real-time problem, the user receiver sends its calculated position to the computation server as well. This transmission of the user position is done in the NMEA format by the Global System for Mobile Communication (GSM) or General Packet Radio Service (GPRS), among others.

In the server, the carrier phase data and pseudorange are geometrically translated from the nearest reference station to the virtual position. The distance dependent errors are interpolated and added, generating data for a new non-physical station. The generated data from the resulting Virtual Reference Station (VRS) can be used in the same way data from a physical receiver would be used. The user can this way perform its position calculation both in Real-Time Kinematic (RTK) or Post-Processed (PP) mode.

The following figure illustrates the distribution of the GNSS Network by the Portuguese Instituto Geográfico do Exército (IgeoE).

It contains already 26 receiver stations covering the whole country. The IgeoE allows users to generate data for any VRS located anywhere within Continental Portuguese territory. The output of these stations is provided in RINEX format.

The notion of VRS provides several improvements: Not only can the reference receiver network density be decreased, but reliability can be increased due to the redundancy introduced by the additional receivers. Another benefit of a VRS is that the reference data are free of site-specific errors such as multipath, because the VRS computation assumes that the virtual station is situated at an ideal location [31].

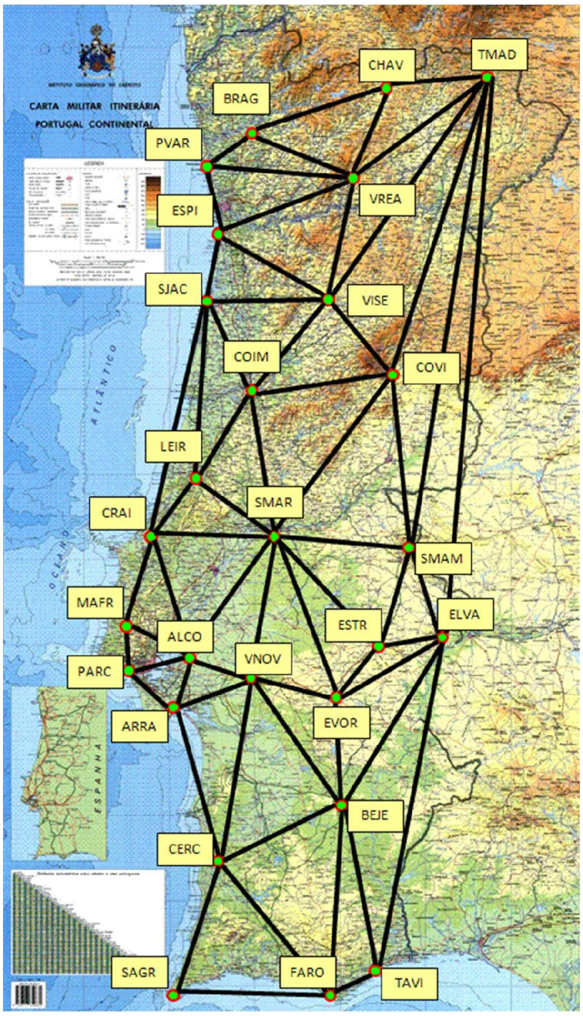

Figure 94 – Geographical Institute of the Army GPS Receiver Network[2]

5.2 Acceptability of VRS Data

Before using VRS Data in our performance evaluation we must first determine whether or not it is similar enough to real data in order to produce reliable results. To do so, PEGASUS is used to analyze data given by a VRS station at the same position as a real station: specifically, the data of a virtual station with the same location as IST4. This virtual station will be referred to as VRS4.

Using the data generated by both stations and PRN 120 on October 10th 2011, Convertor is run on the .o RINEX file from VRS4 and the Septentrio file from IST4. Using FileWatch to look at the resulting .rng file for both, the CNO_L1 parameter, corresponding to the Carrier to Noise ratio, is examined:

[2] www.igoe.pt.

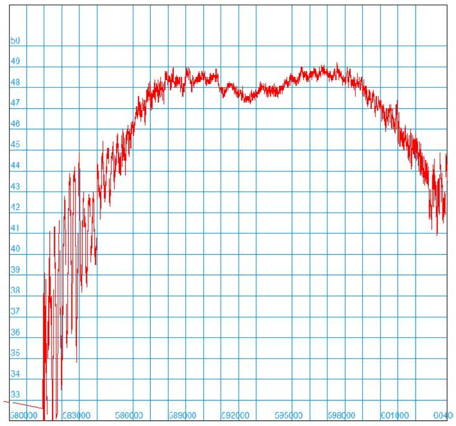

Figure 95 – CNO_L1 of GPS satellite PRN 20 for EGNOS PRN 120 IST4 data during October 10th 2011

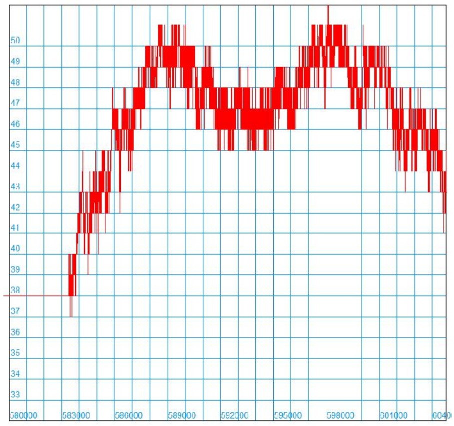

Figure 96 – CNO_L1 of GPS satellite PRN 20 for EGNOS PRN 120 VRS4 data during October 10th 2011

As the graphs show, the Carrier to Noise ratio of the VRS is slightly higher and more discretized, yet very similar to the real station, indicating a good approximation.

The NSV_LOCK parameter (which, as seen before corresponds to the number of satellites in view) in both generated .rng files is compared in the following figures:

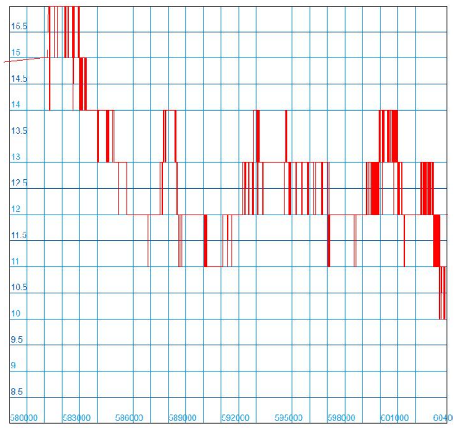

Figure 97 – NSV_LOCK of GPS satellite PRN 20 for EGNOS PRN 120 IST4 data during October 10th 2011

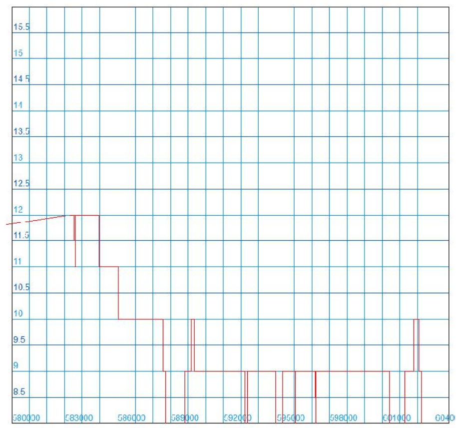

Figure 98 – NSV_LOCK of GPS satellite PRN 20 for EGNOS PRN 120 VRS4 data during October 10th 2011

As the graphics show, VRS data uses fewer satellites in view, thus generating more inaccurate positions. By running the steps described in the following section and using PEGASUS' "Report" function, for both sets of data we get the following results:

Protection level statistics	
	99%
HPL	24.54
VPL	40.18

Table 29 – Protection level statistics for PRN 120 IST4 data during October 10th 2011

APV-I Position error statistics	
	95%
HPE	1.21
VPL	1.47

Table 30 – Position error statistics for PRN 120 IST4 data during October 10th 2011

	APV-I	APV-II	CAT-I
Minimum Required	99%	99%	NA
Availability	98.387%	67.449%	1.539%

Table 31 – Availability statistics for PRN 120 IST4 data during October 10th 2011

Protection level statistics	
	99%
HPL	25.54
VPL	41.81

Table 32 – Protection level statistics for VRS4 data during October 10th 2011

APV-I Position error statistics	
	95%
HPE	0.96
VPL	1.29

Table 33 – Position error statistics for PRN 120 VRS4 data during October 10th 2011

	APV-I	APV-II	CAT-I
Minimum Required	99%	99%	NA
Availability	96.724%	64.400%	1.200%

Table 34 – Availability statistics for PRN 120 VRS4 data during October 10th 2011

As the tables show, not only are the results very similar but VRS data tends to provide a slightly worse estimate of availability and accuracy, meaning that results obtained with real receivers tend to be slightly better than those predicted with VRS stations. Nevertheless, these results prove that VRS stations can be used as adequate replacements for real receivers for the purposes of SBAS evaluation.

5.3 Procedure

The first step in analyzing data from virtual stations is to make sure that data from a real EGNOS compatible receiver from the same time as the VRS data is available. Since the real data is usually separated by hour, it is necessary to concatenate it. PEGASUS does have a concatenation function inside the File Manager option in Tools but often it is not possible to concatenate certain files of the same type due to the program erroneously recognizing them of different types. Therefore, it is necessary to use the concat.exe program inside the Pegasus/Software folder. This program is used via the Windows command line. A simple way to ensure the files are properly concatenated is to ensure the filenames have the common convention of XXXYYYZ where XXX is the receiver name, YYY is the day number and Z is a letter matching the hour of the day (a for 0:00 to 1:00, b for 1:00 to 2:00, etc). This will ensure the filenames remain in alphabetical order so a command of “concat *.12_ outputfilename.12_” will concatenate the files in the proper order.

While data is usually analyzed in 24 hour periods, it is advisable to use 25 hour periods instead as PEGASUS can be unstable during the first hour of operation. The extra hour can be eliminated by opening the .pos file generated by PEGASUS in Notepad and deleting the first 3600 lines after the header.

Opening PEGASUS; the steps are as follows:

1. Run Convertor for the .o RINEX file generated by the VRS
2. Run Convertor for a real Septentrio file of the same date, making sure that both files have the same date, time length of measurement and are both at 1 Hz.
3. Copy the .sXX, .sfc, .smt, .smt, .ssc, .xpl and .alm files from Convertor’s output and copy them into the folder generated by Convertor for the virtual ones. This will add the EGNOS data to the virtual files
4. Run the GNSS Solution module for the .rng file in the combined real and virtual data folder. Make sure to insert the receiver coordinates in order to generate correct results for the position errors and to select the PRN of the EGNOS satellite you wish to use (120, 124 and 126). To get all three, you need to run the module several times (make sure to assign a new job for each, so that PEGASUS won’t overwrite the data).
5. Analyze the generated graphics (found in the “Graphics” option of the main window).

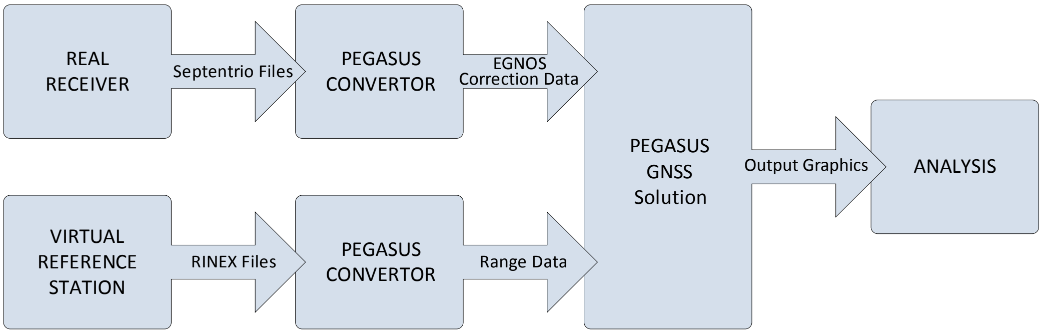

Figure 99 – Virtual Data Evaluation Procedure

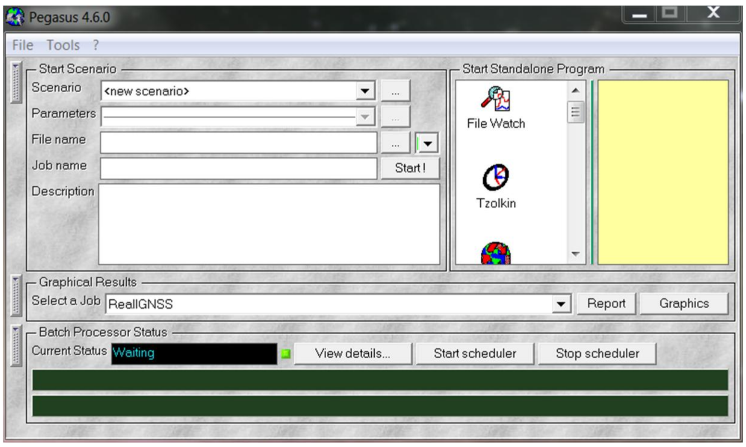

Figure 100 – PEGASUS Main Window

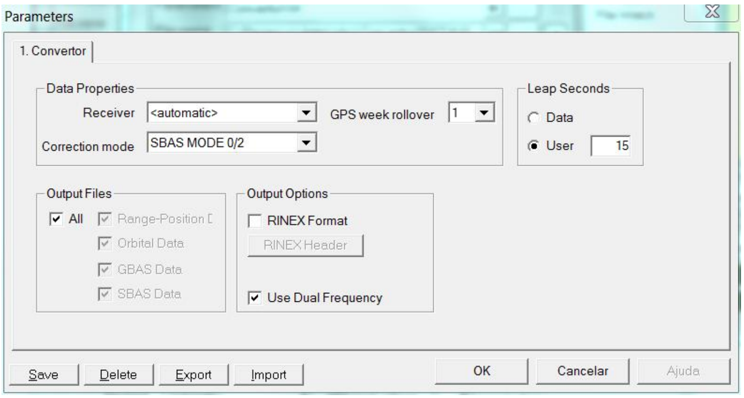

Figure 101 – Convertor Parameters Screen

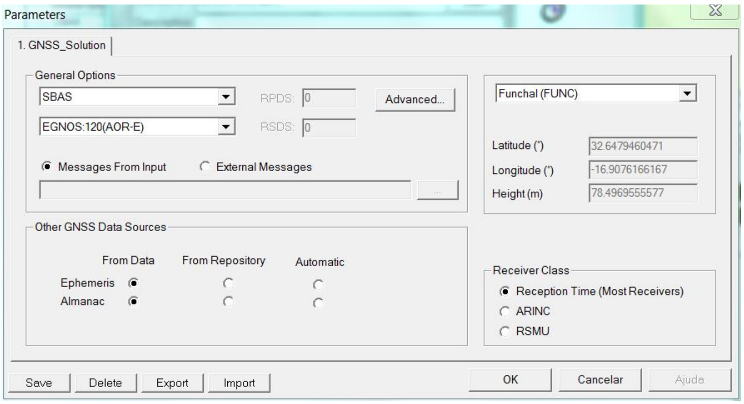

Figure 102 – GNSS Solution Parameter Screen

5.4 Virtual Receiver Station Evaluation

The VRS data analysis methodology will now be used to analyze EGNOS' performance in the Porto and Faro airports on February 9th, 2012. For that purpose, two Virtual Reference Stations are created at both these airports, which we call VirtPorto and VirtFaro, whose locations are included in the annex. After following the steps described in 6.1 with the data from VirtPorto, VirtFaro and IST4, PEGASUS' "Graphics" button on the main screen can be used to examine the graphics for the virtual data.

5.4.1 VirtPorto

In the following figures the distribution of the Vertical and Horizontal Position Errors and Protection Levels is shown:

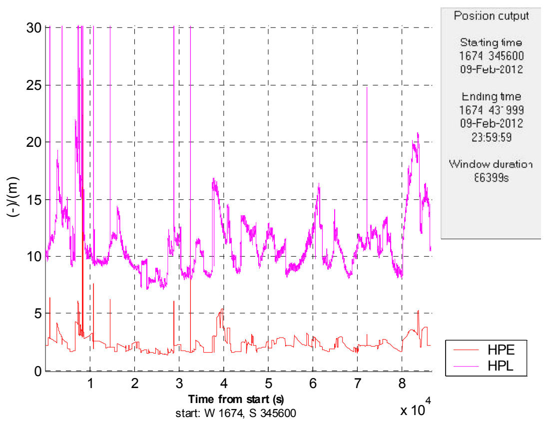

Figure 103 – HPE and HPL for VirtPorto in February 9th 2012 PRN 120

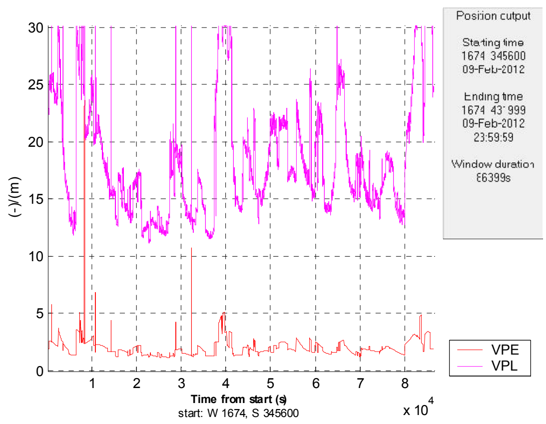

Figure 104 – VPE and VPL for VirtPorto in February 9th 2012 PRN 120

Apart from a few outliers in the Protection Levels, performance was acceptable throughout.

Now the Stanford plots for VirtPorto are examined:

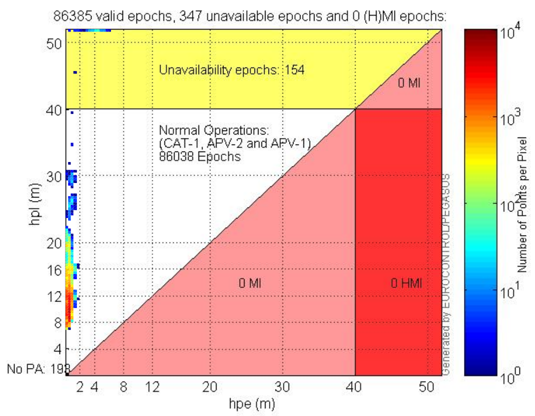

Figure 105 – Horizontal Stanford Plot for VirtPorto in February 9th 2012 PRN 120

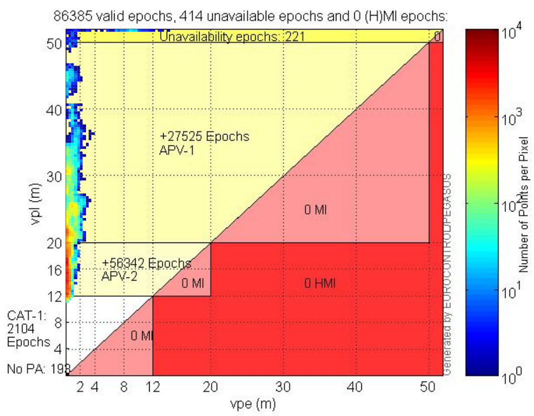

Figure 106 – Vertical Stanford Plot for VirtPorto in February 9th 2012 PRN 120

As the plots show, APV-1 was available for most of the day, with about 6 minutes of unavailability.

The following figure shows the horizontal deviation from reference:

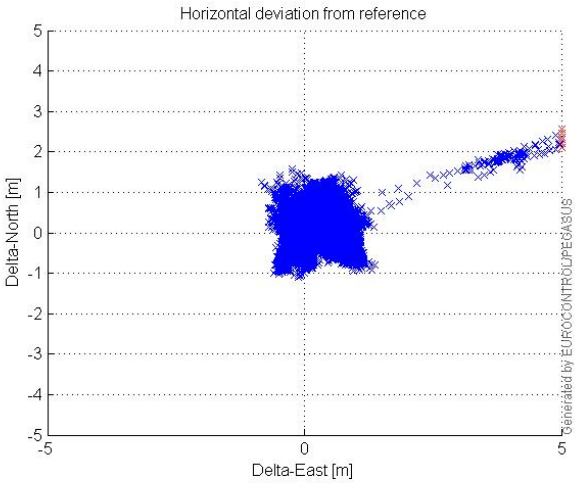

Figure 107 – Horizontal deviation from reference for VirtPorto in February 9th 2012 PRN 120

Despite the presence of the aforementioned outliers, deviation has been limited to less than 2 meters, as the graphics show.

And finally the Position Error and Protection Level histograms are shown here:

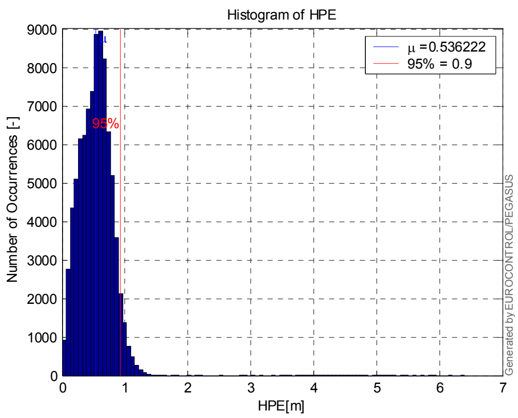

Figure 108 – HPE histogram for VirtPorto in February 9th 2012 PRN 120

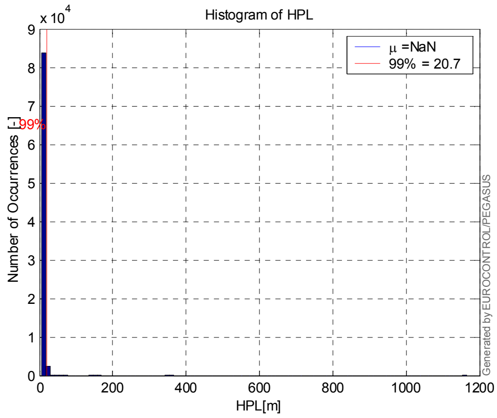

Figure 109 – HPL histogram for VirtPorto in February 9th 2012 PRN 120

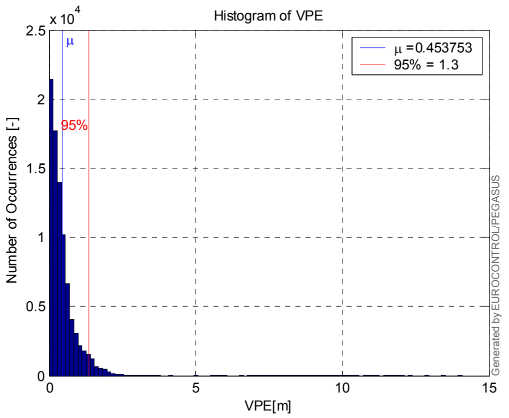

Figure 110 – VPE histogram for VirtPorto in February 9th 2012 PRN 120

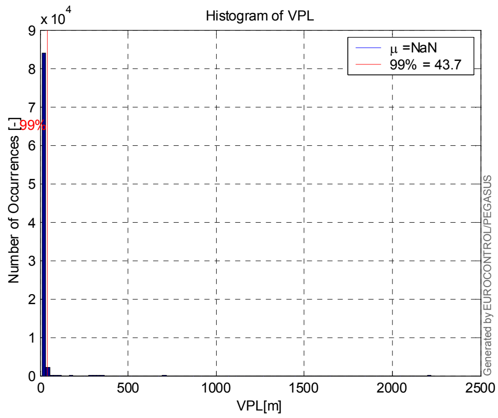

Figure 111 – VPL histogram for VirtPorto in February 9th 2012 PRN 120

The Position Errors and Protection Levels are mostly concentrated around low values, meaning the resulting positions are quite accurate. The aforementioned Protection Level outliers can also be seen in near the bottom of the respective histograms. However, the 99th percentile shows that these make up less than 1% of the results.

Using the "Report" function on the same job, we obtain the information detailed in the following tables (with the simultaneous data from IST4 shown for comparison):

Protection level statistics (99%)		
	VirtPorto	IST4
HPL	19.85	21.28
VPL	37.79	35.51

Table 35 – Protection Level Statistics for VirtPorto and IST4 in February 9th 2012 PRN 120

Position error statistics (95%)		
	VirtPorto	IST4
HPE	0.92	1.21
VPE	1.33	1.47

Table 36 – Position Error Statistics for VirtPorto and IST4 in February 9th 2012 PRN 120

	APV-I	APV-II
Minimum Required	99%	99%
Availability VirtPorto	99.518%	67.658%
Availability IST4	98.387%	67.449%

Table 37 – Availability statistics for VirtPorto and IST4 in February 9th 2012 PRN 120

The tables support the graphics' information that APV-I was available throughout the day, even despite the high protection level outliers. It can be concluded that the PRN 120 satellite provided adequate performance.

Now the graphics for PRN124 are generated:

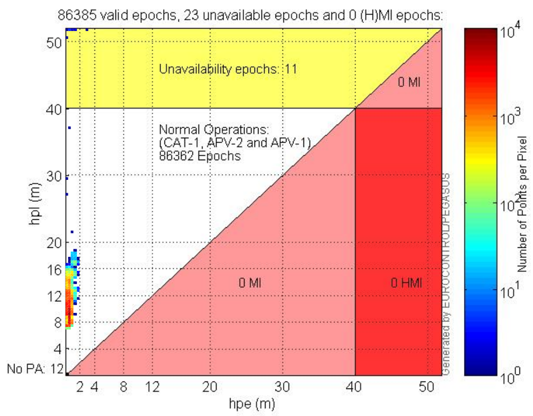

Figure 112 – Horizontal Stanford Plot for VirtPorto in February 9th 2012 PRN 124

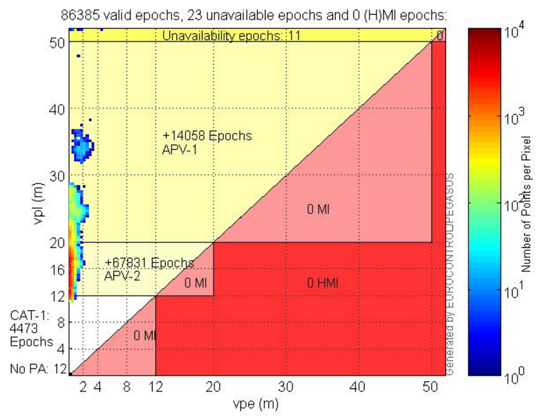

Figure 113 – Vertical Stanford Plot for VirtPorto in February 9th 2012 PRN 124

Once again, APV-I or better was available for most of the day, with only 23 seconds of unavailability.

Next, the Horizontal deviation from reference is shown:

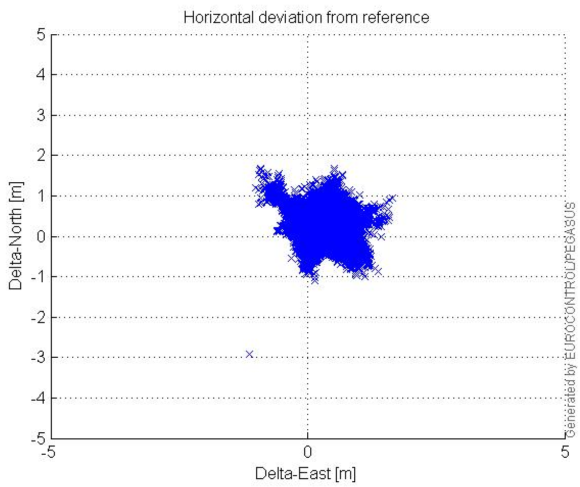

Figure 114 – Horizontal deviation from reference for VirtPorto in February 9th 2012 PRN 124

This time, only a single outlier was found. Overall, the error remained below 2 meters.

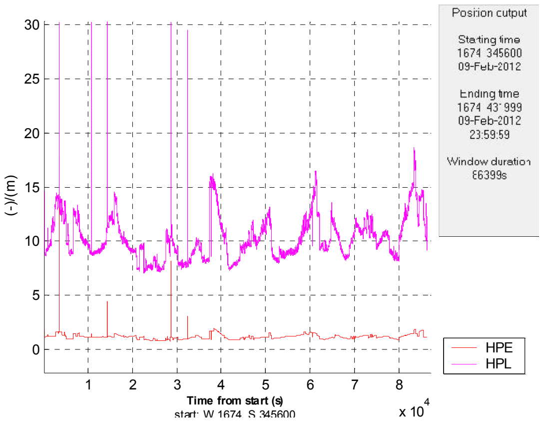

Figure 115 – HPE and HPL for VirtPorto in February 9th 2012 PRN 124

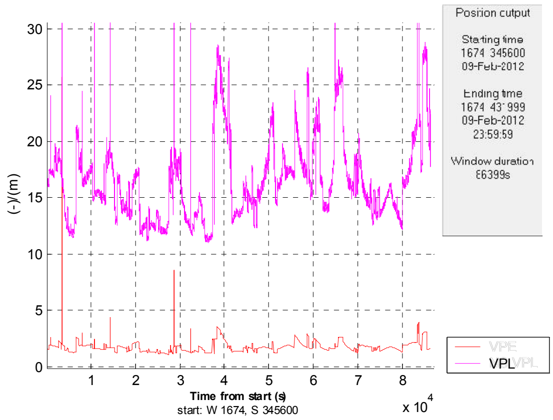

Figure 116 – VPE and VPL for VirtPorto in February 9th 2012 PRN 124

Again, the error remains low apart and the Protection Levels as well, apart from a few outliers.

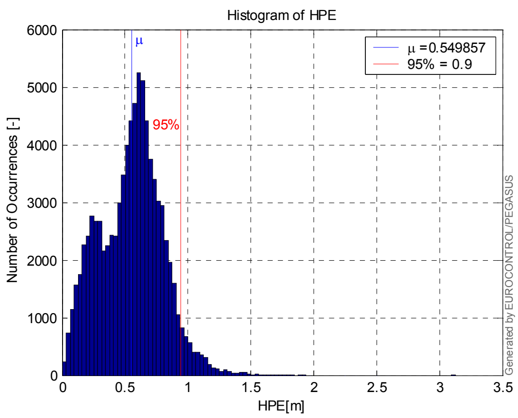

Figure 117 – HPE histogram for VirtPorto in February 9th 2012 PRN 124

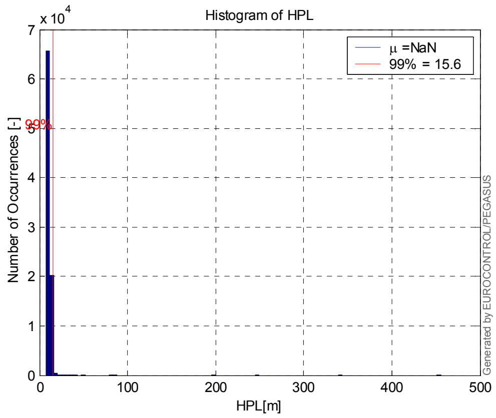

Figure 118 – HPL histogram for VirtPorto in February 9th 2012 PRN 124

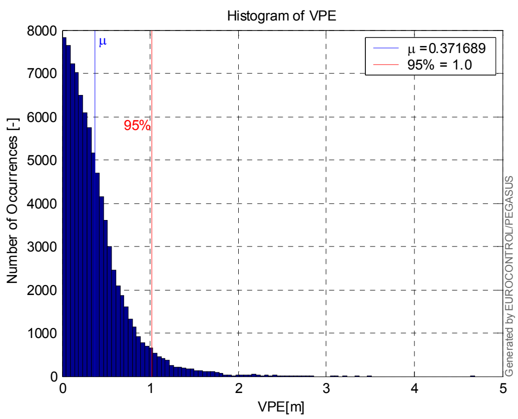

Figure 119 – VPE histogram for VirtPorto in February 9th 2012 PRN 124

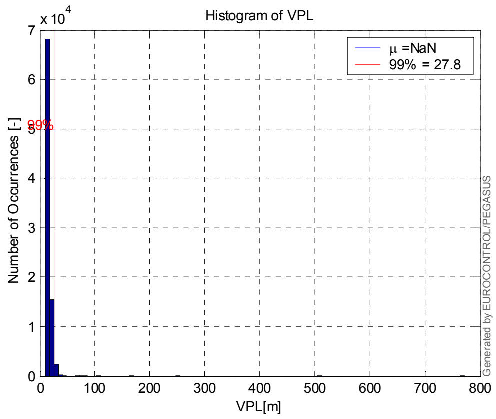

Figure 120 – VPL histogram for VirtPorto in February 9th 2012 PRN 124

Once again, apart from a few outliers, the Position Errors and Protection Levels have remained low. The results are similar to those seen in the PRN 120 satellite.

The respective report provides the following:

Protection level statistics (99%)		
	VirtPorto	IST4
HPL	15.56	15.13
VPL	27.80	25.84

Table 38 – Protection level statistics for VirtPorto and IST4 in February 9th 2012 PRN 124

APV-I Position error statistics (95%)		
	VirtPorto	IST4
HPE	0.94	1.12
VPE	1.02	1.16

Table 39 – Position error statistics for VirtPorto and IST4 in February 9th 2012 PRN 124

	APV-I	APV-II
Minimum Required	99%	99%
Availability VirtPorto	99.972%	83.700%
Availability IST4	99.991%	88.096%

Table 40 – Availability statistics for VirtPorto and IST4 in February 9th 2012 PRN 124

The tables and graphics show that once again, APV-I was available throughout the day, with even greater performance than the PRN120 satellite. Once again, the Protection Level outliers, despite being quite large, didn't affect the overall performance.

Finally, the same procedure is used for PRN126:

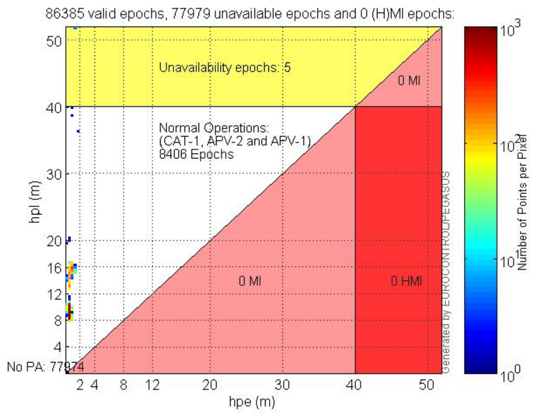

Figure 121 – Horizontal Stanford Plot for VirtPorto in February 9th 2012 PRN 126

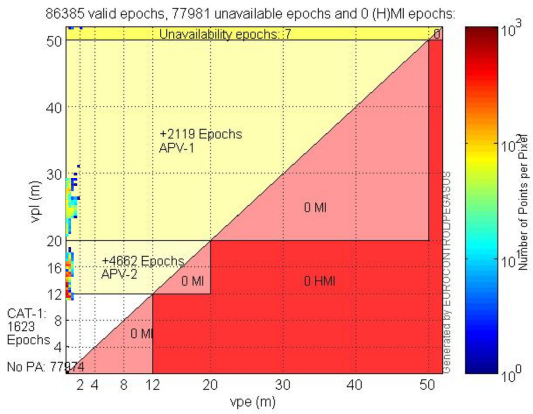

Figure 122 – Vertical Stanford Plot for VirtPorto in February 9th 2012 PRN 126

Here we see that in this satellite, the EGNOS corrections were mostly unavailable. This is supported by the Protection Level graphs, which only show data for a limited time during the day and with quite excessive values:

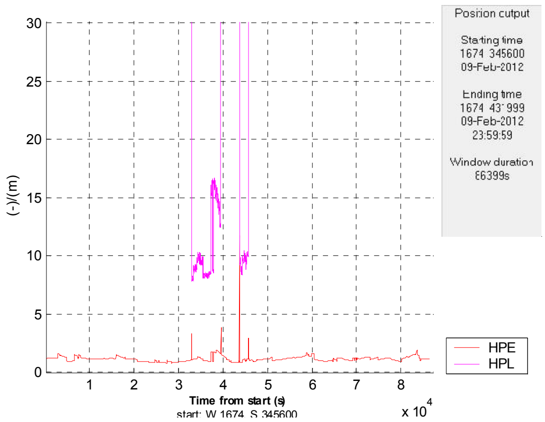

Figure 123 – HPE and HPL for VirtPorto in February 9th 2012 PRN 126

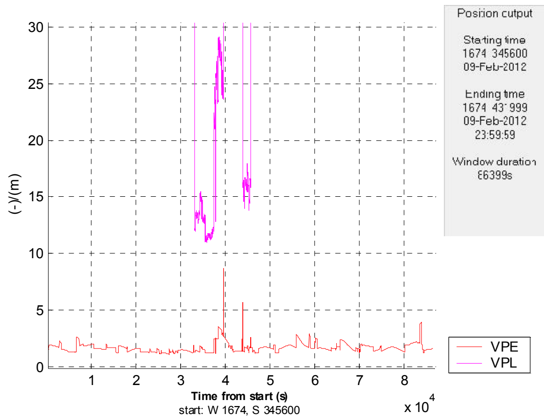

Figure 124 – VPE and VPL for VirtPorto in February 9th 2012 PRN 126

The horizontal deviation from reference graph shows that the error remained low:

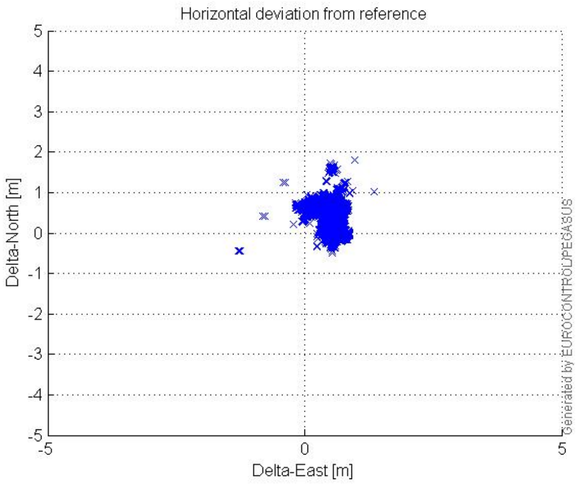

Figure 125 – Horizontal deviation from reference for VirtPorto in February 9th 2012 PRN 126

The histograms show that the Protection Level data is a lot more spread than normal operation:

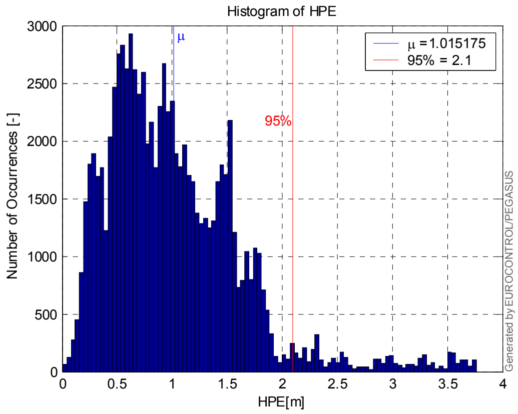

Figure 126 – HPE histogram for VirtPorto in February 9th 2012 PRN 126

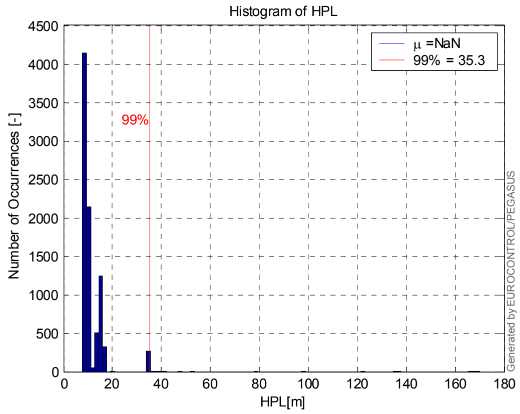

Figure 127 – HPL histogram for VirtPorto in February 9th 2012 PRN 126

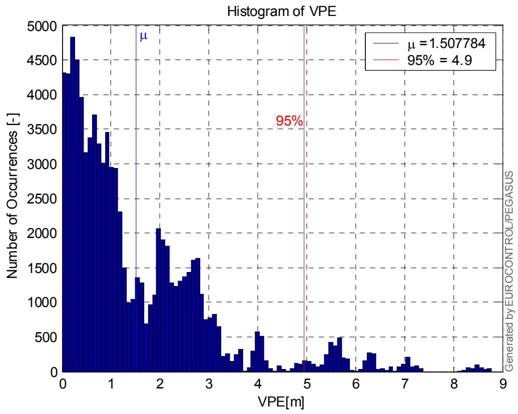

Figure 128 – VPE histogram for VirtPorto in February 9th 2012 PRN 126

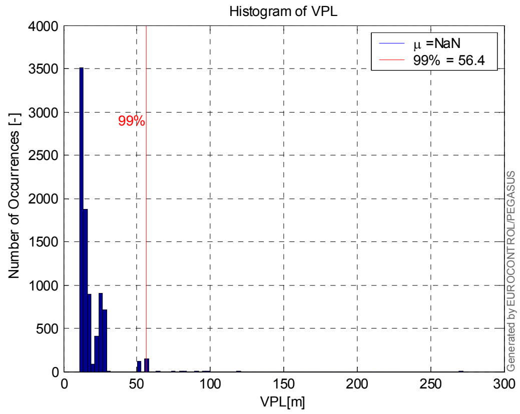

Figure 129 – VPL histogram for VirtPorto in February 9th 2012 PRN 126

Finally, the PEGASUS Report shows the following:

Protection level statistics (99%)		
	VirtPorto	IST4
HPL	15.90	14.59
VPL	27.47	26.20

Table 41 – Protection level statistics for VirtPorto and IST4 in February 9th 2012 PRN 126

APV-I Position error statistics (95%)		
	VirtPorto	IST4
HPL	0.93	1.21
VPL	0.87	1.51

Table 42 – Position error statistics for VirtPorto and IST4 in February 9th 2012 PRN 126

	APV-I	APV-II
Minimum Required	99%	99%
Availability VirtPorto	9.779	8.497%
Availability IST4	9.729%	7.276%

Table 43 – Availability statistics for VirtPorto and IST4 in February 9th 2012 PRN 126

Here we see very little availability of EGNOS data. This is likely due to some sort of outage in the PRN 126 satellite. According to the EGNOS User Support website[3], PRN 126 did suffer an outage several times throughout February 9th, 2012. Thus, the data provided by PRN 126 is discarded.

Taking into account the data of first two satellites, we can conclude that during this day, EGNOS allowed APV-I to be met in the vicinity of the Porto airport. We can also witness the benefits of the EGNOS Space Segment's redundant nature: since only one satellite is needed to benefit from EGNOS' service, two (or in this case one) of the satellites can suffer an outage and the service is still available.

5.4.2 VirtFaro

The same procedure is repeated for the Faro airport:

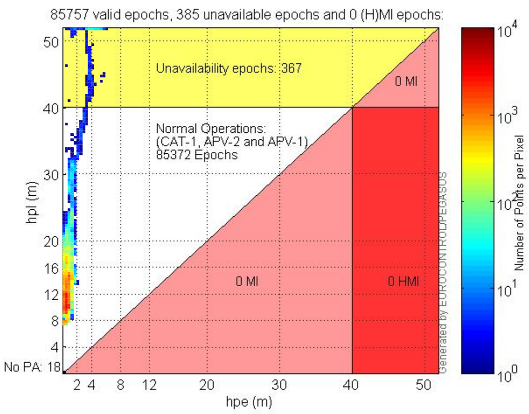

Figure 130 – Horizontal Stanford Plot for VirtFaro in February 9th 2012 PRN 120

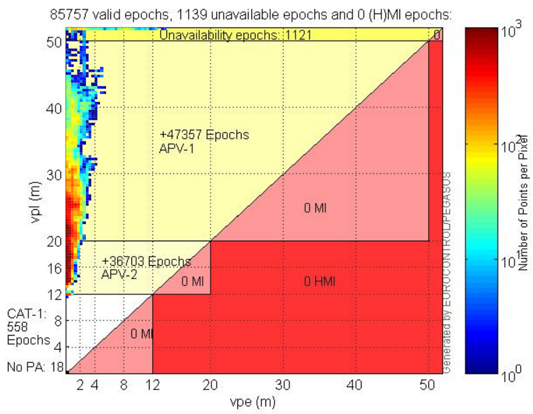

Figure 131 – Vertical Stanford Plot for VirtFaro in February 9th 2012 PRN 120

These plot show that once again, most samples fulfill APV-I requirements though there are more unavailable epochs than in VirtPorto PRN 120. Moving onto the horizontal deviation:

[3] http://egnos-user-support.essp-sas.eu/egnos_ops/data_gaps?sid=18998.

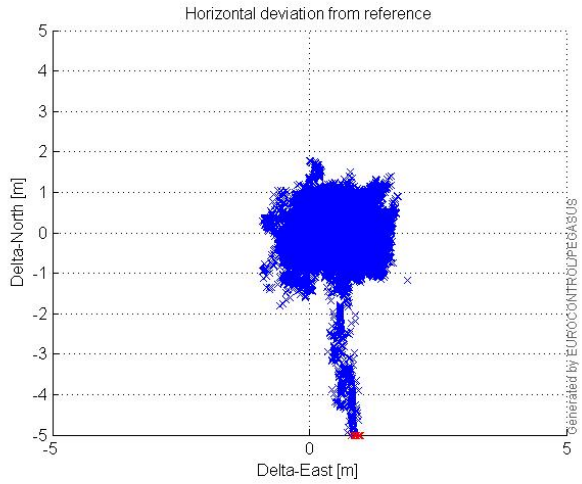

Figure 132 – Horizontal deviation from reference for VirtFaro in February 9th 2012 PRN 120

Here we find a substantial number of outliers, though the performance is otherwise consistent with other seen results.

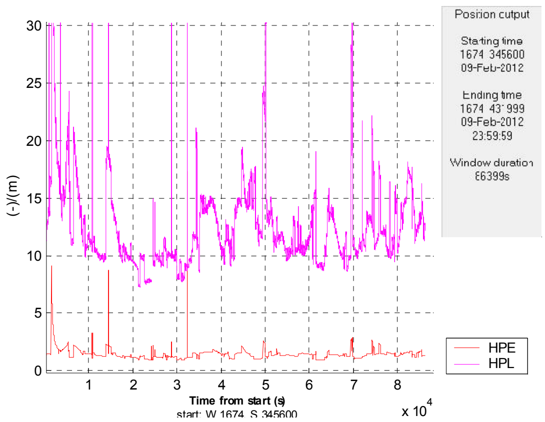

Figure 133 – HPE and HPL for VirtFaro in February 9th 2012 PRN 120

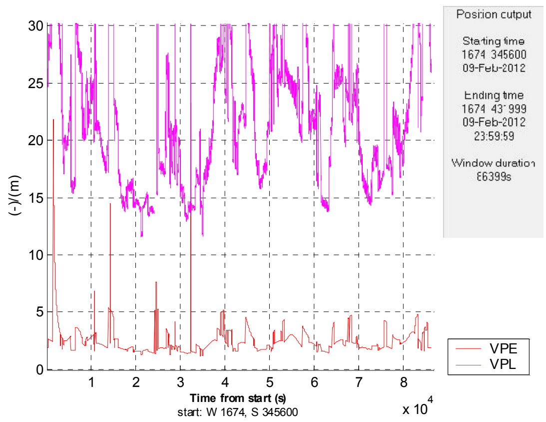

Figure 134 – VPE and VPL for VirtFaro in February 9th 2012 PRN 120

The Position Error and Protection Level graphics show similar results to those of VirtPorto, though a greater number of outliers can be seen in the case of the latter.

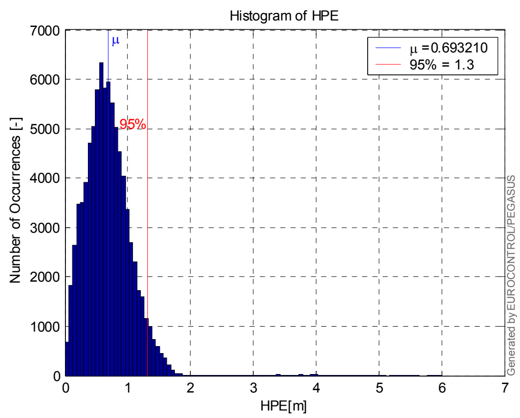

Figure 135 – HPE histogram for VirtFaro in February 9th 2012 PRN 120

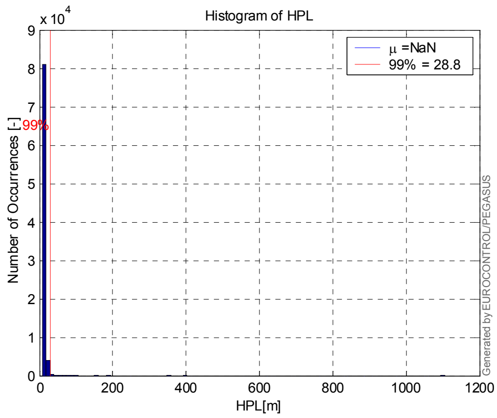

Figure 136 – HPL histogram for VirtFaro in February 9th 2012 PRN 120

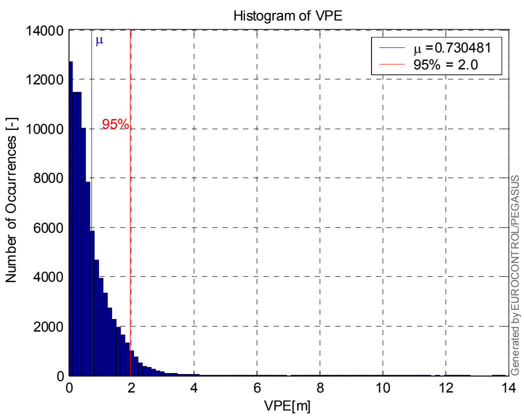

Figure 137 – VPE histogram for VirtFaro in February 9th 2012 PRN 120

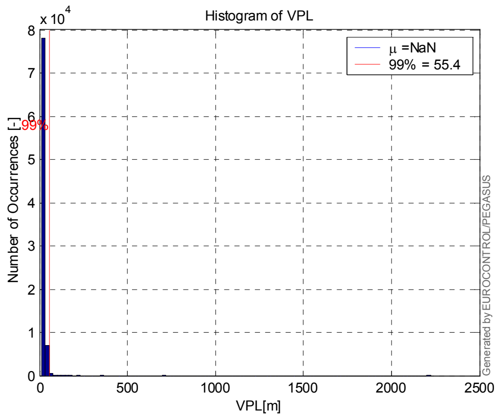

Figure 138 – VPL histogram for VirtFaro in February 9th 2012 PRN 120

As the graphics show, Position Error and Protection Level are once again consistent with what we've seen thus far.

Generating the report produces the following data:

Protection level statistics (99%)		
	VirtFaro	IST4
HPL	20.56	21.28
VPL	38.32	35.51

Table 44 – Protection level statistics for VirtFaro and IST4 in February 9th 2012 PRN 120

Position error statistics (95%)		
	VirtFaro	IST4
HPE	1.28	1.21
VPE	1.90	1.47

Table 45 – Position Error statistics for VirtFaro and IST4 in February 9th 2012 PRN 120

	APV-I	APV-II
Minimum Required	99%	99%
Availability VirtFaro	98.671%	43.450%
Availability IST4	98.387%	67.449%

Table 46 – Availability statistics for VirtFaro and IST4 in February 9th 2012 PRN 120

The tables show that APV-I was not met, albeit by a very small margin. However, the error was very low overall (less than 2 m in the 95th percentile for both horizontal and vertical), thus showing good performance.

The following figures show the results for the PRN124 satellite:

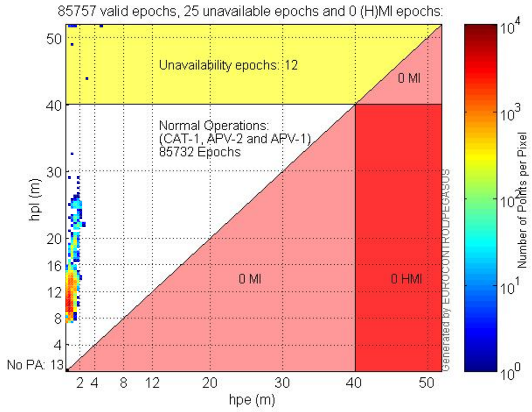

Figure 139 – Horizontal Stanford Plot for VirtFaro in February 9th 2012 PRN 124

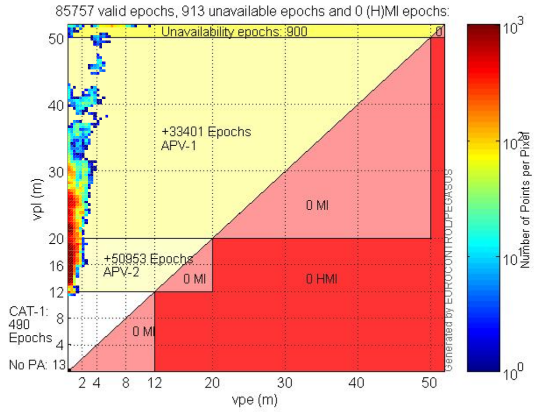

Figure 140 – Vertical Stanford Plot for VirtFaro in February 9th 2012 PRN 124

The Stanford Plots show that there were less unavailable epochs than in PRN 120, meaning that more epochs met APV-I requirements.

Protection level statistics (99%)		
	VirtFaro	IST4
HPL	18.99	15.13
VPL	38.67	25.84

Table 47 – Protection level statistics for VirtFaro and IST4 in February 9th 2012 PRN 124

APV-I Position error statistics (95%)		
	VirtFaro	IST4
HPE	1.33	1.12
VPE	1.70	1.16

Table 48 – Position error statistics for VirtFaro and IST4 in February 9th 2012 PRN 124

	APV-I	APV-II
Minimum Required	99%	99%
Availability VirtFaro	98.935%	59.987%
Availability IST4	99.991%	88.096%

Table 49 – Availability statistics for VirtFaro and IST4 in February 9th 2012 PRN 124

Once again, APV-I was not met but by an even lower margin than in PRN 120. Both Protection Levels and Position Errors were of the same magnitude as in PRN 120.

Finally, the PRN 126 data is examined. Given that this is the same date used for the VirtPorto data, we can expect the same lack of data for this satellite seen in that analysis:

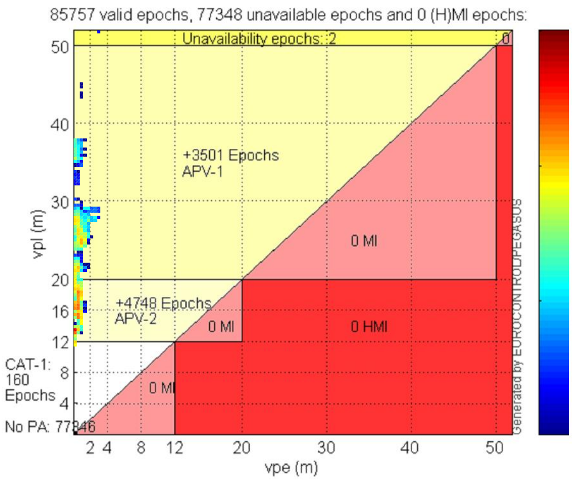

Figure 141 – Horizontal Stanford Plot for VirtFaro in February 9th 2012 PRN 126

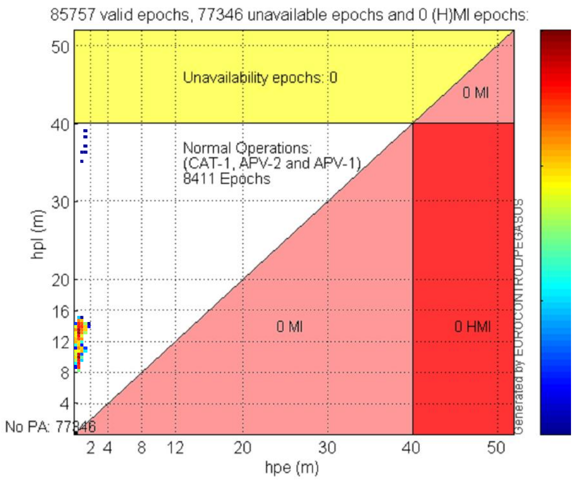

Figure 142 – Vertical Stanford Plot for VirtFaro in February 9th 2012 PRN 126

Protection level statistics (99%)		
	VirtFaro	IST4
HPL	14.61	14.59
VPL	37.04	26.20

Table 50 – Protection level statistics for VirtFaro and IST4 in February 9th 2012 PRN 126

APV-I Position error statistics (95%)		
	VirtPorto	IST4
HPL	1.14	1.21
VPL	1.31	1.51

Table 51 – Position Error statistics for VirtFaro and IST4 in February 9th 2012 PRN 126

	APV-I	APV-II
Minimum Required	99%	99%
Availability VirtPorto	9.806%	5.723%
Availability IST4	9.729%	7.276%

Table 52 – Availability statistics for VirtFaro and IST4 in February 9th 2012 PRN 126

As expected, the PRN 126 satellite is lacking in EGNOS data for the same reasons as mentioned during the VirtPorto analysis and once again that data is discarded. Overall, we can conclude that during this day, EGNOS didn't meet APV-I requirements in the Faro airport. However, since as we have seen earlier, virtual receivers can provide a slightly more pessimistic estimate than real receivers. Therefore, it is possible that APV-I was available in the Faro airport. A more long term study of VRS generated data can disambiguate this question.

Thanks to Virtual Reference Stations, we can judge EGNOS' operational performance without having to install an actual physical station in every airport.

6 Conclusions and Future Work

The goal of this dissertation was to provide a systematic methodology for the operational evaluation of EGNOS.

It began with an overview of GNSS systems nowadays and the various GNSS augmentation system, particularly SBAS. We then described EGNOS in detail, from its various components and inner workings as well as its certification process.

This was followed by a detailed description of a proposed methodology for the operational evaluation of EGNOS using PEGASUS, DoIt, real receivers and virtual reference stations, taking into account both normal operation and the appearance of anomalous data.

6.1 Conclusions

The work done over the course of this thesis led to the following conclusions:

– It is possible to automate the operational evaluation of SBAS via real receivers via the described methodology and use it to monitor performance on a daily basis, with the added possibility of further inspection in the case of anomalies in the data. EGNOS performance can thus be closely and consistently monitored to ensure that it's operating smoothly and effectively, as well as indicate when maintenance is necessary.

– EGNOS data can be analyzed in further detail in order to figure out the cause of any observed anomalies. Examining the various types of corrections allows us to pinpoint a particular satellite as being the cause.

– All three EGNOS satellites (PRN 120, 124 and 126) provide similar performance during normal operation, thus ensuring redundancy in case one of them has an outage. Position errors tend to skew towards the North and the East, due to Portugal's geographic location in relation to the center of Europe. DoIt's estimates for APV-I availability tend to be accurate while those for APV-II tend to be 5% higher than the real result.

– Real receiver data collected during the 15th of January of 2012 showed lower EGNOS performance overall than that of the data collected during the 16th of October of 2012, likely due to RIMS maintenance/upgrade work.

– Virtual Reference Stations can be used as a replacement for real receivers for operational evaluation purposes when the latter are not available. These stations provide a slightly more pessimistic evaluation than real receivers but said evaluation is still very close to reality, meaning evaluation and monitoring can be done in any point where a VRS can be generated without the time and money necessary for the installation of a real station in the desired location.

– EGNOS can be used to provide approach operations with vertical guidance (APV-I) on aircraft with no further equipment necessary other than an EGNOS compatible receiver.

– EGNOS performance in the Lisbon and Porto airports fulfilled APV-I requirements in the examined dates while the Faro airport did not. However, since performance in the Faro airport is below APV-I requirements by a very small margin and the aforementioned pessimistic bias of virtual reference stations, a more long term study with a real receiver can show otherwise.

6.2 Future Work

Future work done in this topic may focus on the following areas:

– Dynamic evaluation of EGNOS: by placing a receiver aboard an airplane in flight, we can determine how EGNOS performs during several phases of flight, namely takeoff and landing as well as cover a large area, providing more data points.

– Analyze data from other points in Portugal, especially Açores and Madeira: seeing as the VRS network is distant from those points, a virtual station cannot be interpolated, meaning a real receiver must be used to evaluate EGNOS performance in those points. Seeing as Açores and Madeira are the most westward points in the EGNOS coverage area, this would provide an interesting study.

– Provide a long term study (perhaps over the course of a year) of EGNOS operational performance in either the airports mentioned in this thesis or others.

– Create a program similar to DoIt capable of automating evaluation using Virtual Receivers. This would allow for a more streamlined process and facilitate long term analysis of performance in places and times where a real receiver is not available.

Annex A: DoIt Sample Report

EUROCONTROL	EGNOS SIS analysis Lisbon Airport 10 September 2011	Site: IST4 PRN: 120 Created: 12/10/11 page 1 of 12

EGNOS SIS analysis

PRN 120

10 September 2011

Lisbon Airport
Lisbon - Portugal

Caution: EGNOS is still under test and development. Results may not be representative of the final EGNOS system performance.
Note: The Pegasus software is still a prototype under validation. Results are not guaranteed and should be treated with care.

1 Introduction

This report constitutes a brief overview of the performance of EGNOS SIS (PRN 120) as observed at Lisbon Airport over a period of 24 hours from 10 of September 00:00 until 10 of September 23:59 with a Septentrio PolaRx 2/3 receiver.

Note that during this period the EGNOS system was still under test and not yet fully deployed. Therefore the results serve only as an indication and can not be used for the final validation

2 First Glance Analysis

The following table provides a quick overview of the most important performance characteristics as obtained during the observed period of 24 hours at Lisbon Airport. Smoothing was set to 100 seconds.

This First Glance Report is generated with Pegasus 4.6.0 and presents the following performance characteristics:

- **Sample validity**: Valid samples are all the samples that are present in the data and are not considered to be affected due to logging or processing tool problems
- **Accuracy** statistics: calculated for horizontal and vertical positioning errors separately.
  For the **measured accuracy**, the samples are taken directly from the horizontal and vertical errors as computed by PEGASUS.
  For the **scaled accuracy**, every sample is scaled with a ratio of AL/PL(i) before taking the 95th percentile.
- User **Availability** percentiles for the different PA operations: determined by dividing the number of samples that are available for an operation by the total number of valid samples
- Number of **discontinuity events** within the period: the total number of discontinuity events for a given operation
- Number of **Integrity** events within the period: the total number of integrity events. The Misleading Information (MI) events are determined based on samples with XPE>XPL. The Hazardous MI (HMI) are counted according to XPE>XAL>XPL for each operation.

All values that exceed a certain required threshold are presented in red.

For more information refer to the FGA Performance algorithms document.

Caution: EGNOS is still under test and development. Results may not be representative of the final EGNOS system performance.

Site	[IST4] Lisbon Airport							Date	10/09/2011	
Location	Lat:	38.789		Lon:	-9.130			Alt:	160.07	
Receiver	Septentrio PolaRx 2/3			Software	Pegasus 4.6.0 300160			PRN	120	
Data set	Duration	Start	Stop	Expected	Total		SBAS Msg	Valid	Valid(%)	
1 Hz	24h00	00:00	23:59	86400	86400		86233	86400	**100%**	
Results per operation										
	all valid samples	APV-I			APV-II			CAT-I		
HAL / VAL		40 / 50			40 / 20			40 / 12		
Accuracy (m)										
		Meas.	Scaled	Req.	Meas.	Scaled	Req.	Meas.	Scaled	Req.
HNSE(95%)	**1.19**	1.19	4.75	16	1.13	5.04	16	1.14	5.57	16
VNSE(95%)	**1.45**	1.45	3.71	20	1.16	1.48	8	0.78	0.81	4
Availability (%)										
samples	86255	86057			61510			2380		
Minimum Required		99%			99%			na		
Availability		**99.603%**			**71.192%**			**2.755%**		
Continuity										
Events		**4**			**558**			**226**		
Integrity										
	MI	HMI APV-I			HMI APV-II			HMI CAT-I		
Total	**0**	0			0			0		
Horizontal	**0**	0			0			0		
Vertical	**0**	0			0			0		

Protection level statistics					
	99%	95%	50%	mean	std deviation
HPL	**24.77**	18.80	10.49	11.79	3.59
VPL	**39.41**	33.52	17.20	19.20	6.18
Position error statistics					
	99%	**95%**	50%	mean	std deviation
HPE	1.76	**1.19**	0.64	0.68	0.31
VPE	2.40	**1.45**	0.44	0.55	0.48

Note: *The Pegasus software is still a prototype under validation. Results are not guaranteed and should be treated with care.*

Note: The following table provides a quick overview of the estimated most important performance characteristics as obtained during the observed period of 24 hours at Lisbon Airport

Estimated availability			
	APV-I	APV-II	CAT-I
Minimum Required	99%	99%	na
Availability	**99.75%**	**73.11%**	-
Estimated continuity			
Events			-

3 Signal In Space Analysis

3.1 GEO broadcast over time period

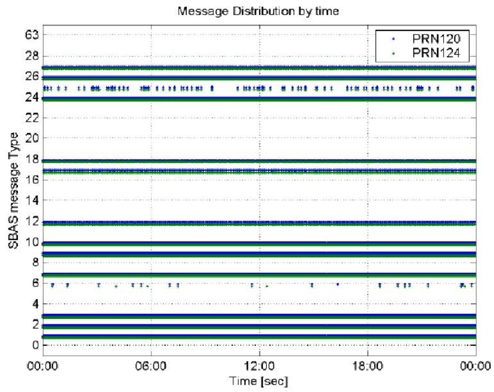

Figure 1: Message types over time

3.2 Message Types Distribution

	PRN 120		PRN 124	
SBAS MT	number	%	number	%
MT 0	0	0.00	0	0.00
MT 1	1340	1.55	1342	1.55
MT 2	21526	24.96	21569	24.96
MT 3	21531	24.97	21569	24.96
MT 4	0	0.00	0	0.00
MT 5	0	0.00	0	0.00
MT 6	92	0.11	96	0.11
MT 7	1339	1.55	1343	1.55
MT 9	1340	1.55	1343	1.55
MT 10	1341	1.56	1342	1.55
MT 12	536	0.62	537	0.62
MT 17	537	0.62	538	0.62
MT 18	2685	3.11	2690	3.11
MT 24	21531	24.97	21568	24.96
MT 25	91	0.11	92	0.11
MT 26	11807	13.69	11833	13.70
MT 27	537	0.62	538	0.62
MT 28	0	0.00	0	0.00
MT 62	0	0.00	0	0.00
MT 63	0	0.00	0	0.00
Total	86233	100.00	86400	100.00

Figure 2: Message type counter

3.3 Message Type 6 Analysis

This figure shows the number of occurrences for consecutive MT6 broadcasts (1, 2, 3, 4 or more repetitions). A normal alert consists of four consecutive MT6 messages, while single occurances indicate CPF switch-overs.

Message Type 6 repetitions

	single	double	3 x	4 x	> 5x
PRN 120	0	0	1	22	0
PRN 124	0	0	1	23	0

Figure 2: Message Type 6 repetitions

4 Position Solution Analysis

4.1 Position errors and Protection levels

All plots have fixed scales that represent nominal behaviour. When the performance does not fit properly within these scales further detailed investigations are needed.

4.1.1 Position solution plots

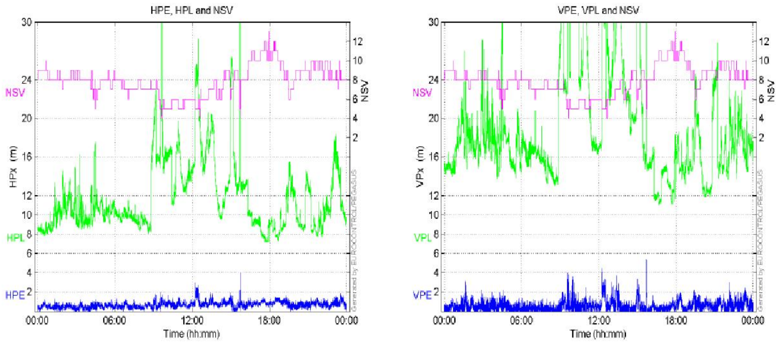

Figure 4: Horizontal and vertical Error, Protection Level and NSV over time

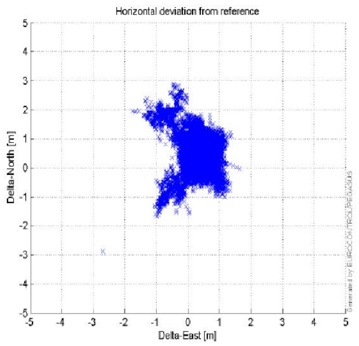

Figure 5: Scatter plot of horizontal deviation from reference position

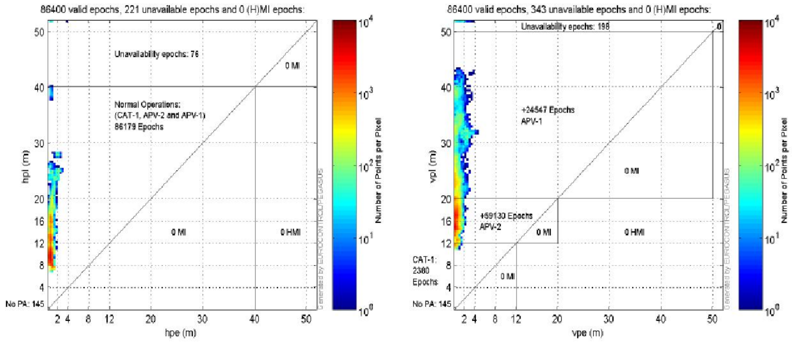

Figure 6: Horizontal and Vertical Stanford graphs

4.1.2 Statistics

Figure 7: Horizontal and Vertical position error distributions

Figure 8: Horizontal and Vertical protection level distributions

Figure 9: Horizontal and Vertical xPE/xPL distributions

4.2 Integrity

In case of a (potential) Misleading Information situation, this section will provide a list of all the epochs where there was an xPE/xPL ratio of more than 1 (real MI) or more than 0.75 (near MI).

4.2.1 Integrity events

There are no Integrity events in the data. The maximum Horizontal PL/PE ratio is 0.191454 and the maximum Vertical PL/PE ratio is 0.143593

The following table represents the most extreme epochs: Highest xPE/xPL ratio, Lowest xPL values and Highest xPE values.

extremes

	Epoch	HPE	HPL	HPE/HPL	VPE	VPL	VPE/VPL
max normHor	584899	1.48417	7.75208	0.19145	-0.44548	13.9153	0.03201
max normVer	524392	0.51572	10.9474	0.04711	-3.15541	21.9747	0.14359
max HPE	575109	3.94855	276.022	0.01431	-0.44189	148.217	0.00298
max VPE	562518	2.84273	25.1036	0.11324	-4.48293	32.2403	0.13905
min HPL	582279	0.65489	7.1639	0.09141	-0.44386	11.179	0.0397
min VPL	578334	0.46851	8.84641	0.05296	-0.27359	10.9929	0.02489

extremes	**-**	**3.94855**	**7.1639**	**0.191454**	**-4.48293**	**10.9929**	**0.143593**

4.2.2 Cumulative Density Function

The Cumulative Density Function (CDF) gives a good indication of the quality of the data in terms of over-bounding. Especially the trend towards lower probabilities becomes clear. The graphs should be read as follows:

- The Red dashed line indicates the ideal trend
- The vertical axis indicates the probabilities, the more data is available, the lower the graphs continue
- The horizontal axis indicates the quality of over-bounding.
- The data points are strictly not allowed to exceed the red-dashed line.
  - However at the start they normally tend to exceed it, and this is acceptable as long as this is only for a small area at the beginning
- The steeper the trend of the data-points, the better.
  - A clear downward trend gives confidence that the over-bounding is sufficient.
  - A clear trend towards exceeding the reference (red-dashed) line is an indication of non over-bounding.
  - In case the trend is parallel and close to the reference, further investigation such as EVT is recommended.
  - A change(s) of the trend suggests that multiple system modes are present in the data. For detailed analysis these should be separated.

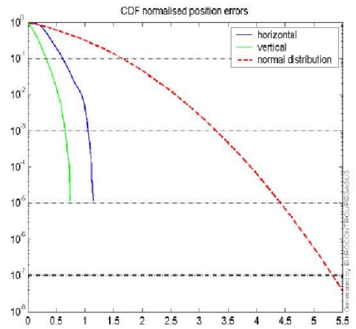

Figure 10: Horizontal and Vertical Position over-bounding in CDF

4.3 Continuity

This section will provide a list of all the discontinuity events. In case there are more than 20 discontinuity events the tables are filtered to a maximum table length of 20. In case there still too many independent events, the table will not be displayed and further investigation is recommended.

The following table presents the discontinuity performance in more detail.

- All discontinuities regardless of duration (same as in firstglance)
- Long discontinuities lasting 3 or more seconds

- Independent discontinuities, lasting 3 or more seconds and after continuously available period of 15 or more seconds
- P(disc.): Continuity Risk determined by multiplying the continuity risk per epoch with 15 seconds
- P(slide): Continuity Risk determined with sliding window of 15 seconds

Discontinuity events

	Valid	APV-1	APV-2	CAT-1	APV-35m
All	8	4	558	226	208
Long	8	4	71	26	10
Independent	2	2	25	2	3
P(disc.)	0.00035	0.00035	0.0061	0.0126	0.00054
P(slide)	0.00118	0.00059	0.0338	0.25966	0.00685

4.3.1 Discontinuity events for Position Solution

The following table presents all Position discontinuity events:

Position discontinuity events

#	Epoch	duration	stable period
1	574940	9	56540
2	574961	8	12
3	574981	8	12
4	575001	28	12
5	575041	28	12
6	575081	24	12
7	575125	20	20
8	575157	20	12

4.3.2 Discontinuity events for APV-I

The following table presents all APV-I discontinuity events:

APV-I discontinuity events

#	Epoch	duration	stable period
1	553158	127	34758
2	574940	169	21655
3	575118	27	9
4	575157	20	12

4.3.3 Discontinuity events for APV-II

There are too many (25) APV-II discontinuity events.

4.3.4 Discontinuity events for CAT-I

The following table presents independent CAT-I discontinuity events:

CAT-I discontinuity events

#	Epoch	duration	stable period
1	579112	2657	782
2	582281	407	512

5 Range Domain Analysis

This chapter is empty. No range information.

6 Estimated Values

6.1 Protection levels

6.2 Availability

			APV-1			APV-2		
Site	**Lat.**	**Lon.**	Avail.	HPL(99%)	VPL(99%)	Avail.	HPL(99%)	VPL(99%)
IST4	38.78	-9.13	99.75%	24.4	39	73.11%	15.8	19.8

6.3 Continuity

Annex B: Location of Real and Virtual Receivers

IST4

Data collection ground station for EGNOS and GBAS date

Receiver: Septentrio PolaRx2 (L1/L2 GPS+SBAS)

Antenna: Septentrio PolaNt (L1/L2)

Lat. N 38º 47' 20.46672''

Lon. W 9º 7' 48.94963''

Alt. (rel. ellipsoid WGS84) 160.070m

Figure 143 – IST4 location

VirtPorto

Data collection virtual station for GPS and GLONASS data

Lat. N 41° 15' 0.4716"

Lon. W 8° 40' 56.2692"

Alt. (rel. ellipsoid WGS84) 61m

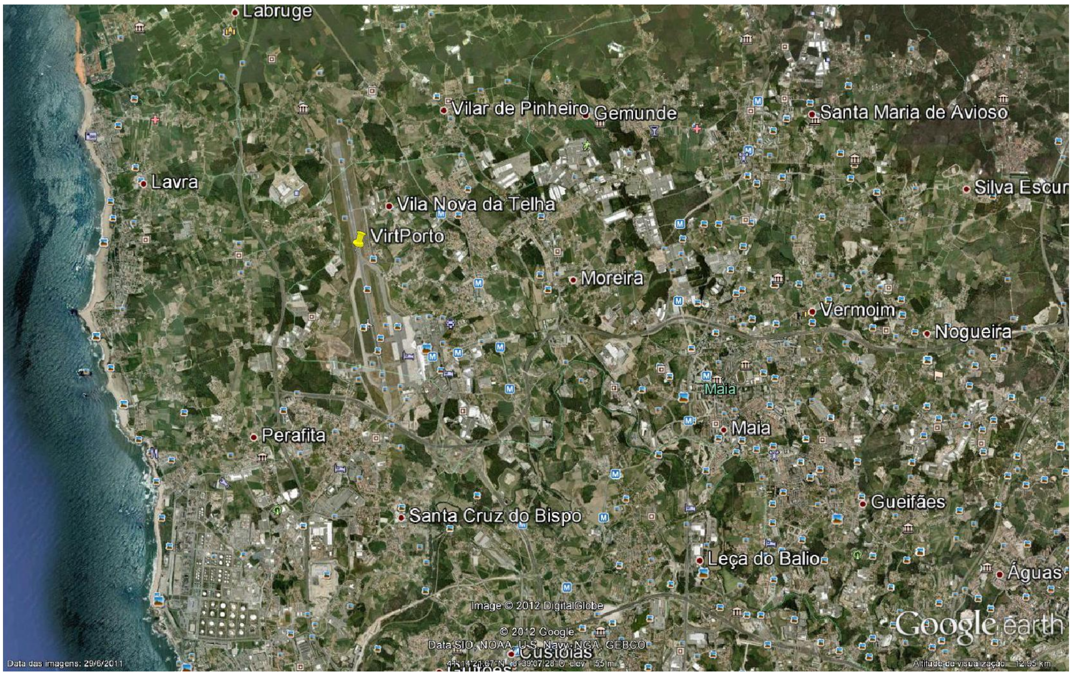

Figure 144 – VirtPorto location

VirtFaro

Data collection virtual station for GPS and GLONASS data

Lat. N 37° 0' 53.9706"

Lon. W 7° 58' 11.8992"

Alt. (rel. ellipsoid WGS84) 6m

Figure 145 – VirtFaro location

Annex C: Evaluation Parameters Calculation

In this section, the mathematical basis of the parameters used in the performance evaluation of SBAS, namely the procedure followed for the calculation of errors and protection levels is described.

As mentioned in Chapter 2.1, the pseudorange estimation formula is:

$$\hat{\rho}_i = \sqrt{(x_i - x_u)^2 + (y_i - y_u)^2 + (z_i - z_u)^2} + c\Delta t_r - \Delta\rho_i \quad \text{(C.3)}$$

Where $\hat{\rho}_i$ is the estimated pseudorange of i-th ranging source, $(x_u,\ y_u,\ z_u)$ are the user estimated position WGS84 coordinates and $\Delta\rho_i$ is the residual pseudorange error for that same ranging source, the difference between true pseudorange and estimated pseudo range [9].

By choosing the reference point $(\hat{x}_u, \hat{y}_u, \hat{z}_u, d\hat{t}_r,)$ for the user position and time and applying a first-order Taylor series expansion to the true pseudorange and deriving the result, we get the following [9]:

$$\rho_i = \hat{\rho}_i + \frac{\partial\hat{\rho}_i}{\partial\hat{x}_u}\Delta x_u + \frac{\partial\hat{\rho}_i}{\partial\hat{y}_u}\Delta y_u + \frac{\partial\hat{\rho}_i}{\partial\hat{z}_u}\Delta z_u + \frac{\partial\hat{\rho}_i}{\partial d\hat{t}_r}\Delta dt_r \quad \text{(C.2)}$$

Where:

$$\frac{\partial\hat{\rho}_i}{\partial\hat{x}_u} = a_{xi}\ ;\ \frac{\partial\hat{\rho}_i}{\partial\hat{y}_u} = a_{yi}\ ;\ \frac{\partial\hat{\rho}_i}{\partial\hat{z}_u} = a_{zi}\ ;\ \frac{\partial\hat{\rho}_i}{\partial d\hat{t}_r} = \mathrm{c} \quad \text{(C.3)}$$

Given that the residual error $\Delta\rho_i$ is:

$$\Delta\rho_i = \hat{\rho}_i - \rho_i \quad \text{(C.4)}$$

We can write the system for error calculation as:

$$\Delta P = \begin{Bmatrix} \Delta\rho_1 \\ \Delta\rho_2 \\ \vdots \\ \Delta\rho_n \end{Bmatrix}\ ;\ \underline{\underline{H}} = \begin{bmatrix} a_{x1} & a_{y1} & a_{z1} & 1 \\ a_{x2} & a_{y2} & a_{z2} & 1 \\ \vdots & \vdots & \vdots & \vdots \\ a_{xn} & a_{yn} & a_{zn} & 1 \end{bmatrix}\ ;\ \overrightarrow{\Delta X} = \begin{Bmatrix} \Delta x_u \\ \Delta y_u \\ \Delta z_u \\ c\Delta t_r \end{Bmatrix} \quad \text{(C.5)}$$

Which derives into:

$$\Delta P = \underline{\underline{H}} \cdot \Delta P \quad \text{(C.6)}$$

As the corrected pseudorange measurement errors are assumed to be jointly zero-mean random Gaussian variables whose covariances depend on satellites' positions it is correct to consider that for different measurements the errors will vary as each measurement is consider to be an stochastic variable, therefore, it is suitable to apply the Weighted Least Square method for the solution of this system [9].

The Weighted Least Square solution for equation (C.6) is:

$$\Delta E = (H^T W H)^{-1} H^T W^{-1} \Delta P = K \Delta P \qquad \text{(C.7)}$$

In which ΔE is the error vector and W the weighting matrix designed to take into account the specific uncertainty of each pseudorange measurement:

$$W = \begin{bmatrix} {\sigma_1}^2 & \cdots & 0 \\ \vdots & \ddots & \vdots \\ 0 & \cdots & {\sigma_n}^2 \end{bmatrix} \quad \text{(C.8)}$$

Since it was assumed that the pseudorange errors are zero-mean random Gaussian variables, the positioning error vector will also be composed of random Gaussian variables with the same characteristics:

$$\Delta E \approx N(0, C) \quad \text{(C.9)}$$

where the covariance matrix C can be expressed as

$$C = \operatorname{cov}(\Delta E) = E(\Delta E \Delta E^T) = K W K^T = \begin{bmatrix} {\sigma_{xx}}^2 & {\sigma_{yx}}^2 & {\sigma_{zx}}^2 & c \cdot {\sigma_{tx}}^2 \\ {\sigma_{xy}}^2 & {\sigma_{yy}}^2 & {\sigma_{zy}}^2 & c \cdot {\sigma_{ty}}^2 \\ {\sigma_{xz}}^2 & {\sigma_{yz}}^2 & {\sigma_{zz}}^2 & c \cdot {\sigma_{tz}}^2 \\ c \cdot {\sigma_{xt}}^2 & c \cdot {\sigma_{yt}}^2 & c \cdot {\sigma_{zt}}^2 & c \cdot {\sigma_{tt}}^2 \end{bmatrix} \qquad \text{(C.10)}$$

The covariance matrix obtained for the position error vector provides an estimate of the standard deviation of 3D position error. It should be noted that, when the error sources affecting GNSS are introduced, satellite geometry has, in fact, a relevant contribution for the Accuracy obtained with these systems.

Furthermore, it has to be noted that the position errors are expressed in the same coordinate system as the one used in the navigation equations from where it was derived, the WGS84. This coordinate frame is not adequate to evaluate the system positioning Accuracy and to calculate the Protection Levels; it is preferable to execute a coordinate transformation from an Earth Centered Earth Fixed (ECEF) to a Local Coordinate Frame (LCF).

To express the position errors in the North-East-Down (NED) coordinate system, a coordinate transformation must be performed. It should be noted that this coordinate transformation can be executed just by a frame rotation, as it is only desired to express the error vector coordinates in another coordinate frame and for this purpose the coordinate frame origin position is irrelevant [9].

$$\Delta E_{NED} = \underline{\underline{T_{WGS}^{NED}}} \Delta E_{WGS} \qquad \text{(C.11)}$$

Where T represents the transformation (rotation) matrix between the WGS84 and the NED coordinate systems.

This matrix is obtained on the basis of geodetic angles (latitude and longitude) [9]:

$$\underline{T_{WGS}^{NED}} = \begin{bmatrix} -\sin\varphi\cos\lambda & -\sin\varphi\sin\lambda & \cos\varphi & 0 \\ -\sin\lambda & \cos\lambda & 0 & 0 \\ -\cos\varphi\cos\lambda & -\cos\varphi\sin\lambda & -\sin\varphi & 0 \\ 0 \quad 0 \quad 0 & & & 1 \end{bmatrix} \qquad \text{(C.12)}$$

Thus, the error covariance matrix is:

$$C_{NED} = T_{WGS}^{NED} K W K^T T_{WGS}^{NED^T} = \begin{bmatrix} \sigma_{NN}{}^2 & \sigma_{EN}{}^2 & \sigma_{DN}{}^2 & c \cdot \sigma_{tN}{}^2 \\ \sigma_{NE}{}^2 & \sigma_{EE}{}^2 & \sigma_{DE}{}^2 & c \cdot \sigma_{tE}{}^2 \\ \sigma_{ND}{}^2 & \sigma_{ED}{}^2 & \sigma_{DD}{}^2 & c \cdot \sigma_{tD}{}^2 \\ c \cdot \sigma_{Nt}{}^2 & c \cdot \sigma_{Et}{}^2 & c \cdot \sigma_{Dt}{}^2 & c^2 \cdot \sigma_{tt}{}^2 \end{bmatrix} \qquad \text{(C.13)}$$

VPE standard deviation is equal to σ_{DD} and the HPE standard deviation is considered to be the maximum deviation in the Horizontal plane σ_M [9]:

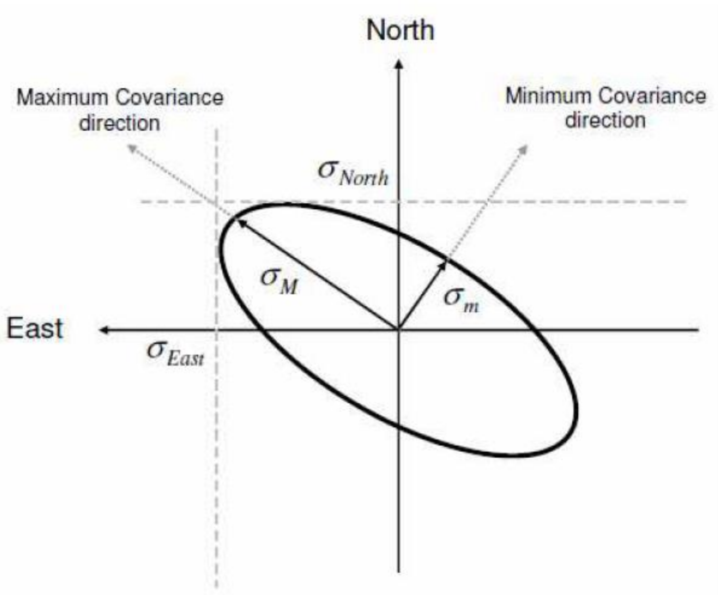

Figure 146 – Horizontal Standard Deviation [9]

$$\sigma_M^2 = \frac{1}{2}(\sigma_{NN}{}^2 + \sigma_{EE}{}^2 + \sqrt{\sigma_{NN}{}^2 + \sigma_{EE}{}^2 + 4\sigma_{NE}{}^2} \quad \text{(C.14)}$$

Protection Level Calculation

The Protection Levels are high confidence bounds for the positioning errors. It is possible to calculate them whenever two or more receivers are interconnected to form a receiving net. Each time a certain number of receivers are connected together the system receives more than one piece of information about each ranging source

It is possible to calculate positioning errors by using the information gathered with the whole net or just by using partial information obtained without taking into account one of the receivers. As briefly introduced in the previous chapter, the first case is named H0 hypothesis and it is defined as “nominal functioning condition” while the second case, named H1 hypothesis, is defined as “one Reference Receiver failure condition”, it represents the error obtainable when one receiver is broken or not available [9].

Considering the conclusions given by equations (C.8) and (C.12), VPE and HPE derivations are defined as

$$HPE \rightarrow \sigma_M = \sqrt{\frac{1}{2}\left(\sigma_{NN}{}^2 + \sigma_{EE}{}^2 + \sqrt{\sigma_{NN}{}^2 + \sigma_{EE}{}^2 + 4\sigma_{NE}{}^2}\right)} \qquad \text{(C.15)}$$

$$VPE \rightarrow \sigma_D \qquad \text{(C.16)}$$

Having a net that incorporates n reference receivers it is possible to repeat these calculations for H1 hypothesis n times, each time excluding a different receiver. Each error calculated in this way is then multiplied by a constant, given by actual regulations, expressing the possibility of fault-free misdetection. The values obtained in this way can be gathered into two vectors [9]:

$$HPL_{H1} = \begin{Bmatrix} k_1 \cdot \left(\left|\sum_{i=1}^{4} B(i)\right| + \sigma_M\right)_1 \\ k_2 \cdot \left(\left|\sum_{i=1}^{4} B(i)\right| + \sigma_M\right)_2 \\ \vdots \\ k_3 \cdot \left(\left|\sum_{i=1}^{4} B(i)\right| + \sigma_M\right)_n \end{Bmatrix} \qquad \text{(C.17)}$$

$$VPL_{H1} = \begin{Bmatrix} k_1 \cdot \left(\left|\sum_{i=1}^{4} B(i)\right| + \sigma_D\right)_1 \\ k_2 \cdot \left(\left|\sum_{i=1}^{4} B(i)\right| + \sigma_D\right)_2 \\ \vdots \\ k_3 \cdot \left(\left|\sum_{i=1}^{4} B(i)\right| + \sigma_D\right)_n \end{Bmatrix} \qquad \text{(C.18)}$$

A similar calculation can also be drawn also for H0 hypothesis:

$$HPL_{H0} = k_{H0} \cdot \sigma_M \qquad \text{(C.19)}$$

$$VPL_{H0} = k_{H0} \cdot \sigma_D \qquad \text{(C.20)}$$

Protection Levels are defined as [9]:

$$HPL = \max\{HPL_{H0}, HPL_{H1}\} \text{ (C.20)} VPL = \max\{VPL_{H0}, VPL_{H1}\} \quad \text{(C.21)}$$

The highest value among those calculated will represent the horizontal protection level and the vertical protection level. Values of the multiplying constants can be found in reference.

In reality it has to be taken into account the possibility of Ephemeris errors, the possibility of large discrepancies between the satellites actual location and broadcast location that could invalidate part of received data. This situation counts as an additional parameter (HPL E and VPL E) for Protection Levels' calculation [9].

$$HPL = \max\{HPL_{H0}, HPL_{H1}, HPL_{E}\} \qquad \text{(C.22)}$$

$$VPL = \max\{VPL_{H0}, VPL_{H1}, VPL_{E}\} \qquad \text{(C.23)}$$

Bibliography

[1] C. Conroy, "A Perspective on GPS/GNSS in Consumer Segment – Especially on Mobile Phones," in *Stanford Center for Position, Navigation and Time*, 2010.

[2] L. Biagi, "GPS Navigation for Precision Farming," in *The 5th International Symposium on Mobile Mapping Technology* , Padua, 2007.

[3] V. Iatsouk, "Development of standards for aeronautical satellite," *Acta Astronautica,* 2004.

[4] ICAO, "ICAO Annex 10 to the Convention on International Civil Aviation," ICAO, 2006.

[5] ICAO, "Global Air Navigation Plan," 2007.

[6] G. Xu, GPS: Theory, Algorithms and Applications, Berlin: Springer, 2007.

[7] A. El-Rabbany, Introduction to Gps: The Global Positioning System, Norwood: Artech House Inc., 2002.

[8] S. Gopi, Global Positioning System: Principles And Applications, Tata Mc-Graw Hill Education, 2005 .

[9] M. Trevisi, *Development of Procedures for the Operational Evaluation of GNSS-SBAS Systems,* Instituto Superior Técnico, 2009.

[10] C. J. H. Elliott D. Kaplan, Understanding GPS - Principles and Applications, Norwood: Artech House, 2006.

[11] P. Enge, "GPS Modernization: Capabilities of the New Civil Signals," in *Australian International Aerospace Congress* , Bribane, 2003.

[12] S. Gleason and D. Gebre-Egziabher, GNSS Applications and Methods, Boston: Artech House, 2009.

[13] I. Leveson, "Benefits of the New GPS Civil Signal - The L2C Study," *Inside GNSS,* July/August 2006.

[14] U.S. General Services Administration, *Federal Standard 1037C,* 1996.

[15] R. B. Langley, "RB Langley," *GPS World,* 1999.

[16] ICAO, Global Navigation Satellite Systems (GNSS) Manual, 2005.

[17] User Guide for EGNOS Application Developers, European Comission, 2009.

[18] EGNOS, "EGNOS Safety of Life Service Definition Document.," European Commission Directorate-General for Energy and Transport., 2011.

[19] RTCA, Minimum Operational Performance Standards for Global Positioning System/Wide Area Augmentation System Airbourne Equipment, 2001.

[20] EGNOS, "EGNOS Service Definition Document - Open Service.," European Commission Directorate-General for Energy and Transport., 2009.

[21] G. T. Team, PEGASUS - Technical Notes on SBAS, EUROCONTROL, 2003.

[22] S. Soley, R. Farnworth, A. v. d. Berg, R. Kremers, J. Sanz, C. Macabiau and A. Fonseca, "The Data Collection Network: EGNOS Revealed," 2004.

[23] ESA, "En Route To Certification," *EGNOS News,* 2008.

[24] "Single European Sky Timeline," EUROCONTROL, [Online]. Available: http://www.eurocontrol.int/articles/single-european-sky-timeline. [Accessed 23 March 2012].

[25] "REGULATION (EC) No 549/2004 of the European Parliament and of the Council of 10 March 2004 laying down the framework for the creation of the single European sky (the framework Regulation)," *Official Journal of the European Union,* 10 March 2004.

[26] "REGULATION (EC) No 550/2004 of the European Parliament and of the Council of 10 March 2004 on the provision of air navigation services in the single European sky (the service provision Regulation)," *Official Journal of the European Union,* 10 March 2004.

[27] "Commission Regulation (EC) No 2096/2005 of 20 December 2005 laying down common requirements for the provision of air navigation services," *Official Journal of the European Union,* 20 December 2005.

[28] "Understanding Egnos," *Coordinates,* September 2007.

[29] "Regulation (EC) No 552/2004 of the European Parliament and of the Council of 10 March 2004 on the interoperability of the European Air Traffic Management network (the interoperability Regulation)," *Official Journal of the European Union,* 10 March 2004.

[30] "EGNOS Open Service Roadmap," ESSP, 2012.

[31] M. Petovello, "What is a virtual reference station and how does it work?," *Inside GNSS,* pp. 28-31, July/August 2011.

[32] PEGASUS User Software Manual: Module CONVERTOR, 2004.

[33] Deloitte, "Transforming the Air Transportation System - A business case for program acceleration," 2011.